Developing an integrated platform for predicting niche and range dynamics: inverse calibration of spatially-explicit eco-evolutionary models

Anne-Kathleen Malchow, M. Sc.

Univ.-Diss.

zur Erlangung des akademischen Grades
Doctor rerum naturalium
(Dr. rer. nat.)

in der Wissenschaftsdisziplin Ökologie

Kumulativ eingereicht an der
Mathematisch-Naturwissenschaftlichen Fakultät
Institut für Biochemie und Biologie
der Universität Potsdam

Tag der Einreichung: 04. Oktober 2022
Ort und Tag der Disputation: Potsdam, 02. Juni 2023

Hauptbetreuerin:
Prof. Dr. Damaris Zurell
Zweitbetreuer:
Prof. Dr. Tobias Krüger

Mentorin: Dr. Leonie Wenz

Gutachter:
Prof. Dr. Damaris Zurell
Prof. Dr. Tobias Krüger
Dr. Tamara Münkemöller

Vorsitz der Prüfungskommission:
PD Dr. Niels Blaum

Online veröffentlicht auf dem
Publikationsserver der Universität Potsdam:
https://doi.org/10.25932/publishup-60273
https://nbn-resolving.org/urn:nbn:de:kobv:517-opus4-602737

Contents

List of Figures

List of Tables

List of Acronyms

ABC	Approximate Bayesian computation
AUC	area under the receiver-operator characteristic curve
BP	breeding pair
CI	credibility interval
cSDM	correlative species distribution model
DCR	demography-environment relationship
DEzs	Differential evolution sampler with snooker update
dSDM	dynamic species distribution model
HSI	Habitat suitability index
IBM	Individual-based model
MCMC	Markov chain Monte Carlo
MHB	Monitoring häufiger Brutvögel (Swiss breeding bird survey)
POM	Pattern-oriented modelling
RMSE	root mean squared error
SDM	species distribution model
WAIC	Watanabe-Akaike information criterion

Abstract

Species are adapted to the environment they live in. Today, most environments are subjected to rapid global changes induced by human activity, most prominently land cover and climate changes. Such transformations can cause adjustments or disruptions in various eco-evolutionary processes. The repercussions of this can appear at the population level as shifted ranges and altered abundance patterns. This is where global change effects on species are usually detected first.

To understand how eco-evolutionary processes act and interact to generate patterns of range and abundance and how these processes themselves are influenced by environmental conditions, spatially-explicit models provide effective tools. They estimate a species' niche as the set of environmental conditions in which it can persist. However, the currently most commonly used models rely on static correlative associations that are established between a set of spatial predictors and observed species distributions. For this, they assume stationary conditions and are therefore unsuitable in contexts of global change. Better equipped are process-based models that explicitly implement algorithmic representations of eco-evolutionary mechanisms and evaluate their joint dynamics. These models have long been regarded as difficult to parameterise, but an increased data availability and improved methods for data integration lessen this challenge. Hence, the goal of this thesis is to further develop process-based models, integrate them into a complete modelling workflow, and provide the tools and guidance for their successful application.

With my thesis, I present an integrated platform for spatially-explicit eco-evolutionary modelling and provid a workflow for their inverse calibration to observational data. In the first chapter, I introduc RangeShiftR, a software tool that implements an individual-based modelling platform for the statistical programming language R. Its open-source licensing, extensive help pages and available tutorials make it accessible to a wide audience. In the second chapter, I demonstrat a comprehensive workflow for the specification, calibration and validation of RangeShiftR by the example of the red kite in Switzerland. The integration of heterogeneous data sources, such as literature and monitoring data,

allowed to successfully calibrate the model. It was then used to make validated, spatio-temporal projections of red kite abundance and identify their most influential processes. The presented workflow can be adopted to any study species if data is available. In the third chapter, I extended RangeShiftR to directly link demographic processes to climatic predictors. This allowed me to explore the climate-change responses of eight Swiss breeding birds in more detail. Specifically, the model could identify the most influential climatic predictors, delineate areas of projected demographic suitability, and attribute current population trends to contemporary climate change.

My work shows that the application of complex, process-based models in conservation-relevant contexts is feasible, utilising available tools and data. Such models can be successfully calibrated and outperform other currently used modelling approaches in terms of predictive accuracy. Their projections can be used to predict future abundances or to assess alternative conservation scenarios. They further improve our mechanistic understanding of niche and range dynamics under climate change. However, only fully mechanistic models, that include all relevant processes, allow to precisely disentangle the effects of single processes on observed abundances. In this respect, the RangeShiftR model still has potential for further extensions that implement missing influential processes, such as species interactions.

Dynamic, process-based models are needed to adequately model a dynamic reality. My work contributes towards the advancement, integration and dissemination of such models. This will facilitate numeric, model-based approaches for species assessments, generate ecological insights and strengthen the reliability of predictions on large spatial scales under changing conditions.

Zusammenfassung

Arten sind an ihren jeweiligen Lebensraum angepasst, doch viele Lebensräume sind heute einem globalen Wandel unterworfen. Dieser äußert sich vor allem in Veränderungen von Landnutzung und Klima, welche durch menschliche Aktivitäten verursacht werden und ganze Ökosysteme in ihrem Gefüge stören können. Störungen der grundlegenden öko-evolutionären Prozesse können auf der Populationsebene in Form von veränderten Verbreitungsgebieten und Häufigkeitsmustern sichtbar werden. Hier werden die Auswirkungen des globalen Wandels auf eine Art oftmals zuerst beobachtet.

Um zu untersuchen, wie die Wirkung und Wechselwirkung der verschiedenen öko-evolutionären Prozesse die beobachteten Verbreitungs- und Häufigkeitsmuster erzeugen, und wie diese Prozesse wiederum von Umweltbedingungen beeinflusst werden, stellen räumlich explizite Modelle wirksame Instrumente dar. Sie beschreiben die ökologische Nische einer Art, also die Gesamtheit aller Umweltbedingungen, unter denen die Art fortbestehen kann. Die derzeit am häufigsten verwendeten Modelle stützen sich auf statische, korrelative Zusammenhänge, die zwischen bestimmten räumlichen Prädiktoren und den beobachteten Artverteilungen hergestellt werden. Allerdings werden dabei stationäre Bedingungen angenommen, was sie im Kontext des globalen Wandels ungeeignet macht. Deutlich besser geeignet sind prozessbasierte Modelle, welche explizite, algorithmische Repräsentationen von ökologischen Prozessen beinhalten und deren gemeinsame Dynamik berechnen. Solche Modelle galten lange Zeit als schwierig zu parametrisieren, doch die zunehmende Verfügbarkeit von Beobachtungsdaten sowie die verbesserten Methoden zur Datenintegration machen ihre Verwendung zunehmend praktikabel. Das Ziel der vorliegenden Arbeit ist es, diese prozessbasierten Modelle weiterzuentwickeln, sie in umfassende Modellierungsabläufe einzubinden, sowie Software und Anleitungen für ihre erfolgreiche Anwendung verfügbar zu machen.

In meiner Dissertation präsentiere ich eine integrierte Plattform für räumlich-explizite, öko-evolutionäre Modellierung und entwickle einen Arbeitsablauf für dessen inverse Kalibrierung an Beobachtungsdaten. Im ersten Kapitel stelle ich RangeShiftR vor: eine Software,

die eine individuenbasierte Modellierungsplattform für die statistische Programmiersprache R implementiert. Durch die Open-Source-Lizenzierung, umfangreichen Hilfeseiten und online verfügbaren Tutorials ist RangeShiftR einem breiten Publikum zugänglich. Im zweiten Kapitel demonstriere ich einen vollständigen Modellierungsablauf am Beispiel des Rotmilans in der Schweiz, der die Spezifikation, Kalibrierung und Validierung von RangeShiftR umfasst. Durch die Integration heterogener Datenquellen, wie Literatur- und Monitoringdaten, konnte das Modell erfolgreich kalibriert werden. Damit konnten anschließend validierte, raum-zeitliche Vorhersagen über das Vorkommen des Rotmilans erstellt und die dafür relevanten Prozesse identifiziert werden. Der vorgestellte Arbeitsablauf kann auf andere Arten übertragen werden, sofern geeignete Daten verfügbar sind. Im dritten Kapitel habe ich RangeShiftR erweitert, sodass demografische Prozessraten direkt mit Klimavariablen verknüpft werden können. Dies ermöglichte es, die Reaktionen von acht Schweizer Brutvogelarten auf den Klimawandel genauer zu untersuchen. Insbesondere konnte das Modell die einflussreichsten klimatischen Faktoren identifizieren, demografisch geeignete Gebiete abgrenzen und aktuelle Populationstrends auf den bisherigen Klimawandel zurückführen.

Meine Arbeit zeigt, dass die Anwendung komplexer, prozessbasierter Modelle in naturschutzrelevanten Kontexten mit verfügbaren Daten möglich ist. Solche Modelle können erfolgreich kalibriert werden und andere, derzeit verwendete Modellierungsansätze in Bezug auf ihre Vorhersagegenauigkeit übertreffen. Ihre Projektionen können zur Vorhersage zukünftiger Artvorkommen und zur Einschätzung alternativer Naturschutzmaßnahmen verwendet werden. Sie verbessern außerdem unser mechanistisches Verständnis von Nischen- und Verbreitungsdynamiken unter dem Einfluss des Klimawandels. Jedoch ermöglichen nur vollständig prozessbasierte Modelle, die alle relevanten Prozesse vereinen, eine korrekte Aufschlüsselung der Auswirkungen einzelner Prozesse auf die beobachteten Abundanzen. In dieser Hinsicht hat das RangeShiftR-Modell noch Potenzial für Weiterentwicklungen, um fehlende, einflussreiche Prozesse hinzuzufügen, wie zum Beispiel die Interaktionen zwischen Arten.

Um eine dynamische Realität adäquat abbilden zu können, werden dynamische, prozessbasierte Modelle benötigt. Meine Arbeit leistet einen Beitrag zur Weiterentwicklung, Integration und Verbreitung solcher Modelle und stärkt somit die Anwendung numerischer, modellbasierter Methoden für die Bewertung des Zustands von Arten, die Untersuchung ökologischer Zusammenhänge und die Steigerung der Zuverlässigkeit von Vorhersagen auf großen räumlichen Skalen unter Umweltveränderungen.

Chapter 1

Introduction

1.1. Global transitions

Anthropogenic threats

Humans are altering the atmosphere and surface of Earth at an accelerating pace (Steffen, Broadgate, et al., 2015). As our industrial and agricultural activities are becoming dominant factors in shaping our planet's state and appearance, it has been proposed to define a new geological epoch characterised by global anthropogenic influence. The Anthropocene marks an age of drastic changes in climate and atmospheric composition (Lewis & Maslin, 2015), after the Holocene had seen approximately 10 000 years of relative stability. This rapidly changing environment entails disadvantageous consequences for us humans as well as many other organisms.

Anthropogenic global effects are embodied in six threats on nature and human well-being: land- and sea-use change, resource extraction, pollution, invasive and alien species, and climate change (Balvanera et al., 2019). 14% of their combined impact is attributed to climate change by the IPBES Global Assessment, after land/sea-use change (30%) and direct exploitation (23%) (IPBES, 2019). Climate change is rated as the most prevalent current threat and the largest potential threat by the IUCN World Heritage Outlook (Osipova et al., 2020). It further exacerbates the adverse effects of all other threats (IPBES, 2019).

Responses to threats

Responses of species and whole ecosystems to these direct drivers have been detected in terrestrial, marine as well as freshwater environments around the globe and on all organisational levels (Parmesan, 2006; Scheffers et al., 2016). Among the observed responses are changes in population dynamics (Selwood et al., 2015) and abundance (Martay et al., 2017), range shifts (I.-C. Chen et al., 2011), altered phenology (Menzel et al., 2020),

impoverished and novel community compositions (Kampichler et al., 2012; Singer et al., 2013) and perturbed ecosystem functions (N. B. Grimm et al., 2013).

Responses in spatio-temporal abundance patterns are relatively well documented as they are detectable with common monitoring schemes. Local population declines and extinctions are reported across continents and taxa (Tilman et al., 2017; Wiens, 2016) and overall population trends are measured by indicators like the Living Planet Index (WWF, 2020). Many species also counter climate change effects by shifting their distributions towards the poles, into deeper waters, or towards higher altitudes, thereby tracking their required climatic conditions (Lenoir & Svenning, 2015). Most notably, such range shifts are established for mobile and comparably well monitored taxa like birds (Maggini et al., 2011; Brommer et al., 2012; Thomas & Lennon, 1999).

Threatening ourselves

The effects of anthropogenic threats on nature amount to a beginning biodiversity crisis (Convention on Biological Diversity - CBD, 2020) with yet unpredictable implications for humanity. As many human societies trade off current against future well-being, the ongoing degradation of Earth's ecosystems causes disruptions in essential ecosystem services such as provisioning of food, water and resources as well as stabilising climate and buffering weather extremes (Sarukhan et al., 2005).

Action plans for reversing ecosystem degradation and transitioning to a sustainable pathway have been devised, but require fundamental transformations. A comprehensive framework for this is given by the UN's Sustainable Development Goals and the 2050 Vision for Biodiversity (CBD, 2020). The necessary effort to reach these goals may be encouraged by a range of successful conservation actions that provide proof of concept that a reversal of current biodiversity trends is possible (Hoffmann et al., 2010; Bolam et al., 2021; Duarte et al., 2020).

1.2. Modelling species distributions

A cross-scale problem

Understanding regional, population-level shifts in species abundance is crucial because it can provide a cross-scale link between global forcings and local responses, even before large-scale biodiversity changes are observed (Dornelas et al., 2014). Such insights can support potential mitigation and management measures whose planning depends on small-scale information, since they are usually carried out at smaller spatial scales and, furthermore, are often time-critical (Guisan et al., 2013). A well-established, direct and

quantitative link between global-scale human activities, that drive anthropogenic threats, and their local and regional effects on biodiversity can help to communicate the manifold and severe consequences of global change and thus emphasise the urgency to counteract. Therefore, a sound scientific basis for the representation and analysis of observed and expected spatio-temporal population patterns is needed and can be provided by species distribution models.

Models as a tool

Models of natural systems are an abstraction and no full representation of reality (Fig. 1.1). They isolate a set of considered phenomena to describe and leave everything else outside their system boundary (Getz et al., 2018). Deciding where exactly this boundary is meaningfully drawn requires a structural understanding of the study system and often determines whether a model can be useful. Further, profound process understanding is necessary to formulate adequate representations of the modelled processes. Incorporating too much detail can lead to overparameterisation and non-identifiability, whereas missing important aspects can restrict model flexibility to an extent where it fails to adequately reflect reality (Bell & Schlaepfer, 2016; Cabral et al., 2017). This structural and process understanding, on which model building is based, is often formulated as theories and conceptual frameworks that delineate central entities, state spaces and processes.

Niche theory

A basic framework for the modelling of species distributions is the concept of the ecological niche (MacArthur, 1968). The ecological niche defines a volume in a space spanned by a set of environmental variables in which a species occurs or can persist, respectively, depending on whether it models the realised or potential distribution (Soberón & Nakamura, 2009). The types of considered abiotic and biotic variables as well as their spatio-temporal scales, however, vary by the exact definition of the niche type (Chase & Leibold, 2009). Hutchinson (1957) introduced the notions of the fundamental and the realised niche. A refinement of this concept for species distribution modelling was proposed by Soberón (2007), who distinguishes between the Grinellian (fundamental) and Eltonian (realised) niche and their different spatial scales. The fundamental niche represents large-scale, non-interacting climatic conditions, that describe physiological limits (the bioclimatic envelope, Pearson & Dawson, 2003). The realised niche, in contrast, includes small-scale, interacting variables such as consumable resources and biotic interactions (both antagonistic and synergistic). The intersection of fundamental and realised niche, projected into geographical space, is then considered to describe the species' potential distribution.

Inferring the realised niche (and even more so, the fundamental niche) from observed

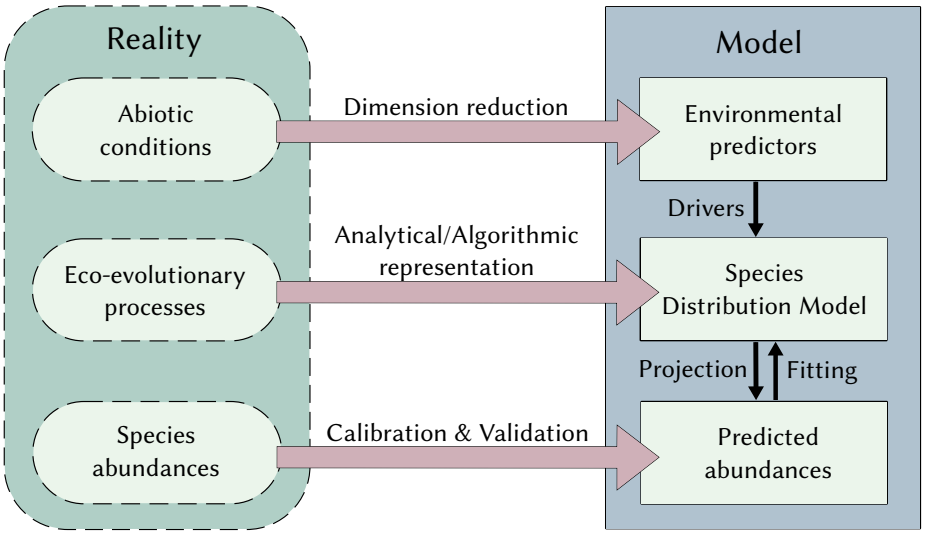

Figure 1.1.: Models as a tool to formalise reality. By selecting a set of environmental predictors, the true complexity of the causal structure is reduced to a few dimensions. The natural eco-evolutionary processes are separated into defined mechanisms with analytical or algorithmic representations. The resulting species distribution model generates predictions which are compared with the true species abundances for both calibration and validation.

occurrences in hindered by several effects (Jiménez-Valverde et al., 2008): The potential distribution is in many cases not fully occupied by a species, for example if it is still in the process of colonising suitable areas or if fundamental dispersal barriers are present (Jackson & Overpeck, 2000). Further, species can be present outside their potential distribution due to source–sink dynamics (Pulliam, 2000). Lastly, species are not always detected even tough they do occur due to imperfect detection. These effects cause a mismatch between the environmental conditions under which species are detected and their theoretic realised niche. Therefore, without further understanding of these confounding effects, the ecological niche can not be fully inferred from observed presences and absences (Sillero, 2011). As an alternative, a species' niche can be derived from ecological principles that account for combined effects of biotic and abiotic factors using mechanistic niche models (Kearney, 2006).

Avenues for species distribution modelling

A multitude of approaches to species distribution modelling has been developed to describe, understand, and predict a species' geographic distribution (Buckley et al., 2010; Dormann et al., 2012; Schurr et al., 2012; Ehrlén & W. F. Morris, 2015; Singer et al., 2016;

Fordham et al., 2018; Briscoe et al., 2019). While also spatially-implicit models exist that are useful for studying population dynamics and dispersal in patchy or fragmented landscapes (Hanski, 1994; McFarland et al., 2012), I will focus on spatially-explicit models in the following. Such distribution models are useful tools for testing ecological hypotheses, gaining insights into a species' ecology and estimating (parts of) its niche. They also have significance in conservation planning, as they are used to identify suitable sites for additional monitoring efforts or for management interventions such as area protection, habitat restoration or species reintroductions and to assess invasion potential (Guisan et al., 2013). Species distribution models (SDMs) are usually classified into correlative SDMs and process-based (or mechanistic) SDMs, although this is not a clear-cut distinction and intermediate forms exist (Dormann et al., 2012).

Correlative species distribution models

Correlative SDMs have been the standard for a long time (Araújo et al., 2019), as they work with common data types (presence-only or presence-absence data), are comparably easy to apply, and are backed by published tools and user recommendations. Depending on the context, correlative SDMs are also known as habitat suitability models, bioclimatic envelope models or ecological niche models (Araújo & Peterson, 2012). Their central method is to correlate the observed spatial distribution of a species with a number of selected environmental predictors (usually large-scale bioclimatic and land cover variables). To achieve this, many techniques exist, such as regression models and machine-learning algorithms, that differ in the shapes of relationship to fit (Guisan & Zimmermann, 2000; Elith & Leathwick, 2009). The fitted relationship is interpolated (or extrapolated) to unsampled environments and projected to geographic space in order to make predictions of past, current or future distributions. This step makes the crucial assumption that the environment is sufficiently described by the selected predictors. Therefore, predictors should be chosen which have a causal relationship with the modelled distribution. Otherwise, the fitted correlation structure is unlikely to continue into unsampled region of the predictor space, leading to low model transferability (Fourcade et al., 2018). Further, niche theory tells us that a mismatch can even arise between a causal –but incomplete– set of predictors and observed distribution, if large-scale non-interacting variables are used to describe a distribution that is shaped by additional local-scale processes such as dispersal and species interactions (Guisan & Thuiller, 2005). Another assumption made by correlative SDMs is that species distribution dynamics are quasi-stationary, that is, an equilibrium distribution is always maintained and tracked instantaneously when the environment changes. Therefore, dynamic distributions can only be implicitly described by evolving

the predictors, but transient dynamics are not representable (Araújo & Peterson, 2012). When projecting to other times or places, there is the additional risk of extrapolation error. For example, the fitted relationship may not validly extend to unsampled conditions or it may be different for other populations of the same species or change through time due to evolution and adaptation (Wiens & Graham, 2005). These limitations of correlative SDMs make them inadequate for modelling species' responses to global change, and more advanced approaches have been devised.

Process-based species distribution models

Recent years have seen an effort towards modelling species distributions more dynamically and more mechanistically with process-based SDMs (Q. Chen et al., 2011; Connolly et al., 2017; Lurgi et al., 2015; Cabral et al., 2017; Briscoe et al., 2019). Process-based (or mechanistic) SDMs aim to represent the mechanisms that underlie the formation of species distributions by explicitly formulating representations of the acting processes (Higgins et al., 2012). Urban et al. (2016) proposed six key eco-evolutionary processes that should be be considered when modelling range dynamics: (i) physiology; (ii) demography, life history, and phenology; (iii) species interactions; (iv) evolutionary potential and population differentiation; (v) dispersal, colonization, and range dynamics; and (vi) responses to environmental variation. With this integration of ecological theory and causal relationships, process-based SDMs are expected to be more readily transferable to non-analog conditions and to provide more robust predictions under extrapolation into the future or past.

Ideally, a complete model would incorporate all six eco-evolutionary processes. Since they act and interact on different ecological, spatial and temporal scales, however, this is a challenging endeavour. Currently existing models, therefore, each focus on a certain subset of processes only. For example, eco-physiological models describe the physiological responses and constraints of organisms, effectively delineating their fundamental niche (Kearney & Porter, 2009). Another example are hybrid models that supplement a correlative SDMs with selected processes (Franklin, 2010), such as local population dynamics (Keith et al., 2008), dispersal (Brotons et al., 2012; Smolik et al., 2010), or trophic interactions (Pellissier et al., 2013). Thanks to the added dynamic population model, hybrid models can represent abundance (instead of occurrence only) and transients, which makes them suitable for modelling non-equilibrium situations like species invasions or reintroductions (Gallien et al., 2010). However, they still rely heavily on the underlying correlative SDM and thus inherit their weaknesses in transferability. Another approach are dynamic range models, which directly relate environmental predictors with local demographic rates and include explicit dispersal and observer models (Schurr et al., 2012; Pagel & Schurr, 2012).

This allows to disentangle the effects of demography and dispersal, so that the species' niche can be inferred from the fitted model as the predictor-space volume for which demographic growth is positive. (Still, which part of the niche is described exactly depends on the selected predictors.) The inclusion of dispersal further allows to extract information on locations of sink and source populations (Gilroy & Edwards, 2017) and the observer component increases the ability to reflect the structure of monitoring data.

The above-mentioned model types operate principally on the population scale. They can be extended to include intra-specific trait variation and adaptation on the individual level (Moran et al., 2016) and inter-specific interaction on the community level (Pellissier et al., 2013; Kissling & Schleuning, 2015). Progress towards this scale-integration is being made by mechanistic general ecosystem models (Harfoot et al., 2014).

Process-based SDMs are still, despite their clear advantages for modelling species distributions and range shifts, much less commonly applied than correlative SDMs. There are several potential reasons for this (Briscoe et al., 2019): Process-based SDMs are usually more difficult to construct and need more programming work. Their specification can be challenging as specific ecological knowledge is required to define analytical or algorithmic process representations and certain types of data are necessary to identify the values of their process parameters. Further, less supporting resources are available for process-based SDMs than correlative SDMs, such as accessible software tools and published guidelines or workflows.

Individual-based modelling

A powerful modelling framework that can incorporate complex and interacting eco-evolutionary processes is provided by individual-based models (IBMs; Railsback & V. Grimm (2019); sometimes also called agent-based models). In a bottom-up approach, key processes like reproduction, survival, movement, and species interactions are described and evaluated at the individual level and can include stochasticity, individual behaviour, intra-specific variation, inheritance and (genetic) adaptation to local conditions (DeAngelis & Mooij, 2005). IBMs are inherently difficult to treat analytically because of the central role of interactions among the individual agents (but see Ovaskainen et al., 2014). Therefore, IBMs are usually scaled up to the population level by numerical simulation. This allows to reveal large-scale abundance patterns and investigate collective phenomena like emergence and self-organisation. IBMs thus allow for very complex, species- and case-specific formulations of a modelling problem. Examples include the host-tree selection of a pine beetle (Chubaty et al., 2009) or the complex life history of Atlantic salmon (Hedger et al., 2013), which demonstrate the vast potential for complex model building. Since IBMs have a comparably

long history (that originated from the study of cellular automata and thus dates back to the very beginning of numerical simulation) and are used in many different fields of complexity science, such as epidemiology, sociology and economics, a profound body of literature on their theory and application exists. However, the often highly case-specific nature of IBMs also means that they are usually built without the intention of application to other study systems and are thus rarely re-used, which increases the programming workload for each new model. Advances towards standardising the conceptualisation and documentation of IBMs have been made by the development of the "Overview, Design concepts, and Details" (ODD) protocol (V. Grimm et al., 2006; V. Grimm et al., 2010; V. Grimm et al., 2020). Another common problem is, that because of their high flexibility IBMs can be made arbitrarily complex. However, care must be taken to avoid including more processes than are parameterisable from available data (Manson et al., 2020).

1.3. Parametrisation and Calibration

Direct and inverse parametrisation

Fully specifying a model encompasses not only the choice of model type and structure, but also the identification of appropriate values for all model parameters. One option to achieve this is direct parametrisation, where a parameter value is directly measured from the respective isolated process. For example, a population model may include a 'fecundity' parameter that describes the number of offspring per season. This value can be obtained from experiments or observations and subsequently be used in the model. Here, process-based models have the advantage that their parameters have clear ecological meanings and can in principle be measured. In contrast, the parameters of correlative models are not accessible in this way and are thus always inferred from observed occurrences. This second option is inverse (or indirect) parametrisation and is often simply called 'model fitting'. It uses data of the response-type of the model which, in the case of species distribution models, is spatial (and temporal, for dynamic models) data of species occurrence or abundance. Most correlative models use maximum likelihood, maximum entropy, or machine learning approaches for this step, where model fit is measured by an objective function that is then optimised. The optimisation result is a point estimate, i.e. the set of parameter values that yielded the best model fit, and is often reported as is. In order to quantify its uncertainty, additional steps are necessary since no information about the relative performance of this best parametrisation is retained during the optimisation.

Bayesian calibration

An elegant framework, in which direct and inverse parametrisation are combined and quantification of parameter uncertainty is integrated, is given by Bayesian calibration (Gelman et al., 2013). In this framework, parameter specifications are expressed as probability distributions, that quantify the relative support for all possible parameter values under a given state of knowledge. The available direct knowledge on model parameters is expressed as a prior distribution. It can be understood as reflecting the state of knowledge before seeing the response data. The response data constitutes the indirect knowledge and is taken into account by the likelihood function. The likelihood measures the probability with which the model reproduces the data, given a parameterisation. The posterior distribution is then calculated via Bayes' rule and represents the support for all possible parameter values from both types of data sources, direct and indirect, combined. This approach provides a consistent quantification of parameter uncertainty which originates from the input data, is expressed in the prior and the likelihood, and propagated to the posterior via Bayes' rule.

In most applications of Bayesian inference, Bayes' rule can not be evaluated in a closed form for the whole parameter domain, either because already the likelihood can not be evaluated or because the integral in the denominator (the normalisation constant) can not be solved analytically. Instead, the posterior can be approximated by repeated sampling via Monte Carlo methods (Luengo et al., 2020). In the former case, when the likelihood function itself can not be evaluated (because it is either not known or it is intractable), so-called approximate or likelihood-free Bayesian inference is used where the sampling target is only an approximation of the true posterior (Beaumont, 2010). In the latter case, when the likelihood function is tractable but the integral in Bayes' rule can not be solved, the sampling target is the exact posterior that will be obtained in the limit of infinite sampling (so-called exact Bayesian inference). Exact Bayesian inference has been demonstrated for analytical population-based models for various ecological applications (Ellison, 2004; Gillespie & Golightly, 2010; Rosenbaum et al., 2019). For individual-based models, however, this often proves challenging as they possess intractable likelihoods due to the represented complex and stochastic processes and their hidden states (but see Johnson & Briggs, 2011). A solution to this are simulation-based methods (Hartig et al., 2011). One possibility is to define an informal likelihood that describes an error distribution and compares the IBM output with the data. The likelihood constructed in this way is usually stochastic as most IBMs are stochastic, In order to still be able to use Monte Carlo methods for sampling the posterior, pseudo-marginal methods can be employed (Andrieu & G. O. Roberts, 2009; Warne et al., 2020). They guarantee that even using an unbiased likelihood estimate,

e.g. obtained by taking the mean over repeated stoachstic likelihood evaluations, lets the Monte Carlo sample converge to the exact posterior. Simulation-based calibration methods exist for both likelihood-free calibration (e.g. an IBM for little owls; Hauenstein et al., 2019) and exact calibration (Hartig et al., 2011, e.g. an IBM for a simulated species; Kattwinkel & Reichert, 2017). In the context of Bayesian inference, adequate models are thus used to extract relevant information from monitoring data that informs process rates and, in this way, generates ecological knowledge.

1.4. In summary

Usefulness of process-based models

Reliable models of current species distributions and future range shifts are needed to forecast the effects of environmental change on biodiversity and to anticipate and mitigate biodiversity loss. Range shifts arise from the interaction of local population dynamics and dispersal. Therefore, dynamic spatially-explicit process-based population models are appropriate tools for the task. They can represent transient dynamics that arise from slow responses to rapid environmental change and they model patterns of abundance which constitute important information for spatial population assessment (Oliver et al., 2012; Yin & He, 2014). Further, models that explicitly include ecological processes are robust under extrapolation to novel conditions, because they represent fundamental mechanisms of a species' biology that are unlikely to be altered. For their mechanistic underpinnings, process-based SDMs rely on expert knowledge and ecological theory to specify the model structure and the functional representation of processes. A suitable framework for their parametrisation is given by Bayesian calibration, which provide the means to efficiently and consistently integrate heterogeneous data to inform the values of process parameters as well as their uncertainties. The efficient use of data can be decisive in ecological applications, where sparse and uncertain data sources are common. Further, the quantification of parameter uncertainty is crucial to be able to make useful predictions of future species distributions (Zylstra & Zipkin, 2021). Only if predictions include an assessment of their reliability are they trustworthy enough to be a basis for conservation planning and decision making.

Objective and structure of this thesis

The overarching objective of this thesis was to contribute to the development of tools and workflows for the application of spatially-explicit, eco-evolutionary models of species' niche dynamics that are well founded in ecological theory and provide improved forecasts

of range shifts and future distributions.

I pursued this objective within three independent articles. The first article (Chapter 2) introduced the RangeShiftR package, a software that implements an individual-based modelling platform for spatial eco-evolutionary dynamics for the widely-used statistical programming language R. I used the RangeShiftR simulation model in the subsequent two research articles to model the spatial population dynamics of Swiss breeding birds. In my second article (Chapter 3), I demonstrated how to specify, calibrate and validate the RangeShiftR IBM with heterogeneous data by the example of the Swiss red kite population. This allowed to improve estimates of the red kite's demographic rates and to identify the processes that contribute most to the currently observed population increase. In my third article (Chapter 4), I extended the RangeShiftR IBM to explicitly model demography-environment relationships that relat demographic rates (survival and fecundity) to climatic predictors. I applied this model to eight Swiss breeding birds using the modelling workflow presented in Chapter 3. With the calibrated models I created spatial assessments of climatic suitability and attributed current population trends to recent climate change. The article concludes with a discussion of the interpretations and limitations of the model. Chapter 5 of this thesis provides a synthesis of my work, a discussion of related research, and future perspectives.

List of publications

I have lead the following manuscripts that pertain to this cumulative dissertation:

- Malchow, A.-K., Bocedi, G., Palmer, S. C. F., Travis, J. M. J., and Zurell, D. (2021): „RangeShiftR: an R package for individual-based simulation of spatial eco-evolutionary dynamics and species' responses to environmental changes". *Ecography* **44.10** 1443–1452, https://doi.org/10.1111/ecog.05689.

- Malchow, A.-K., Fandos, G., Kormann, U., Grüebler, M., Kéry, M., Hartig, F., and Zurell, D. (2023): "Fitting an individual-based model of spatial population dynamics to long-term monitoring data". Revision submitted to: *Ecological Applications*. Preprint in *bioRxiv*, https://doi.org/10.1101/2022.09.26.509574.

- Malchow, A.-K., Hartig, F., Reeg, J., Kéry, M., and Zurell, D. (2023): "Demography-environment relationships improve mechanistic understanding of range dynamics under climate change". *Philosophical Transactions B* **378** 20220194, https://doi.org/10.1098/rstb.2022.0194.

I have further co-authored five publications that are relevant to the field. Their titles and abstracts can be found in Appendix A.

Chapter 2

RangeShiftR: an R package for individual-based simulation of spatial eco-evolutionary dynamics and species' responses to environmental changes

Abstract

Reliably modelling the demographic and distributional responses of a species to environmental changes can be crucial for successful conservation and management planning. Process-based models have the potential to achieve this goal, but so far they remain underused for predictions of species' distributions. Individual-based models offer the additional capability to model inter-individual variation and evolutionary dynamics and thus capture adaptive responses to environmental change.

We present RangeShiftR, an R implementation of a flexible individual-based modelling platform which simulates eco-evolutionary dynamics in a spatially explicit way. The package provides flexible and fast simulations by making the software RangeShifter available for the widely used statistical programming platform R. The package features additional auxiliary functions to support model specification and analysis of results. We provide an outline of the package's functionality, describe the underlying model structure with its main components and present a short example.

RangeShiftR offers substantial model complexity, especially for the demographic and

dispersal processes. It comes with elaborate tutorials and comprehensive documentation to facilitate learning the software and provide help at all levels. As the core code is implemented in C++, the computations are fast. The complete source code is published under a public licence, making adaptations and contributions feasible.

The RangeShiftR package facilitates the application of individual-based and mechanistic modelling to eco-evolutionary questions by operating a flexible and powerful simulation model from R. It allows effortless interoperation with existing packages to create streamlined workflows that can include data preparation, integrated model specification, and results analysis. Moreover, the implementation in R strengthens the potential for coupling RangeShiftR with other models.

2.1. Introduction

Under anthropogenic exploitation and rapid environmental changes, one of the most urgent challenges biologists face today is to understand and predict if and how species will persist, by adapting or undergoing changes in their geographic range (McGill et al., 2015; IPBES, 2019). To infer a species' niche from data and make predictions in space and time, correlative species distribution models (SDMs) are commonly used tools (Guisan & Zimmermann, 2000; Elith et al., 2008; Qiao et al., 2015). The widespread use of SDMs has been facilitated by accessible and ready-to-use software, most notably Maxent (Phillips et al., 2017) and dedicated R packages such as biomod2 (Thuiller et al., 2009) and dismo (Hijmans et al., 2017). However, these methods often incorporate little ecological theory (Guisan & Thuiller, 2005; Austin, 2007) and usually require making assumptions that are routinely violated in natural observed systems (Elith et al., 2010; Jarnevich et al., 2015; Martínez-Minaya et al., 2018). For example, SDMs assume that species are at equilibrium with their environment and ignore any transient dynamics (Zurell et al., 2016). An alternative that avoids some of these drawbacks is the development and application of process-based (or mechanistic) models, which aim to simulate relevant eco-evolutionary processes such as dispersal, demography and evolution (Urban et al., 2016; Cabral et al., 2017). Despite repeated calls for more mechanistic understanding of range dynamics (Kearney & Porter, 2009; Schurr et al., 2012; Connolly et al., 2017), such models remain underused, arguably due to challenges such as poor availability of the data needed for parametrisation and restricted accessibility to the software required to run them (Dormann et al., 2012; Briscoe et al., 2019).

The ambition for a more prominent representation of process-based models in ecological research led to the development of the standalone software RangeShifter (Bocedi et al.,

2014), a flexible individual-based model (IBM) that simulates spatial eco-evolutionary dynamics for a given species. It models population dynamics, dispersal, and evolution as interacting processes, organised within a modular structure in which each process has a number of modelling options. This makes RangeShifter a highly adaptable platform with a wide range of applications, including conducting population viability or connectivity analyses (Aben et al., 2016; Henry et al., 2017) and assessing the dynamics of genetic variation across complex landscapes. The new RangeShifter version 2.0 (Bocedi et al., 2021) adds novel features including the option for dynamic landscapes and a completely revised genetics module. Here, we present RangeShiftR version 1.0, a package that implements the RangeShifter 2.0 simulation in R (R Core Team, 2023), making it multi-platform software.

With the RangeShiftR package, we take a step towards more accessible and integrated use of mechanistic individual-based models. RangeShiftR extends the existing suite of R packages for ecological modelling, which includes software like the spatially explicit population models steps (Visintin et al., 2020) and demoniche (Nenzén et al., 2012), by a complete and flexible IBM with detailed dispersal dynamics, thus expanding the range of representable ecological levels from the population to the individual. The package augments the RangeShifter platform with functionality to assist in model specification and output visualisation. As part of the R environment, RangeShiftR offers the powerful potential to interoperate with other packages in order to form integrated workflows, drawing on the extensive functionality for data preparation, output analysis, and easy reporting that is available for R. RangeShiftR is published under the public licence GPLv3 and hence may be used, modified and shared under the terms of the GPLv3. In order to provide easy access for all users, the package includes extensive built-in documentation and comes with elaborate tutorials presented on the accompanying website (https://rangeshifter.github.io/RangeshiftR-tutorials/).

2.2. Package Structure and Implementation

The RangeShiftR package inherits its model structure from the underlying RangeShifter platform (Fig. 2.1). It models the abundance and distribution of a population of a single species by explicitly and stochastically simulating three main interacting processes – demography, dispersal, and evolution (genetics) – at the individual level. The simulation is based on a regularly gridded landscape and runs over discrete yearly or seasonal time steps. Various levels of output can be written to text files at specified time intervals during the simulation, recording data including abundance, individual traits, connectivity between patches, or dispersal paths.

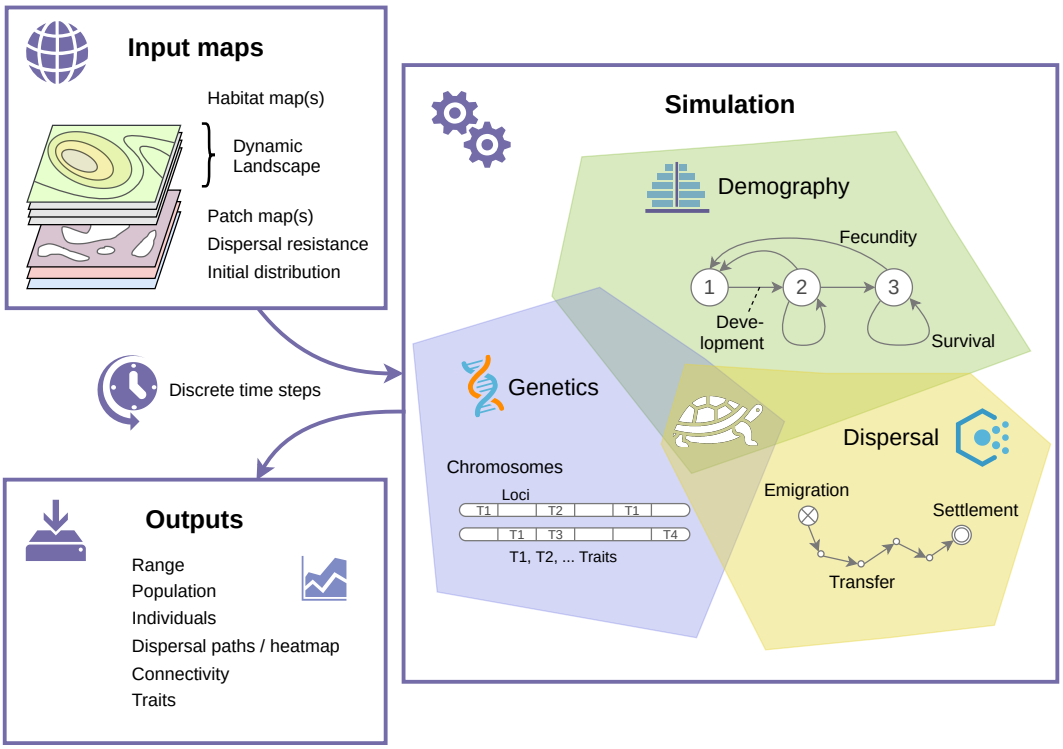

Figure 2.1.: Conceptual overview of a RangeShiftR simulation. The user provides input maps to characterise the landscape, and specifies parameter options that define the three interacting processes of demography, dispersal and evolution (genetics). One option for representing each process is symbolised here as an exemplary model configuration. For example, demography is represented using a stage-structured model with three stages. Different outputs are generated during the simulation and stored in files.

To reflect this conceptual structure, the RangeShiftR package contains a suite of functions and classes (Fig. 2.2), comprising three groups: model functions to set up the simulation, helper functions to assist with parameter specification, and output functions to process and visualise the simulation output. The helper and output functions are provided to enhance usability and constitute unique functionality of the R package not available in RangeShifter.

Model functions A RangeShiftR model is defined by the assembly of various modules, each of which is represented in R by its own class. The model functions are their corresponding class constructors: They are used to create objects that hold the given (numeric) values of all model parameters relevant to the respective module. The species model, i.e. the part of the model that describes the study species, comprises three modules

that represent the distinct simulated processes and are constructed by *Demography()*, *Dispersal()* and the optional *Genetics()*. Modules may have optional or obligatory sub-modules: demography can have a *StageStructure()*, and dispersal always comprises three phases (J. M. J. Travis et al., 2012), namely *Emigration()*, one of the '*Transfer*' sub-modules, and *Settlement()*. The '*Transfer*' class is implemented as a virtual class that can take the form of one of the three possible sub-modules *DispersalKernel()*, *SMS()* (stochastic movement simulator; Palmer et al., 2011) or *CorrRW()* (correlated random walk). The choice of the sub-modules thus determines the structure of the species model. The parameters of each model function set the corresponding model parameters, e.g. the maximum growth rate of the population, 'Rmax', in *Demography()*. Apart from the species model, there is a module that handles the input of the landscape, providing two alternative model functions for importing a raster map, *ImportedLandscape()*, or generating an artificial landscape internally, *ArtificialLandscape()*. Two more modules determine the *Initialisation()* of the simulation as well as some general *Simulation()* settings.

The choices made when selecting certain (sub-)modules and specifying their parameters collectively define a RangeShiftR simulation. However, there exists a number of interdependencies among the modules as well as certain compatibility restrictions with some options (Bocedi et al., 2014). To cover them, there is a *ParameterMaster* class whose constructor *RSsim()* takes and consolidates all components of the model and gives informative error messages or warnings to the user in case of incompatible parameter settings. An object of this class defines a RangeShiftR simulation uniquely and can optionally contain a set seed for the random number generator. Using *RunRS()* on the *ParameterMaster* runs the simulation. The set of model functions constitutes the R interface to the C++ core code, which offers the functionalities of the RangeShifter platform for use from within R while ensuring high computational performance. To integrate the C++ code, the package uses Rcpp ($\geq$ 1.0.0; Eddelbuettel et al., 2011).

The run time and memory requirements of a RangeShifter simulation can vary widely. Both depend on the number of modelled individuals as well as the represented detail. For example, simulating a movement process involves many more steps than using a dispersal kernel for the transfer phase, and including the genetics module means that the genome of each individual has to be stored. The writing of output files contributes significantly to the run time, and it is recommended to generate only necessary output.

Helper functions To aid parameter specification, RangeShiftR includes additional helper functions to estimate or visualise the effect of some parameters (Fig. 2.2). The function *plotProbs()* can be used on a demography or dispersal (sub-)module to plot the shape of

density-dependent relationships, for example the fecundity or emigration probability. Most modules in a RangeShiftR simulation influence each other either directly or indirectly, and certain parameters may have implications in various places. Therefore, it can prove challenging to express knowledge about the system by directly specifying separate numerical parameter values. For example, specifying a stage-structured demographic model requires estimates for at least one parameter that determines the nature of density-dependence in survival or fecundity. We typically will not have a direct estimate for that parameter, but are much more likely to have an estimate of overall carrying capacity or equilibrium density, which in the model is an emergent outcome of all the demographic parameters. Thus, to guide the choice of suitable parameter values, RangeShiftR contains the novel function *getLocalisedEquilPop()* to estimate the combined effect of density-dependent population dynamics on a closed population (cf. example below). Finally, the function *validateRSparams()* can be used on any (sub-)module to check if all parameters are set within their admissible ranges.

Output functions All simulation output is written to text files in the formats provided by the RangeShifter platform. The RangeShiftR package also includes dedicated output functions that facilitate the inspection of these results by processing and visualising the output files. These include *plotOcc()* and *plotAbund()* to show the simulated time series of occupancy and abundance, *ColonisationsStats()* for the computation of spatial statistics such as the occupancy probability and the time to colonisation, and *SMSpathLengths()* to display the distribution of dispersal path lengths. A novel output option is provided by the creation of dispersal heatmaps for SMS in the form of raster files, which show the number of dispersers that passed through each location and can be readily processed and plotted with R. Some output functions use basic functionality from the raster package ($\geq$ 3.0.0; Hijmans & Etten, 2016) to generate and plot maps. All documentation pages use Rdpack ($\geq$ 0.7) to include references.

2.3. Simulation Modules

In the modular structure of RangeShiftR, each module represents a different aspect of the simulation (Fig. 2.2), allowing for adaptable levels of model complexity. Below, the main modules are described briefly. For comprehensive documentation, covering all parameters and options, we refer to the package documentation and the RangeShifter manual (Bocedi et al. (2014) and Bocedi et al. (2021) https://rangeshifter.github.io).

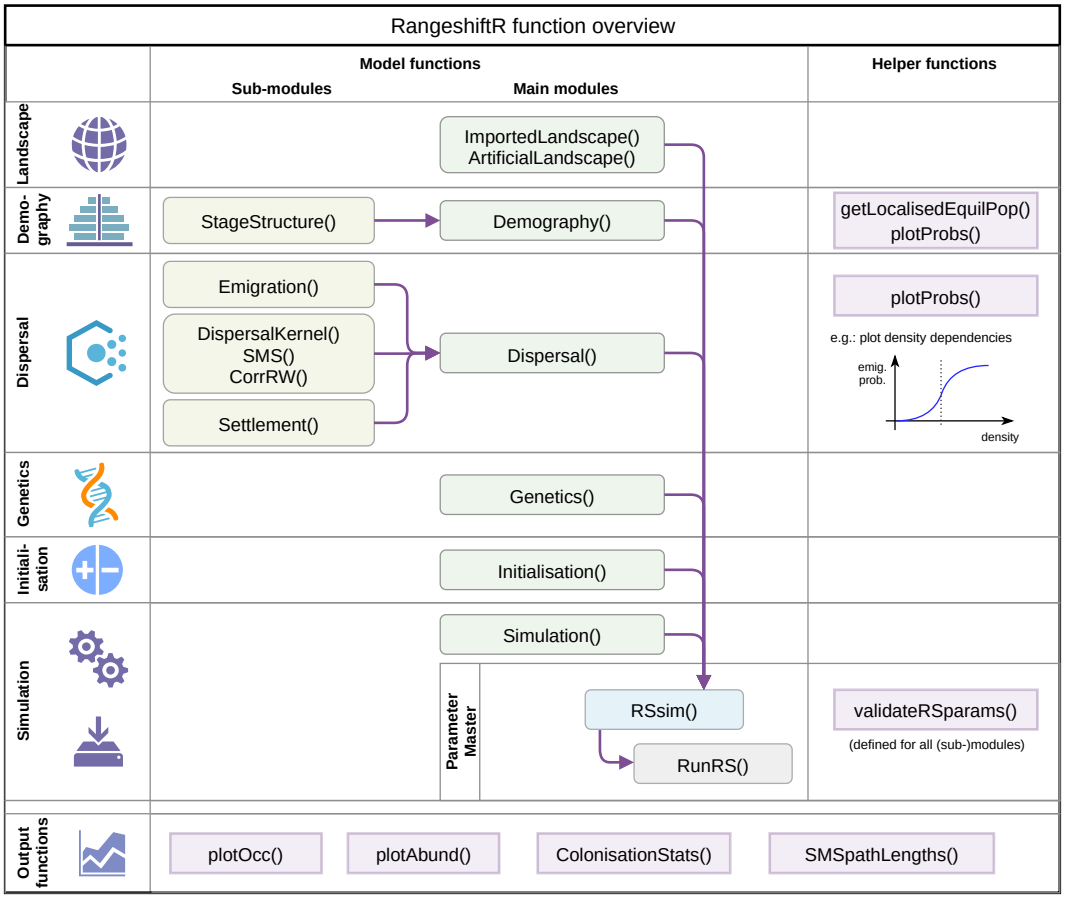

Figure 2.2.: RangeShiftR function overview. The first column introduces the various modules with their respective icons, as reference to Fig. 2.1. The rounded boxes and arrows in columns 2 and 3 indicate model functions and their respective hierarchical relations. They are class constructors used to define the sub-modules (column 2, yellow) and main modules (column 3, green), which can be combined to a parameter master (blue) to compose the RangeShiftR model. The function RunRS (grey) then starts the simulation. The angled boxes in the last column indicate helper functions that are related to their respective modules. The angled boxes in the bottom row are separate from the columns and itemise the output functions that can be used for processing the simulation results.

Landscape A RangeShiftR simulation runs on a cartesian grid in which each cell holds information about its cover. This is described by a single layer that represents cells of either a land class or a habitat quality score ranging from zero to 100%. To relate this layer to a cell's habitat suitability for the study species, a value for its demographic density-dependence must be provided: either one for each land class or that for a 100% habitat cell.

There are two variants of the landscape module: Usually, the landscape map will be imported from an ASCII raster file but it can also be artificially created by a built-in function. Imported landscapes have additional options: they can be patch-based, in which case a second raster file is required to indicate each cell's patch ID. Additionally, a raster of dispersal resistance values and a presence-absence raster of the initial distribution can be loaded. With the new functionality of dynamic landscapes introduced in RangeShifter 2.0, the cover, patch and dispersal resistance layer can be changed at any given year during the simulation.

Demography The modelled demography is determined by two main choices: Firstly, the population can have overlapping or non-overlapping generations, meaning it can be stage-structured or not. In the former case, the sub-processes fecundity, survival and development are explicitly simulated each year, whereas in the latter case only fecundity is modelled. Depending on this choice, the value of the demographic density-dependence defined in the landscape module is interpreted differently: for a stage-structured population it represents the strength of demographic density-dependence ($1/b$), which can act on all three sub-processes, while for a non-structured population it is interpreted as the carrying capacity (K). A stage-structure is an optional sub-module that is represented by its own class and that can be added to the demography module and which allows various parameters in the demography and dispersal modules to be stage-specific. Secondly, the population can be modelled as sexual or asexual. In sexual models, individuals are characterised by their sex so that various parameters can be sex-specific and the reproductive dynamics may include an explicit mating system. Asexual models can be applied to asexually reproducing species or to species for which only the female sex is modelled as they are assumed to be the limiting sex for the demographic or spatial dynamics.

Dispersal The dispersal module has three obligatory sub-modules, which represent the explicitly modelled phases of dispersal (J. M. J. Travis et al., 2012). The first phase is emigration, in which an individual decides whether to leave its natal cell or patch. During the subsequent transfer phase the individual moves through the landscape, which can

be simulated by three alternative methods: either with a dispersal kernel or with explicit consideration of the movement processes using the stochastic movement simulator (SMS; Palmer et al., 2011) or a correlated random walk. The dispersal event is concluded with the settlement phase, when the individual stops in a different habitable cell or patch. Individuals are allowed to disperse only once during their lives. Various dispersal attributes can be, if applicable, sex- and stage-specific, and the emigration and settlement probabilities can additionally be density-dependent (using the value for demographic density-dependence given in the landscape module). The modelling options for the settlement decision depend on the chosen transfer method and may include an option of mate finding.

Genetics Individuals can carry a genome that they inherit from their parent(s) at birth. The genome may consist of multiple autosomal loci that can either be neutral or coding for traits (Bocedi et al., 2021). Currently, only the dispersal parameters can be treated as heritable traits, which allows evolution of dispersal strategies. The genetic architecture is highly flexible and processes such as recombination, mutation and pleiotropy can be explicitly modelled. Modelling of neutral loci allows explicit and individual-based population genetic simulations to address questions on how environmental features and processes, in interaction with population dynamics and dispersal behaviours, shape the genetic structure and diversity of populations (Manel et al., 2003).

Initialisation The initial state of the simulation in the starting year can be defined in three different ways: with an initial distribution map specified in the landscape module, with a list of individuals and their location, or at a given population density in randomly selected locations.

Simulation This module specifies the general simulation settings like the number of simulated time steps (years) and replicates, the types of generated output, and some more specialised options, such as imposing a (shifting) gradient or enabling environmental stochasticity.

2.4. Using RangeShiftR

The RangeShiftR 1.0 package can be readily installed from the github repository 'RangeShifter/RangeShiftR-package'. As a widely applicable simulation software, RangeShiftR aims to provide easy access via a range of resources to support the user: all functions are comprehensively documented on R help pages, an extensive user manual is available online,

and the webpage (https://rangeshifter.github.io) features a support forum as well as a collection of detailed tutorials that illustrate the model's scope and introduce the available modelling options. The tutorials include adaptations of the three original RangeShifter examples (Bocedi et al., 2014), accompanied by sample code for analysis and visualisation. Additionally, we provide a fourth tutorial that demonstrates novel features of RangeShifter 2.0 (Bocedi et al., 2021) by simulating the range dynamics of a species in a changing landscape. Here, we present a shortened form of this fourth tutorial as an example to introduce the RangeShiftR syntax. All required input files can be found on our webpage or downloaded directly via https://rangeshifter.github.io/RangeshiftR-tutorials/files/Tutorial3_Inputs.zip.

Landscape When using the novel RangeShifter feature of dynamic landscapes, we specify the file names of the changing habitat maps, their corresponding patch files, and the order of years in which these become effective. All maps are imported as ASCII rasters by the function *ImportedLandscape()*. Further arguments are the (optional) map of initial distribution, the number of land cover types 'Nhabitats', as well as their respective demographic density-dependence 'K_or_DensDep'.

```
landnames <- c( "map_01.asc",
                "map_02.asc",
                "map_03.asc",
                "map_04.asc")

pchs <- c( "patches_01.asc",
           "patches_02.asc",
           "patches_03.asc",
           "patches_03.asc")

land <- ImportedLandscape( LandscapeFile = landnames,
                           PatchFile = pchs,
                           DynamicLandYears = c(0, 80, 110, 140),
                           SpDistFile = "init_dist.asc",
                           Nhabitats = 5,
                           Resolution = 10,
                           K_or_DensDep = c(125, 0, 150, 75, 0),
                           SpDistResolution = 10)
```

Demography The population model is set up to use explicit sexes and a stage-structure, i.e. generations are overlapping. In the *Demography()* module the coded argument 'ReproductionType' determines whether both sexes are modelled. The *StageStructure()* sub-module takes the transition matrix and can set optional density-dependencies on the sub-processes of fecundity, survival and development.

```
TraMa <- matrix( c( 0.0, 0.0, 0.0, 5.0 ,
                    1.0, 0.1, 0.0, 0.0 ,
                    0.0, 0.6, 0.2, 0.0 ,
                    0.0, 0.0, 0.45, 0.85),
                  ncol = 4, byrow = TRUE)
demog <- Demography( ReproductionType = 1,
                     StageStruct = StageStructure(
                                   Stages = 4,
                                   TransMatrix = TraMa,
                                   FecDensDep = T,
                                   SurvDensDep = T,
                                   SurvDensCoeff = 0.4) )
```

The helper function *getLocalisedEquilPop()* can assist in understanding how the demographic rates set in the demography module and the local density-dependence ($1/b$) affect the simulated abundances:

```
getLocalisedEquilPop( demog = demog,
                      DensDep_values = seq(50, 300, 50))
```

It simulates a time series of the population density (in individuals per hectare) of a single closed population for varying values of $1/b$ (given by 'DensDep_values'). This is achieved by repeated matrix multiplication with the density-dependent transition matrix until an equilibrium is reached. The function returns these equilibrium densities by stages at the given density-dependence values and generates a bar graph (Fig. 2.3a). The generated densities approximate the equilibrium densities of a closed patch in the RangeShiftR simulation, and can thus be used to guide the choice of the parameter $1/b$. However, the matrix approach neglects stochasticity, the scheduling of survival and reproduction, and the integer units of abundance, so that the quality of the estimate is lower for smaller populations.

Dispersal The three phases of dispersal are first defined independently as sub-modules before assembling them in the dispersal module. In the *Emigration()* sub-module, the emigration probability is modelled as stage- and density-dependent, therefore we provide a matrix with one row per stage containing three parameters each, which define how emigration probability relates to population density:

```
emig <- Emigration( StageDep = T,
                    DensDep = T,
                    EmigProb = cbind(0:3, c(0.55,0.45,0,0),
                                          c(5,5,0,0),
                                          c(1,1,0,0) ))
```

The transition phase uses *SMS()* as a method. It implements a step-wise process which is defined by the directional persistence ('DP') and size of memory ('MemSize'). Additionally, we set a dispersal bias (second line) that describes the strength and decay of an additional bias to move away from the original patch, as well as habitat-specific dispersal resistances and a constant per-step mortality:

```
tran <- SMS( DP = 1.8,
             MemSize = 4,
             GoalType = 2,
             GoalBias = 2.5,
             AlphaDB = 0.4,
             BetaDB = 10,
             Costs = c(3, 5, 1, 2, 30),
             StepMort = 0.01)
```

The *Settlement()* sub-module defines the minimum and maximum number of steps permitted and sets the mate-finding requirement:

```
sett <- Settlement( MinSteps = 15,
                    MaxSteps = 80,
                    MaxStepsYear = 20,
                    FindMate = T)
```

Now, the previously defined sub-modules can be combined in the *Dispersal()* module:

```
disp <- Dispersal( Emigration = emig,
                   Transfer = tran,
                   Settlement = sett)
```

Genetics The *Genetics()* module is optional and we leave it disabled here (but see Bocedi et al. (2021) and the online tutorials for an example of this functionality). Although this implies missing inter-individual variation in dispersal traits in our example, individuals are still characterised by their sex, stage and age, which can affect some demographic and dispersal attributes.

Initialisation The function *Initialisation()* uses mostly coded arguments to define the spatial distribution and density of the initial population. The simulation in this example is initialised in all locations indicated by the initial distribution map (provided to the landscape module) at the density given in 'IndsHaCell'. Further, the stage- and age-distributions of the initial population are set.

```
init <- Initialise( InitType = 1,
                    SpType = 0,
                    InitDens = 2,
                    IndsHaCell = 75,
```

```
                        PropStages = c(0, 0.6, 0.2, 0.2),
                        InitAge = 2)
```

Simulation The *Simulation()* runs for 200 years and over twenty replicates. The population, range and SMS paths outputs are enabled and will be generated at the given time intervals:

```
simul <- Simulation( Years = 200,
                     Replicates = 20,
                     OutIntPop = 5,
                     OutIntRange = 5)
```

Model run and results All defined model components are combined into the parameter master with *RSsim()*, which optionally takes a seed to pass to the random number generator and make the simulation reproducible. Every RangeShiftR simulation is defined by an instance of this class and the path to its directory and is run using *RunRS()*:

```
s <- RSsim( land = land,
            demog = demog,
            dispersal = disp,
            init = init,
            simul = simul,
            seed = 123456 )
dirpath <- "RS_example/"
RunRS(s, dirpath = dirpath)
```

The simulation output is written to text files in the 'Outputs' folder of the directory. These can be further processed and visualised using the auxiliary output functions. For example Fig. 2.3b shows a result that is returned by the function *ColonisationStats()*. It calculates the time to colonisation and the occupancy probability at given years and can map the values onto the landscape:

```
col <- ColonisationStats(s, dirpath, maps=T)
raster::plot(col$map_col_time)
```

In the resulting plot, the non-suitable landscape matrix appears grey and all habitat patches are coloured according to their averaged time to colonisation over all replicates. In this example, smaller patches tend to get colonised later than larger ones.

2.5. Discussion

RangeShiftR 1.0 provides, for the first time, an open-source individual-based, eco-evolutionary simulation platform in R, which includes a diversity of processes and offers various levels

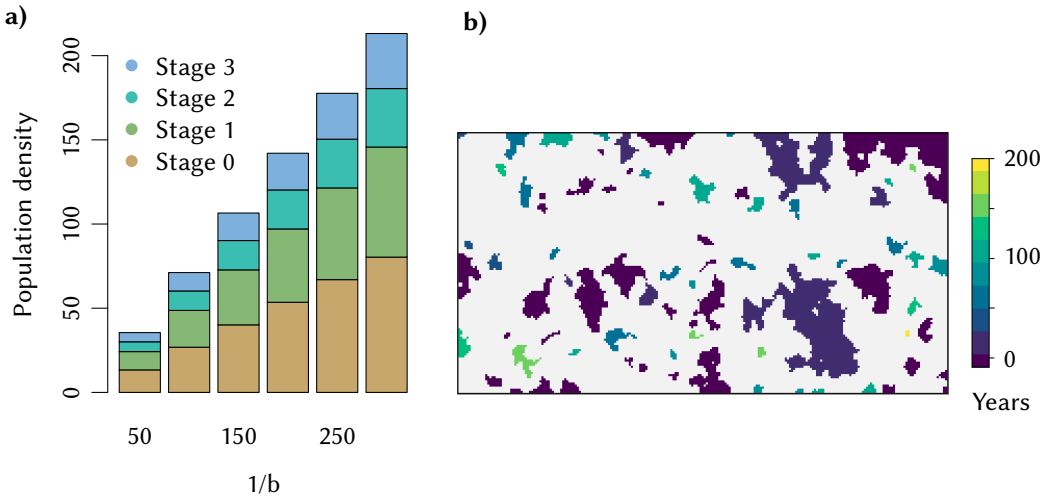

Figure 2.3.: RangeShiftR example. (a) Bar graph generated by the helper function *getLocalisedEquilPop()*, showing the localised equilibrium densities classified by stages over the parameter 1/b (both in units of Inds/ha). They serve as a quick approximation to assess the effect of density-dependent demographic rates. (b) Raster generated by the output function *ColonisationStats()*, showing the average time to colonisation.

of complexity, especially for the demographic and dispersal processes. It gives access to the established RangeShifter platform (Bocedi et al., 2014; Bocedi et al., 2021), adds supporting functionality for model specification and analysis in R, and provides comprehensive documentation to guide the user.

RangeShiftR complements the existing toolbox of R packages, as it offers some important features that have not been available so far. Existing R implementations of spatially-explicit population modelling frameworks, such as the recently published package steps (Visintin et al., 2020) or the demoniche package (Nenzén et al., 2012), are population-based. In contrast, RangeShiftR is individual-based and hence allows for an explicit representation of genetics and evolutionary dynamics. The package vortexR (Pacioni & Mayer, 2017) implements post-analysis functions for the prominent, spatially-implicit, Vortex model (Lacy, 1993) that is also individual-based and commonly applied for population viability analysis (PVA). Here, RangeShiftR provides a useful alternative that allows conducting spatially-explicit PVA under more complex dispersal assumptions.

The RangeShifter GUI (Bocedi et al., 2014; Bocedi et al., 2021) and the RangeShiftR package constitute two complementary entities, as they represent alternative interfaces

to the same software core. The GUI version offers an intuitive handling of the model and visual tracking of simulation outcomes, making it particularly suited for the use by stakeholders or for undergraduate education. The RangeShiftR package, on the other hand, is especially useful for research purposes. It offers transparent, reproducible workflows, as the entire simulation can be scripted in R, along with the visualisation and post-analysis of simulation results. This also facilitates large-scale parameter comparisons, as required in sensitivity and robustness analyses. The use of Rcpp (Eddelbuettel et al., 2011) allows running of the simulation in a C++ module and thereby yields high performance, while the integration in R makes RangeShiftR available for multiple platforms and provides the infrastructure for parallel and cluster computing without having to adapt the C++ back end.

RangeShiftR holds many opportunities for interoperation with other R packages. Firstly, it can be readily integrated with packages for describing the landscape context (e.g. raster; Hijmans & Etten, 2016) or species distribution modelling (e.g. biomod2; Thuiller et al., 2009, sdm; Naimi & Araújo, 2016). Secondly, it permits coupling of different model types, as exemplified by coupling RangeShifter with the land-use model CRAFTY (Murray-Rust et al., 2014; Synes et al., 2019). Thirdly, it enables integrated use with existing methodological devices, like inverse parameterisation through Bayesian inference, for example using the package BayesianTools (Hartig et al., 2019).

RangeShiftR can help overcome some of the challenges that have prevented more widespread use of mechanistic range models (Briscoe et al., 2019) by offering high accessibility. In the future, we plan to enhance the platform further to improve forecasts under global change. For example, the model currently operates on a single habitat layer that contains either land classes or habitat quality. Therefore, demographic rates are related to the environment only indirectly via the user-defined carrying capacities or density-dependence coefficients. Further, all density-dependent relationships have a predetermined shape that is controlled by specified parameters but cannot be replaced by a user-specified function. Moreover, RangeShiftR currently models only a single species and does not incorporate species interactions. Lastly, the genetics module is currently restricted to modelling evolution of dispersal traits while demographic traits cannot evolve. Thus, potential future extensions of the platform will involve explicitly modelling demography-environment relationships (Pagel & Schurr, 2012) species interactions, and genetic evolution of demographic traits. As the code is open source, there is now an opportunity for a broad community of researchers and modellers to contribute to representing these important processes in future versions of the platform.

The RangeShiftR package constitutes an important step towards making frameworks

for modelling range dynamics under global change accessible to a wider audience (Schurr et al., 2012; Lurgi et al., 2015; Zurell et al., 2016). We hope that this will inspire a more widespread use of mechanistic distribution models, for example to guide conservation efforts and ecosystem management, and facilitate more seamless integration with other modelling tools.

Chapter 3

Fitting an individual-based model of spatial population dynamics to long-term monitoring data

3.1. Abstract

Generating spatial predictions of species distribution is a central task for research and policy. Among the currently most widely used tools for this purpose are correlative species distribution models (cSDMs). Their basic assumption of a species distribution in equilibrium with its environment, however, is rarely met in real data and prevents dynamic projections. Process-based, dynamic SDMs (dSDMs) promise to overcome these limitations as they explicitly represent transient dynamics and enhance spatio-temporal transferability. Software tools for implementing dSDMs become increasingly available, yet their parameterisation can be complex.

Here, we test the feasibility of calibrating and validating a dSDM using long-term monitoring data of Swiss red kites (*Milvus milvus*). This population has shown strong increases in abundance and a progressive range expansion over the last decades, indicating a non-equilibrium situation. We construct an individual-based model with the RangeShiftR modelling platform and calibrate it using Bayesian inference. This allows the integration of heterogeneous data sources, such as parameter estimates from published literature and observational data from monitoring schemes, and consistent quantification of parameter uncertainties. Our monitoring data encompass counts of breeding pairs at 267 sites across Switzerland over an annual time series of 22 years. We validate our model using a spatial-block cross-validation scheme and assess predictive performance with a rank-correlation

coefficient.

Our model showed very good and excellent predictive accuracy of spatial and temporal projections, respectively, well representing the observed population dynamics over the last two decades. Results suggest that reproductive success was the most decisive factor driving the observed range expansion. According to our model, the Swiss red kite population fills large parts of its current range but has potential for further density increases.

With our case study we demonstrate the practicality of data integration and validation for dSDMs using available tools. This approach can improve predictive performance compared to cSDMs. The workflow exemplified here can be adopted for any population for which prior knowledge on demographic and dispersal parameters as well as spatio-temporal observations of abundance or occupancy are available. The resulting calibrated model provides refined insights into the ecology of a species and its predictions can inform conservation and management.

3.2. Introduction

In response to multiple anthropogenic pressures and environmental shifts, the abundance and distribution of many species are changing (Selwood et al., 2015; Newbold et al., 2015; Díaz et al., 2019). Negatively affected populations can potentially be stabilised or even recovered through targeted and effective conservation measures (Hoffmann et al., 2010; Bolam et al., 2021; Duarte et al., 2020). But also expanding populations may be in the focus of conservation interest, for example when exploring scenarios of future threats or evaluating the invasive potential of a species (Thompson et al., 2021). The basis for efficient conservation planning thus lies in reliable knowledge about the spatio-temporal patterns of abundances and the expected effects of conservation measures (Guisan et al., 2013; Zurell et al., 2022).

Various approaches have been developed for spatially-explicit population modelling, ranging from purely correlative to detailed mechanistic species distribution models (SDMs; Dormann et al., 2012; Guisan et al., 2013). Currently, most spatial model assessments for conservation planning are based on projections of correlative SDMs (cSDMs) (Franklin, 2013; Zurell et al., 2022), that statistically relate species occurrences to environmental predictors (Elith & Leathwick, 2009). This class of models can achieve high flexibility and may be readily fitted to available occurrence data, but their geographical and temporal transferability is limited (Araújo & Peterson, 2012; Wenger & Olden, 2012). They further provide only stationary or time-implicit predictions, which rely on the assumption that the observed distribution is in equilibrium with its environment (Guisan & Thuiller, 2005).

However, this assumption is commonly violated in conservation-relevant cases such as invasive species, reintroduction programs, or threatened populations that are subjected to ongoing environmental change. This leads to inaccurate predictions because the true species distribution is actually transient and thus dependent on time and history (Santos et al., 2020; Watts et al., 2020; Semper-Pascual et al., 2021).

This dynamic nature of spatial abundance patterns is recognized in dynamic spatially-explicit process-based SDMs (hereafter called dSDMs). They understand present species distributions and abundances as the result of the effects and interplay of a number of eco-evolutionary processes (Urban et al., 2016). dSDMs include an explicit description of at least one of these processes to model spatio-temporal and potentially transient population dynamics. Examples include representations of local population dynamics (Keith et al., 2008; Barber-O'Malley et al., 2022) and limiting processes like dispersal (Risk et al., 2011; Broms et al., 2016; Smolik et al., 2010), physiology (Rodríguez et al., 2019), or species interactions (Schweiger et al., 2012; Pellissier et al., 2013). Further, dSDMs often include stochastic elements to account for processes not explicitly described by the model. Thanks to the integration of ecological theory, dSDMs are expected to provide more accurate predictions under extrapolation and thus to be more readily transferable to non-analog conditions than cSDMs (Gallien et al., 2010).

The application of a dSDM requires its specification and validation (Schmolke et al., 2010). Fully specifying a dSDM includes two main steps, both of which require distinct types of knowledge about the population of interest (Singer et al., 2018; Fig. 3.1). First, in the model building step, the model structure and the functional description of the relevant processes are established. They are usually chosen based on ecological theory and expert opinion. Second, in the parameterisation step, the numeric values of all process rates, such as demographic and dispersal rates, are determined by direct or inverse (indirect) parameterisation or a combination of both. Direct parameterisation uses estimates of process parameters based on data collected in the field or from experiments. Conversely, inverse parameterisation is based on spatio-temporal observations of the modelled response variables, typically abundance or occurrence. To make efficient use of all sources of information and combine direct and inverse parameterisation, a Bayesian calibration framework can be employed. In this, the direct parameterisation and its uncertainty are expressed as prior distributions. The prior is updated via Bayes' rule using a likelihood, that measures how well a given set of parameter values is able to reproduce the observed response data. This updated prior yields the posterior distribution. The procedure thus identifies parameterisations that are consolidated with the data and can generate new knowledge on the studied population, as prior estimates of process parameters are cor-

rected and their uncertainty may be reduced. This approach further allows the consistent propagation of uncertainty from the data sources through to model predictions (Hartig et al., 2012; Marion et al., 2012; Jaatinen et al., 2021). The predictive performance of the specified model is then assessed in the validation step. For this, the model is evaluated on a set of testing data that, preferably, is independent of the training data. A way to generate the training and testing data are cross-validation schemes that partition the full data set in a prescribed way, e.g. in leave-p-out or k-fold cross-validations (Arlot & Celisse, 2010). The final, validated model can be used to generate projections to other times or places and to compare alternative management scenarios (Bleyhl et al., 2021).

To date, the widespread use of dSDMs for conservation applications has been hampered by technical challenges with respect to their parameterisation and validation (Briscoe et al., 2019). With the proliferation of novel methods for the various model building steps, software tools are being developed that assist their case-specific implementation. In R, these are available as packages for building different types of complex dSDMs (Visintin et al., 2020; Malchow et al., 2021; Fordham et al., 2021; Moulin et al., 2021; Landguth et al., 2017; Hagen et al., 2021), for model calibration (Hartig et al., 2019; Csilléry et al., 2012), and for cross-validation (Valavi et al., 2019). However, their combined application in integrated modelling workflows is still demanding and rarely undertaken.

In this study, we present a complete calibration and validation workflow for dSDMs, utilising heterogeneous data for direct and indirect parameterisation. As a case study, we modelled the Swiss population of red kite (*Milvus milvus*). This population has a highly dynamic and volatile history that has seen accelerating increases in recent decades (Aebischer & Scherler, 2021), rendering a dynamic modelling approach adequate. We first built a dSDM with the individual-based modelling (IBM) platform RangeShiftR, that explicitly simulates the processes of population dynamics and dispersal (Malchow et al., 2021). Then, its process parameters were directly parameterised using published literature data. This direct parameterisation was subsequently updated by integrating information from long-term, structured survey data using Bayesian inference with BayesianTools (Hartig et al., 2019). Finally, the predictive performance of the calibrated model was evaluated by cross-validation on spatially-blocked data folds (D. R. Roberts et al., 2017). To test our workflow, we investigated whether the calibration could successfully inform parameter estimates and which process parameters were most sensitive to the survey data. Comparing the prior and posterior predictions of our model, we assessed if the calibration considerably improved model fit and reduced uncertainty. Predictive performance of the fitted model was evaluated in spatial-block cross-validation and compared to a comparable cSDM. Lastly, the calibrated model was used to explore the potential population size and

distribution of red kite in Switzerland.

The presented workflow (Fig. 3.1) is intended to guide the application of complex dSDMs to populations that exhibits variable dynamics and for which suitable data sources for direct and inverse parameterisation are available. It is suited for linking process-based models with monitoring data to obtain a solid quantitative basis for management decisions while being explicit about involved uncertainties (Zylstra & Zipkin, 2021).

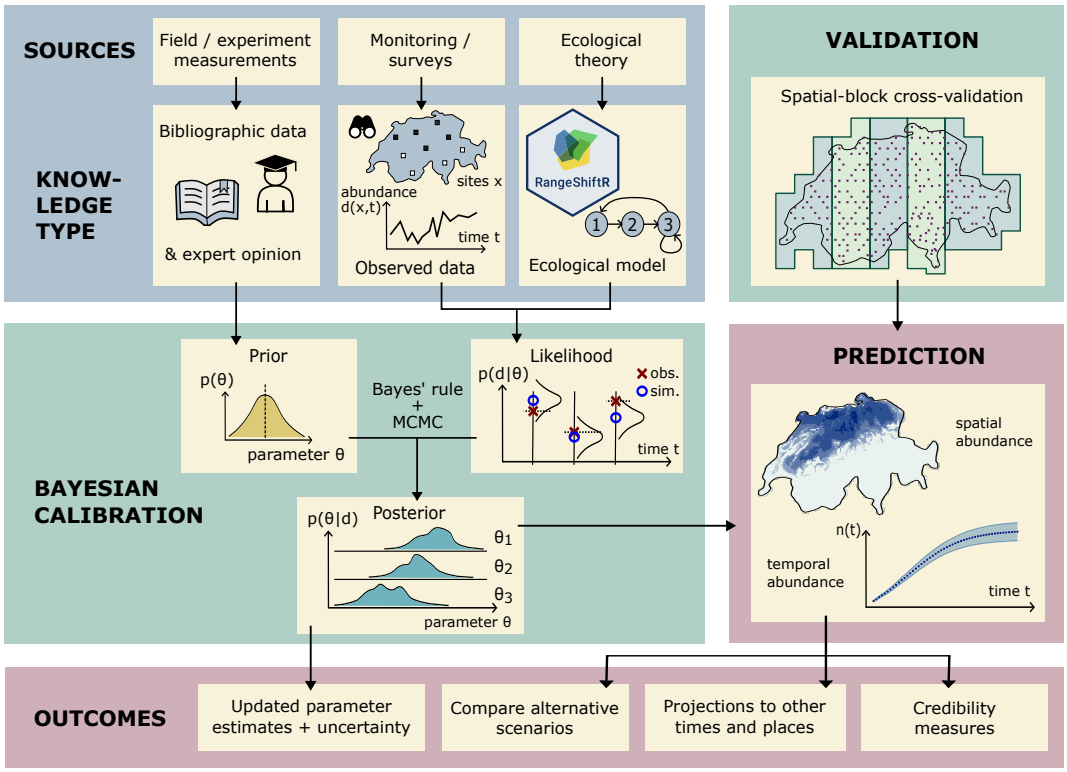

Figure 3.1.: Calibration and validation workflow for process-based, dynamic species distribution models. Different types of knowledge are needed to specify the model structure and parameterisation. Their direct specification can be informed from literature data, expert opinion, and ecological theory. In a calibration, the direct knowledge on model parameters is combined with observations of the model's response quantity. In a Bayesian inference, for example, this is done via the likelihood function. For cross-validation, the calibration is repeated for different subsets of data, using the held-out data to measure predictive performance. Various outcomes can be derived, both from the posterior distribution directly and from model projections.

3.3. Materials and Methods

3.3.1. Data

An overview of all data sources and their use in the modelling process is given in Table B.2. We utilised two sources of monitoring data of the red kite across Switzerland: the Swiss breeding bird atlas that provides snapshot data from two periods (1993-1996, Schmid et al. (1998); and 2013-2016, Knaus et al. (2018)) and the Swiss breeding bird survey (MHB, Schmid et al., 2004) that provides abundance time series for the years 1999-2019. Both schemes are based on so-called simplified territory mapping of representative 1 km^2 squares across Switzerland and record the number of observed breeding pairs during two to three repeat surveys per year along a fixed survey route in each square (Schmid et al., 2004). The Atlas survey data used here included 2318 sites, each of which is sampled in one year within each five-year period. The MHB survey includes 267 sites (1 km^2 sampling quadrats) laid out across Switzerland in a regular grid, which are sampled yearly since 1999. Further, we used land cover and bioclimatic data as environmental predictors. Land cover was represented with the CORINE Land Cover (European Union, 2022) classification (44 classes), obtained for the years 2000, 2006, 2012, and 2018 at a spatial resolution of 100 m. Climate was represented by the nineteen WorldClim bioclimatic variables. We used averaged annual values from the time period 1979–2013 with a spatial resolution of 30 arcsec ($\approx$ 1 km) obtained from CHELSA Bioclim v1.2 (Karger et al., 2017; Karger et al., 2018b).

3.3.2. Modelling

Our dSDM comprised two components, that are detailed in the following section: (1) a static habitat model that describes the habitat suitability in each year over the study region, and (2) a mechanistic individual-based model (IBM; Railsback & V. Grimm, 2019) that describes the population and range dynamics. IBMs use a bottom-up approach in which key processes are formulated at the individual level and are scaled up to the population level by numerical simulation (DeAngelis & Mooij, 2005). All analyses were conducted using the statistical programming language R (R Core Team, 2023).

Habitat suitability of the Swiss landscape

Habitat suitability was derived from a cSDM based on presence-absence data generated from the second atlas (2013-'16) data set. Because the red kite has been expanding its range in Switzerland during the past 30 years, this most recent data best reflects the underlying habitat requirements. For the cSDM, we assumed that most suitable habitats are already occupied even though they may not have reached their potential capacities yet. The red

kite is a generalist and opportunistic raptor that breeds in a wide range of climates and habitats. Typical nesting habitat consists of forest patches with suitable roosting sites and open areas like grassland or agricultural fields that provide prey, which mostly consists of small mammals. Food sources like open waste dumps and carrion are readily exploited if present. To represent the availability of resources relevant for the occurrence of red kites, we used the CORINE 2012 land cover data and aggregated its 44 classes to seven land cover types (Table B.1). To represent climatic influences, all nineteen Bioclim variables were included (Table B.3). Since the red kite requires different habitats for nesting and foraging, it is a highly mobile species and occupies breeding home range sizes of about 4 to 5 km^2 for males (Baucks, 2018; Nachtigall, 2008). To allow the cSDM to consider the diversity of habitat types, we used a grid cell size of 4 km^2. Since the IBM was based on the same grid, this also constitutes a trade-off between the abilities to resolve both the effects of density-dependence on the one hand and dispersal displacements on the other hand. The high-resolution land cover data was aggregated to the target resolution of 2 km by calculating the proportional land cover in each cell. The bioclimatic data was coarsened to the 2 km-resolution by bi-linear interpolation between the grid cells.

To fit the cSDM habitat model, we first selected predictors from all land-cover and bioclimatic variables based on their univariate importance (assessed by the AIC of linear models with second-order polynomials) under the constraint that pairwise Spearman correlation must not exceed 0.7 (Dormann et al., 2013). The variables selected are labelled with an asterisk in Tables B.1 and B.3. We then created an ensemble cSDM by taking the mean occurrence probability predicted by four different algorithms: binomial linear model with second-order polynomials and step-wise variable selection; binomial additive model with splines; random forest; and boosted regression trees. The predicted probabilities are subsequently interpreted as a habitat suitability index (HSI). The ensemble cSDM was then projected to Switzerland and a 12 km buffer around its border in the years 2000, 2006, 2012, and 2018, with varying land-cover data and constant bioclimatic variables. Climate was kept constant because it was considered only a minor driver of change in resource availability over the study period. The buffer was applied to reduce potential boundary effects in the IBM simulations. It was large enough to capture most dispersal events in the Swiss population. For all other years in the period of 1999-2019, the HSI values were linearly interpolated. To distinguish between habitat and non-habitat cells, we derived a binarisation threshold ($\widehat{\mathrm{HSI}}$ =0.51) as the value yielding equal sensitivity and specificity ($\approx$ 90%) and considered all cells with lower HSI values non-habitat.

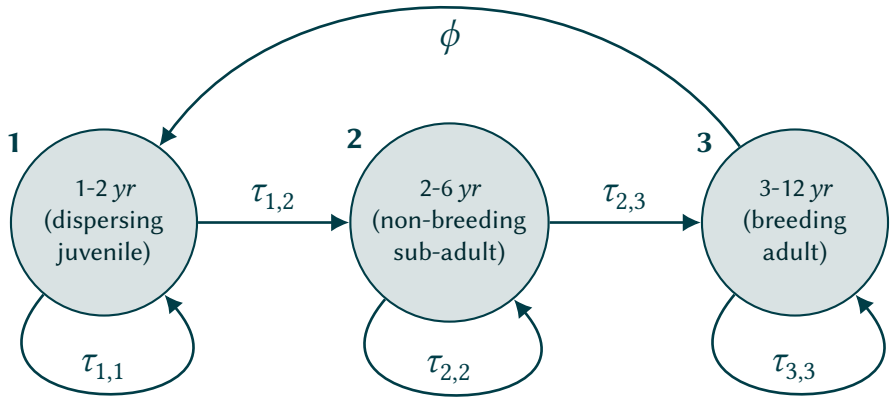

Figure 3.2.: Life-cycle graph of the stage-structured population model for the red kite with three developmental stages. The probability for an individual in stage s to stay in its stage over one time step (1 year) is denoted by $\tau_{s,s}$, and to move to the next stage is denoted $\tau_{s,s+1}$. Only stage 3 produces offspring, with a fecundity of ϕ.

Table 3.1.: Process parameters of the IBM that were included in the Bayesian calibration and the parameters of their truncated normal prior distributions.

Parameter name	**Lower bound**	**Mean**	**SD**	**Upper bound**
Density-dependence b^{-1}	0.001	0.006	0.0025	0.020
Fecundity ϕ_0	0.5	1.66	0.51	5.0
Survival prob. σ_1	0.01	0.42	0.08	0.99
Survival prob. σ_2	0.01	0.68	0.09	0.99
Survival prob. σ_3	0.01	0.80	0.05	0.99
Development prob. $\gamma_{1\to2}$	0.01	0.80	0.10	0.99
Development prob. $\gamma_{2\to3}$	0.01	0.55	0.10	0.99
Emigration prob. e_1	0.01	0.80	0.10	0.99
Settlement inflection pt. β_s	-15.0	4.0	4.0	15.0
Dispersion parameter ν	1.0	50.0	250.0	500.0

Individual-based model

We used the R-package RangeShiftR (Malchow et al., 2021), that interfaces to the individual-based modelling platform RangeShifter 2.0 (Bocedi et al., 2021), to construct a dSDM based on the gridded habitat suitability maps described above. In the following, we describe the main steps of the direct parameterisation, and refer to the full ODD (Overview, Design concepts and Details) protocol (V. Grimm et al., 2020) in Appendix D for all details. RangeShiftR explicitly simulates demography and dispersal in discrete unit-time steps, which here describe one year. During each year, the processes "reproduction", "juvenile dispersal", "survival", "development", and "aging" are evaluated in this order for all individuals. The prior distributions on the respective process parameters (Table 3.1) were informed by literature data and expert knowledge. They were then updated with information contained in the survey data via Bayesian inference as described below.

Our model is female-based, since females primarily determine the population dynamics in red kite. Their development is described in three stages (Fig. 3.2), with classifications and age ranges adopted from Sergio et al. (2021) and Newton et al. (1989): Dispersing juveniles are one to two years old, sub-adults establish a territory within their second to sixth year, and breeding adults can be as young as three but maximally twelve years of age. A senescent stage was not included in the model because it does not contribute to the overall fecundity and non-breeding adults are not monitored in the survey. The age limits are not strict, as the stage transitions are modelled probabilistically (Fig. 3.2). The transition probabilities $\tau_{m,n}$ are expressed as survival probabilities of stage s, $\sigma_s = \tau_{s,s} + \tau_{s,s+1}$, and the development probabilities $\gamma_s = \tau_{s,s+1}\,\sigma_s^{-1}$. Both can independently vary between zero and one. The development probabilities are assumed as $\gamma_1 = 0.80 \pm 0.10$ for stage 1 and $\gamma_2 = 0.55 \pm 0.10$ for stage 2, to approximately yield the given age classes (Fig. B.1). The survival probabilities σ are taken from Katzenberger et al. (2019) for all three stages: $\sigma_1 = 0.42 \pm 0.08$ and $\sigma_2 = 0.68 \pm 0.09$ and $\sigma_3 = 0.80 \pm 0.05$, which is also in accordance with Schaub (2012) and Newton et al. (1989).

Fecundity ϕ was assumed to be density-dependent and was modelled as an exponential decay with population density. Each cell i is characterised by a local strength of demographic density-dependence b_i, which is obtained as the global strength b divided by the cell habitat suitability HSI_i, $b_i = b\ \mathrm{HSI}_i^{-1}$, given in units of cell area ($a_c = 4\ \mathrm{km}^2$). Fecundity follows the relation $\phi_i(n_i) = \phi_0\ \mathrm{e}^{-b_i\, n_i}$, where n_i denotes the density of adults in stages 2 and 3 in cell i (i.e. juveniles do not count towards this density-dependence). The base value ϕ_0 is the required process parameter and denotes the theoretical fecundity at zero population density. Nägeli et al. (2021) report a realised fecundity of 1.77 ± 0.70, which agrees with Schaub (2012) and Nachtigall (2008). We assumed that this value is reached at a density of

25 breeding pairs (BP) per 100 km^2 (i.e. 1 BP per cell) and halved it for our female-only model: $\phi_1 = \phi(n = 1/a_c) = 0.88 \pm 0.35$. We can then get ϕ_0 from $\phi_0(b) = \phi_1 \, e^{b/\mathrm{HSI}}$, with b as a calibration parameter that controls the degree of density-dependent decay in fecundity. The HSI over all habitat cells had a mean and standard deviation of 80% ± 12% and we assumed that the lower and higher fecundities were attained in the lower and higher quality habitats. This was given with a range of $b = (0.50 \pm 0.15)\, a_c$ (Fig. B.2), yielding $\phi_0 = 1.65 \pm 0.51$.

Dispersal is explicitly modelled in three stages: emigration, transfer and settlement (J. M. J. Travis et al., 2012). Red kites are strongly philopatric (Newton et al., 1989) so that emigration was modelled as occurring in the first stage only. The emigration probability was assumed constant at $e_1 = 0.64 \pm 0.10$, meaning that an expected proportion of 87% of juveniles have dispersed within their first two years. This value best matched observations in which 42% of females of a cohort have emigrated after year one and 45% after year two (own unpublished data), suggesting a larger proportion of emigrants among two-year-old juveniles than one-year-old juveniles. The transfer phase described the movement of a dispersing individual through the landscape. It was modelled as a strongly correlated random walk in a random direction with a step length equal to the cell size. After each step, the option to end the movement and settle was evaluated. Settlement was only possible in habitat cells and its probability was density-dependent with a sigmoid relationship (Fig. B.3). Its inflection point β_s was a calibrated parameter and was estimated as $\hat{\beta}_s = \beta_s/b = (4 \pm 4)\, a_c^{-1}$. The maximum settlement probability and the slope parameter were both fixed parameters and were assumed as $\alpha_s = -1$ and $s_0 = 0.75$, respectively. The maximum number of steps in the random walk was set to 10. Therefore, depending on the availability of sparsely populated habitat, individuals exhibit dispersal distances between 2 and maximal 20 kilometres, which is consistent with observations (own unpublished data; Newton et al., 1989; Nachtigall, 2008). Longer-range dispersal events are also frequently observed, but excluded from the model due to the small study region and the mountainous terrain. In- or outflux of individuals across the system boundaries was not considered.

The initial conditions of each simulation were stochastic. The number of adult individuals in each cell was drawn from a Poisson distribution whose mean values were predicted from a generalised linear model. This model of the initial red kite distribution was an autoregressive distribution model (Dormann et al., 2007) of the earlier atlas data (1993-'96) with the spatially interpolated values of atlas counts as its sole predictor (Fig. B.4). The number of juveniles and sub-adults was subsequently estimated from the demographic rates under the assumption of a stable stage distribution.

3.3.3. Bayesian calibration

In a Bayesian calibration, a joint posterior distribution was estimated for nine model parameters θ based on their prior distributions $p(\theta)$ and the likelihood $l(\theta)$ (Fig. 3.1). The priors express the a-priori information that we assumed about likely parameter values as summarised in Table 3.1. The likelihood function $l(\theta)$ measures the fit of a model M, parameterised with θ, to the monitoring data. The calibrated model parameters are: the strength of density-dependence $1/b$; six demographic probabilities for survival of all stages ($\sigma_1, \sigma_2, \sigma_3$), juvenile and sub-adult development (γ_1, γ_2), and the base adult fecundity (ϕ_0); as well as two dispersal parameters to control the emigration (e_1) and settlement probabilities (β_s). Additionally, a dispersion parameter ν is calibrated, which is introduced below.

All priors $p(\theta)$ were chosen as truncated normal distributions. Their means and standard deviations were informed from the literature and expert opinion and they were bounded to their respective valid parameter ranges (Table 3.1). As calibration data, we used observed abundances from the MHB survey, D_{MHB}. Based on this data, we defined a likelihood $l(\theta) = p(D_{\text{MHB}} \mid \theta, M)$ as follows: For a given parameter vector θ, the RangeShiftR simulation model (M) is run and the output abundance data are aggregated and averaged over twenty replicate runs of the model. The result D_{sim} is compared with the MHB data under the assumption of a negative-binomial error distribution (NB), so that for an observation at site i and time t, $l_{i,t}(\theta) = Pr_{\text{NB}}(D_{\text{MHB,i,t}} \mid \mu{=}D_{\text{sim,i,t}}, \nu)$. The parameter ν describes the error over-dispersion and was also calibrated. It arises in an alternative formulation of the negative-binomial probability mass function Pr_{NB} formulated in terms of its mean μ and dispersion ν, instead of the success probability $r = \nu/\mu{+}\nu$ and the target number of successes $n = \nu$. Therefore, its variance is given by $\sigma^2 = \mu + \mu^2/\nu$. It approaches μ from above when $\nu \to \infty$, as the negative binomial converges to the Poisson distribution. The variance can thus be tuned by ν, rendering it an appropriate error description for over-dispersed count data.

Due to the stochasticity inherent in our simulation model, the likelihood values calculated from repeat simulations were also stochastic. They thus represent an estimator of the exact likelihood. Conceptually, this not a problem for the applied Markov chain Monte Carlo approach (MCMC, details below), since the pseudo-marginal theorem guarantees that the MCMC sample still converges to the exact posterior distribution (Andrieu & G. O. Roberts, 2009; Warne et al., 2020). Practically, however, large variances in the likelihood estimator can increase the convergence time dramatically if the sampler gets stuck at occasional high likelihood values. To reduce the variance in the likelihood estimates, we aggregated the abundance data within spatio-temporal blocks of 14 ×14 grid cells in space

and three years in time (Figs. B.5 and B.6). These aggregation factors were chosen with the target of reaching a variance below ten on the logarithmic scale in repeated likelihood evaluations for a given θ. The aggregation resulted in 57 spatial and 5 temporal blocks, within which the observed and simulated red kite densities were compared. Under the usual independence assumptions, the total likelihood was then expressed as the product over all blocks: $l(\theta) = \prod_{i=1}^{57} \prod_{t=1}^{5} l_{i,t}(\theta)$.

To validate the calibration setup and assess the sensitivity of the likelihood estimates $l(\theta)$ to changes in the model parameters θ, we performed a local sensitivity analysis (Fig. B.7). For this, a test data set D_{SA} was simulated from the model with all parameters at their mean prior values. Then, one parameter at a time was varied within the boundaries of its prior distribution while keeping all other parameters at their mean and estimating the likelihood with respect to D_{SA}. Further, we performed a global sensitivity analysis with Morris' elementary effects screening method (M. D. Morris, 1991).

To estimate the joint posterior distribution based on the defined $p(\theta)$ and $l(\theta)$, we used a MCMC sampling scheme (Luengo et al., 2020). Therein, the posterior density $p(\theta | D_{\mathrm{MHB}}, M)$ of a series of given parameter sets θ is evaluated according to Bayes' rule. The utilised MCMC algorithm was a variant of the adaptive Metropolis sampler, namely the differential evolution sampler with snooker update (DEzs, Braak & Vrugt, 2008), as implemented in the BayesianTools R-package (Hartig et al., 2019). Every calibration run included three independent DEzs-MCMCs with a length of 2×10^5 iterations, of which the first 5×10^4 were discarded as an initial burn-in period. Each DEzs, in turn, consisted of three inter-dependent internal chains, so that each calibration comprised a total of nine chains. The chains were checked for convergence using trace plots, trace rank plots (Vehtari et al., 2021) and the multivariate potential scale reduction factor (psrf; Gelman & Rubin (1992)). A chain was considered approximately converged if its multivariate psrf value had dropped below 1.10.

To assess the information gained in the calibration, the sampled posterior distributions were contrasted with the prior distribution. To this end, the parameter estimates were compared with respect to the medians and quantiles of their respective marginal distributions. To evaluate if and by how much the uncertainty was reduced, we assessed and compared the distribution breadth by calculating the width of the highest-posterior-density intervals (HPDIs).

3.3.4. Cross-validation and prediction

We employed a spatial block cross-validation scheme to evaluate the model fit without duplicate use of data for both model calibration and validation (D. R. Roberts et al., 2017).

To this end, the data was split into five spatially contiguous folds (Fig. 3.1 and Fig. B.5). For each fold, the respective subset of MHB data was held out and the model was fit to the remainder of the data. To ensure that the folds covered largely identical spaces of environmental conditions, we chose longitudinally structured folds that include a similar altitudinal profile. For model validation, the respective calibration results for each fold were used. For final model projections, in turn, a separate calibration on the full data set was used.

Posterior model predictions were generated by taking a sample of 1000 draws from the joint posterior, running the dSDM with each drawn parameter vector, and calculating the mean, median and 95%-credibility interval (CI) of the simulated abundances. Prior predictions were obtained in the same way but using draws from the prior distribution. Both prior and posterior predictions were run for the time covered by the MHB data and additional 30 years forward with constant habitat suitabilities, i.e. no changes in land cover or climate were considered. This projection provides an estimate of the potential current population size and distribution, without making a prediction to future conditions.

To assess the model's predictive performance, we calculated Harrell's c-index (Newson, 2006, using the function *rcorr.cens* from the Hmisc R-package), a rank correlation index that generalises the AUC index to non-binary response variables. It quantifies the probability that for a given pair of data points the ranking of predictions matches the ranking of observations. This measure was used in Briscoe et al. (2021) as a form of temporal AUC to assess the fit to temporal trends. We use it here as an index that is applicable to abundance predictions and can be interpreted like the AUC for occurrence predictions.

3.4. Results

3.4.1. Sensitivity analysis

Based on the local and global sensitivity analyses (Fig. B.7 and Fig. B.8), we found that the likelihood estimates responded most strongly to variation in the strength of density-dependence $1/b$, the adult base fecundity ϕ_0 and the three survival probabilities σ_1, σ_2, and σ_3. Therefore, we expected that these parameters will calibrate best under our setup, while the development probabilities γ_1, γ_2, and the emigration probability e_1 would be only weakly informed by our survey data through the specified likelihood.

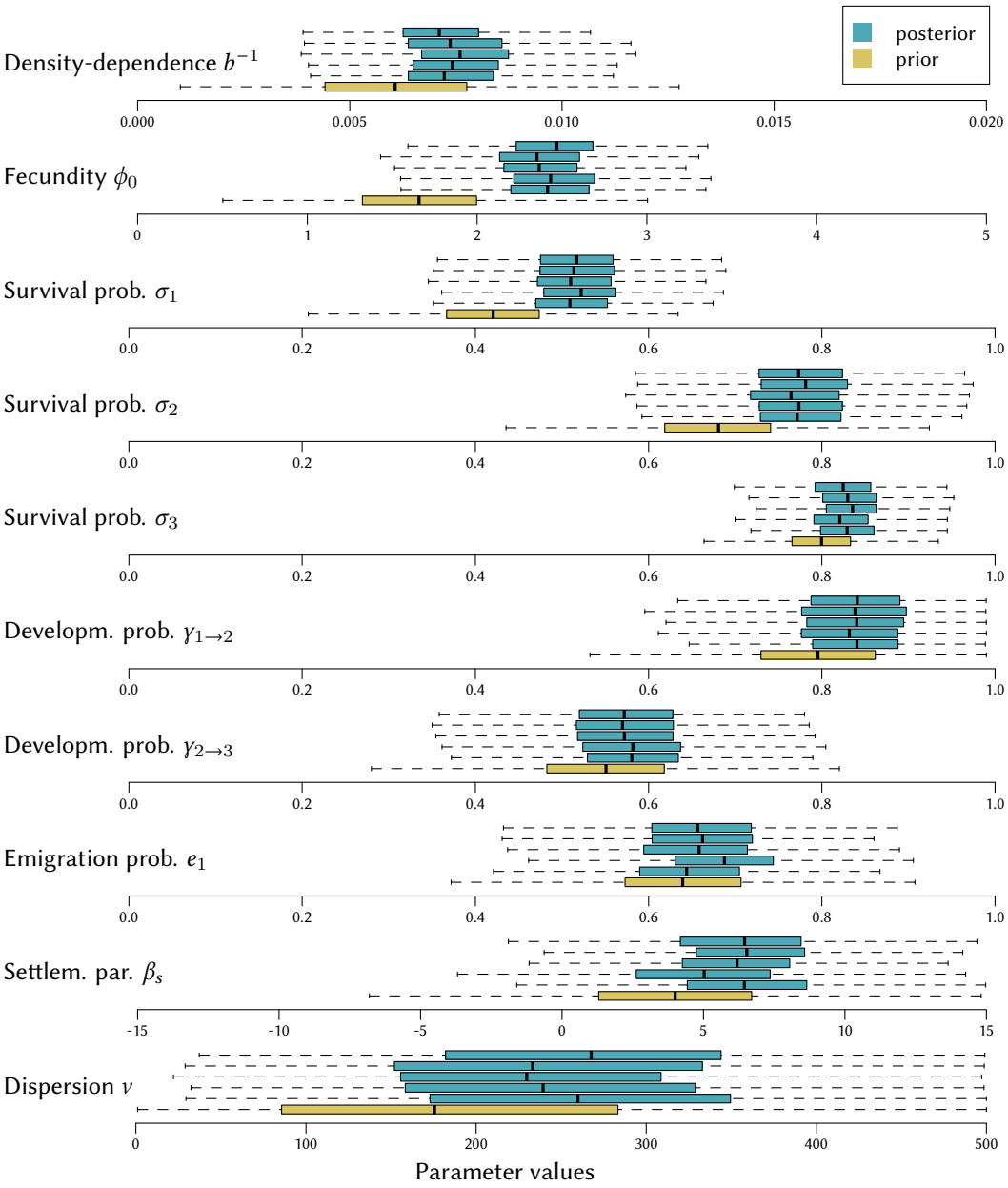

Figure 3.3.: Box plots summarise the marginal prior (yellow) and posterior (blue) distribution for each calibration parameter and for all five spatial folds. The black bar marks the median, the boxes show the inter-quartile range, the whiskers extend to the most extreme data point which is no further away from the box than 1.5 times its length.

3.4.2. Model calibration

To calibrate the model parameters, we ran independent DEzs-MCMC chains on different training data sets: five chains were run on the separate folds of the cross validation and one on the full data set. Differences between the respective sampled posterior distributions can therefore arise both because of differing convergence and because of the data selection. We find that all posteriors converged roughly in the same area of the parameter space, as the variance over the five folds was small. Their marginal distributions take on similar medians and quantiles.

A comparison between the prior and posterior distributions revealed how the consideration of the MHB survey data informs the initial parameter estimates that were obtained directly from literature data. Notably, the medians of the marginal distributions for fecundity ϕ_0 and the survival probabilities of the first and second stage, σ_1 and σ_2, have shifted significantly, whereas those of the other parameters remained largely unchanged. The marginal posterior distributions for each parameter and each spatial fold are represented by box plots in Fig. 3.3, and those for the calibration to the full data set are shown in Fig. B.12. Comparing the HPDIs of the prior and posterior distributions, we found substantially narrower posteriors and thus reduced uncertainty for the strength of density dependence $1/b$, fecundity ϕ_0 and the survival probabilities of stages one and two, σ_1 and σ_2. These parameters had already responded strongly in the sensitivity analysis. No uncertainty reduction nor a significant change in point estimate were found for adult survival σ_3 (Fig. B.13). This was contrary to our expectation based on the sensitivity analysis, but this parameter already had the most informative priors to begin with. The dispersion parameter of the negative binomial error model was calibrated to a very large value, yielding a variance that was close to that of a Poisson distribution. Thus, only slight over-dispersion was detected relative to a Poisson-distributed error.

The convergence of all DEzs-MCMCs was regarded sufficient, based on the conducted diagnostics. However, there were considerable differences between the folds due to the varying number of MHB sites included: The chains reached multivariate psrf values of 1.05, 1.02, 1.05, 1.09, and 1.04, respectively, for folds 1 to 5. Convergence was further assessed using trace plots (Fig. B.9), trace rank plots (Fig. B.10) and psrf plots (Fig. B.11), which were all satisfactory. No substantial correlations between the parameters were detected (Fig. B.14).

Table 3.2.: Evaluation of the spatially-blocked cross-validation (CV). Each fold was used as test data for a separate calibration, which used the remaining folds as training data. Predictions to the test data were evaluated using the c-index, given per row by its mean and standard deviation in brackets. The c-index was computed on different subsets of the MHB data, given per column: The spatio-temporal c-index compares each observation (site-year) independently, the temporal c-index compares time series of total abundance per fold, and the last column gives the c-index over the sites with the 15% highest variance.

Spatial CV fold	Spatio-temporal	Temporal	High variance
Fold 1	0.69 (0.05)	0.94 (0.05)	0.67 (0.11)
Fold 2	0.86 (0.02)	0.93 (0.05)	0.59 (0.06)
Fold 3	0.89 (0.02)	0.94 (0.04)	0.65 (0.07)
Fold 4	0.92 (0.01)	0.92 (0.05)	0.75 (0.05)
Fold 5	0.85 (0.04)	0.92 (0.06)	0.73 (0.07)
All folds	0.88 (0.01)	0.94 (0.04)	0.66 (0.03)

3.4.3. Model validation

The spatial-block cross-validation was evaluated by calculating the c-index per spatial fold and for different subsets of the MHB data (Table 3.2). First, it was calculated over all observations, i.e. all site-year combinations within a fold, independently. The overall value of 0.88 indicates an excellent fit to the validation data. However, the results were quite variable across folds (see also Fig. B.15), which is likely due to the differing number and information content of the included MHB sites. Second, focusing on regional abundance dynamics, we calculated the c-index for the time series of the total abundance within each fold, consistently yielding excellent values between 0.92 and 0.94 (see also Fig. B.16). This confirms that averaging the abundance over large regions further increases the accuracy of temporal predictions. Third, we were interested in the performance of our dSDMs at those MHB sites that showed the highest variance in red kite counts, since highly fluctuating population sizes are often of special conservation interest but are usually harder to predict. To this end, we ranked all MHB sites by their count variance and computed the c-index over the top 15% most variable sites. The folds scored significantly lower, showing an overall value of 0.66 (see also Fig. B.17), which signifies a substantial drop in performance and indicates fair predictions for highly variable sites. Again, the different folds show very variable results that range from 0.59 to 0.75, depending on the specific sites they include.

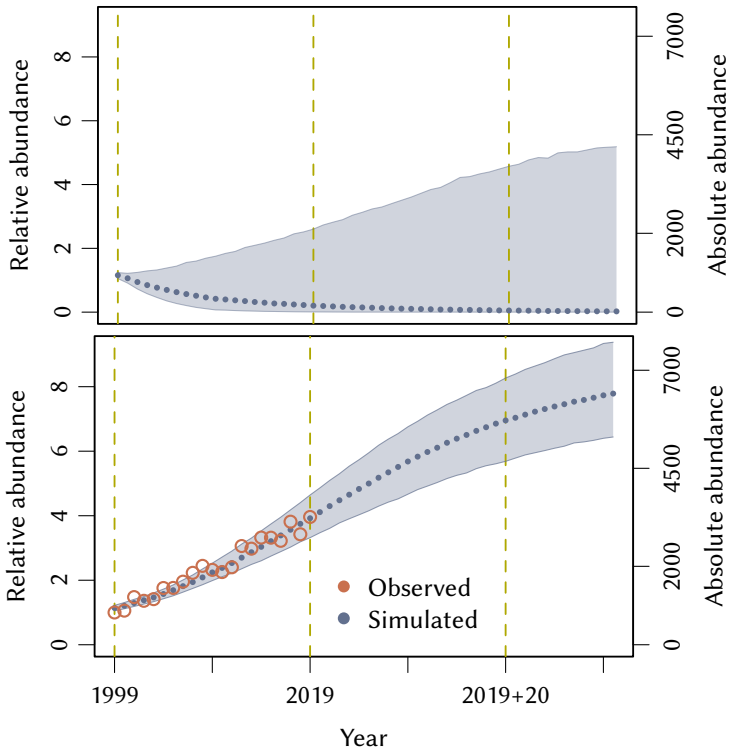

Figure 3.4.: Prior (top) and posterior (bottom) simulations of the abundance time series of red kite in Switzerland. The blue line and band show the median and 95%-credibility interval of total number of predicted breeding pairs (#BP), with relative values (with respect to year 1999) on the left and absolute values on the right y-axis. The bottom panel shows the cross-validated posterior predictions together with the breeding bird index (red circles, relative y-axis only) for comparison. The dashed vertical lines mark the years for which spatial predictions are depicted in Fig. 3.5. After the last year of survey data, 2019, the environmental conditions are kept constant.

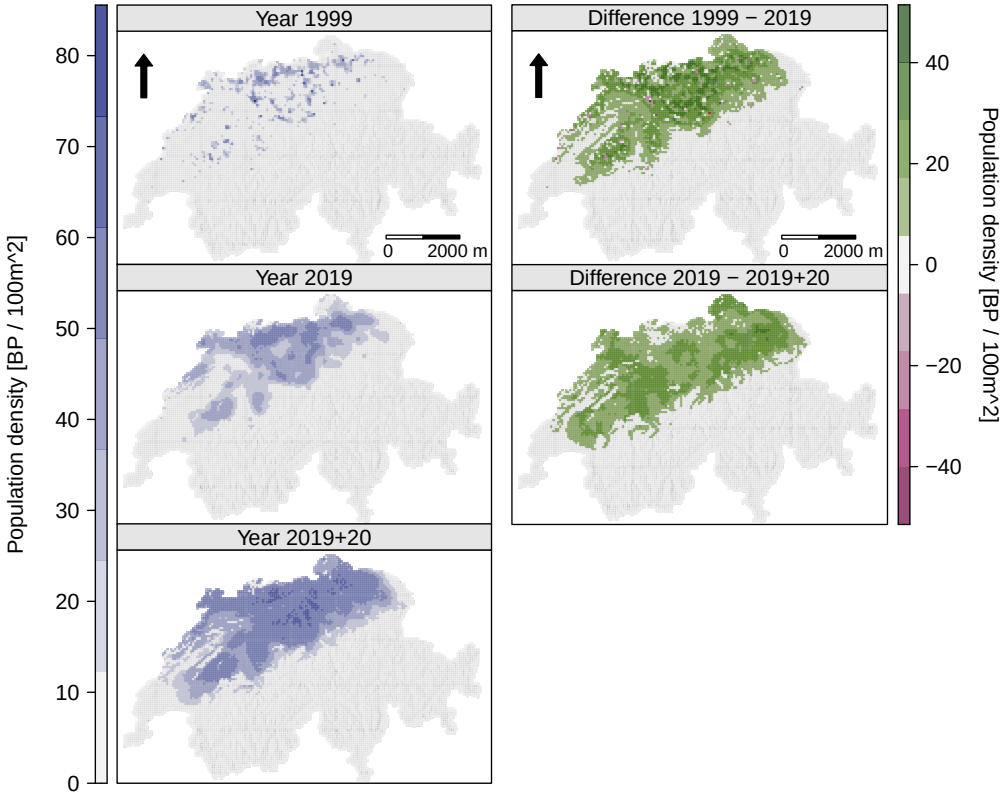

Figure 3.5.: Mean posterior predicted population densities for the years 1999 and 2019, and after 20 further years under constant conditions (left column) as well as the differences between those years (right column).

3.4.4. Model projections

The model was used to generate projections to places not covered by the MHB survey by simulating red kite abundance over the whole extent of Switzerland. This allows to compare these projections to the Swiss breeding bird index, which estimates the total population trend relative to the year 1999 (Knaus et al., 2022) and thus offers an additional source of validation data. Further, by running the model forward beyond the MHB data period and under stable environmental conditions, we estimated the size and range of the current potential population.

Prior and posterior predictions of total red kite abundance during the entire survey period and thirty years onward, assuming constant habitat suitabilities, are shown in Fig. 3.4. The posterior predictions show very good fit to the Swiss breeding bird index. Comparing the prior and posterior predictions of our model gives more evidence that the calibration was able to gain substantial information from the survey data: the model fit

was improved considerably and output uncertainty was reduced. Simulations from the prior show negative population trends in most cases, and they have a large 95%-CI that includes predictions of 5 to 2100 breeding pairs in year 2019. The posterior predictions, in contrast, show increasing trends throughout, and a much narrower CI. They exhibit a comparably steep increase in abundance over the past twenty years, in accordance with the strong increases in red kite abundance that were recorded during this time. Forward simulation shows that today's potential equilibrium population size amounts to 6400 (95%-CI: 5300-7700) breeding pairs.

Spatial projections were made to the whole country as three snapshots in time (Fig. 3.5): at the beginning (1999) and end (2019) of the survey data set, as well as after a continuation of further twenty years (2019+20). These projections mirror the rapid range expansion of red kite range that Switzerland has seen in the past two decades. However, the continuation shows a relatively stable range with increasing population densities, suggesting that the current population has not yet reached the carrying capacity in all colonised areas. The same maps were created from prior predictions for comparison (Fig. B.19). They exhibit a contracting range over time, that deviates substantially from the posterior maps, again indicating the effective inclusion of information from the MHB data.

This comparison of prior and posterior distributions and their respective predictions can shed light on the main drivers of the presented results. While the prior predictions exhibit a tendency towards decreasing populations and contracting ranges, the posterior predictions reproduce the observed patterns closely. Comparing the marginal distributions (Fig. 3.3), the main drivers of these disparate predictions appear to be fecundity and early survival rates. They responded most strongly to the information incorporated from the MHB data via the Bayesian calibration. Taken together, these three influential parameters suggest that reproductive success was determined to play a key role in driving the resulting increases in local density and distribution. In contrast, changes in habitat suitability over the study period seem to have had a lesser effect on the resulting population. This was assessed in a simple analysis of the sensitivity of simulated abundance to habitat suitability. We compared the abundance time series from Fig. 3.4 with two counter-factual scenarios in which the habitat suitabilities of each year were raised or reduced by five (out of 100) points (Fig. B.18). By the last year of MHB data, 2019, this intervention had an effect of 9-10% on total abundance, which is small compared to the effect of the calibration (Fig. 3.4). We thus conclude that the population increases are not driven by a changing environment, but by transient dynamics to an equilibrium with much higher population size.

3.5. Discussion

Reliable methodology for understanding and predicting a species' population and range dynamics will be crucial to inform decision making in the future. Dynamic, spatially-explicit, process-based distribution models (dSDMs) provide valuable advances towards improved biodiversity forecasts (Urban et al., 2016) but are currently underused due to technical and data challenges and limited guidance for applications (Briscoe et al., 2019; Zurell et al., 2022). This study contributes to overcoming these challenges. We demonstrated the practicability of a complete modelling workflow for dSDMs with a case study of a conservation-relevant population, the red kite in Switzerland. This included calibrating a complex stochastic simulation model to heterogeneous empirical data, interpreting the results, and validating the model by cross-validation. Thanks to the use of Bayesian inference, we can integrate direct and indirect knowledge on the process parameters, account for their uncertainty and propagate it to model predictions. Our model captures the Swiss red kite population trends with higher spatial and temporal predictive accuracy than achieved with correlative models in a previous study (details below, Briscoe et al., 2021). The model suggests that the potential population size under current environmental conditions is much larger than presently realised and that this is may be a result of the population's history. The workflow exemplified here can be readily adapted to other species, if an adequate model, prior parameter estimates, as well as response data (e.g. occupancy or abundance data) are available, and it promises to yield improved parameter estimates and more accurate, validated model projections.

The process-based dSDM used here to demonstrate our workflow was built with the individual-based modeling platform RangeShiftR (Malchow et al., 2021). It explicitly considers relevant ecological processes such as demography and dispersal and includes crucial mechanisms such as density-dependence. Therefore, transient dynamics, that arise when a distribution is not in equilibrium with its environment, can be reproduced and dynamic responses to change can be represented. The IBM structure was determined based on expert opinion and the direct (prior) parametrisations of the process parameters were derived from literature data. IBM approaches are particularly suited for the direct estimation of their model parameters (e.g. survival probability or dispersal distance) because they formulate all processes from the perspective of the individual (Railsback & V. Grimm, 2019), where they can be estimated from data obtained in observational studies (e.g. mark-recapture). The prior estimates were updated using the MHB abundance data within a Bayesian inference. Here, IBMs have the advantage of realistically modelling small local populations of a few individuals by incorporating demographic stochasticity, so

that the survey data can be used at a high spatial resolution. Depending on the research question and the available data, however, a different model formulation may be more adequate, such as spatially-explicit population-based models (implemented for example in steps Visintin et al. (2020)). For a successful parameterisation using the presented framework, certain data requirements should be met: the utilised model should have model parameters whose priors can be informed by ecological theory and direct estimates and it should generate outputs that can be compared to observational data via a plausible error model that can be expressed as a likelihood function.

The successful calibration of parameters in process-based dSDMs can produce new insights, since they have a well-defined ecological meaning. Comparing the prior and posterior distributions of our model, we found that some parameters in particular, e.g. the adult fecundity ϕ_0, its density-dependence $1/b$, and the survival probabilities of juveniles and sub-adults, σ_1 and σ_2, responded strongly to the inclusion of additional information from survey data. This behaviour was predicted well from the local and global sensitivity analyses. The detected sensitivity further indicates that the model projections are responsive to these parameters, thereby suggesting potential pathways for conservation measures, e.g. highlighting the protection of young individuals and supporting nest success. Pfeiffer & Schaub (2023) reached the same conclusion and "identified productivity, i.e. the number of fledglings per breeding pair, as the main demographic driver, followed by adult survival" when modelling the German red kite population with an integrated population model. Further, their estimates of stage-wise survival probabilities are in strong agreement with ours. The prior estimate of $1/b$ was corroborated and those of ϕ_0, σ_1 and σ_2 were corrected to higher values, while the uncertainty around all four estimates was reduced. These corrections in parameter distributions also drive the better fit of the calibrated model projections to the data as well as the reduced output uncertainty. Interestingly, it was shown that the calibration could gain information even on the early developmental stages (1 and 2) that were not recorded in the calibration data, which held abundances of stage 3 only. This is facilitated by the ecological assumptions that are imposed by the model structure which discerns the stages by their ability to disperse (only stage 1) or reproduce (only stage 3).

The discrepancies found between prior and posterior parameter estimates are driven by different factors (Cailleret et al., 2020): Firstly, there can be a true difference, for example, if the prior estimates were obtained from different study populations. In our case, the prior fecundity was based on a measurement from a Swiss sub-population with a high breeding density, which may have a lower fecundity than the Swiss average. The prior survival probabilities are taken from a German red kite population, that shows a slightly

negative population trend, and the upward correction seems to better match the increasing Swiss population. Red kite in Switzerland benefit from public feeding (Cereghetti et al., 2019) and many sub-adult individuals change from migratory to resident behaviour, which can also increase survival. Secondly, an important source of deviations between empirical and calibrated parameter estimates is model error. Our IBM captured only a subset of the multiple eco-evolutionary processes that underlie the observed abundance patterns. Therefore, the calibrated parameters will account for missing processes to some extent. This highlights the need for further development of dSDMs to include more mechanisms and thus to fit observed data more closely. It further emphasises the importance of effective integration of direct and inverse calibration to estimate parameter values and their uncertainties, since predictions and derived management decisions can be highly sensitive to the final parameterisation.

The validation of model predictions to assess model performance is common practice in the application of cSDMs (Sillero et al., 2021), but is often missing with dSDMs. With the presented workflow, we have successfully applied spatial-block cross-validation to a dSDMs by calibrating the model to each of five spatially contiguous regions within the study area. By spatially blocking the hold-out data we reduced the amount of spatial autocorrelation between the training and testing data, which is often present in abundance data and only insufficiently reduced by other cross-validation schemes such as randomised leave-p-out. This yields a more realistic assessment of predictive performance for interpolation. For other types of data, different blocking techniques may be more adequate (D. R. Roberts et al., 2017). The folds were selected carefully in a way that the same range of environmental conditions is represented in each one, so that model evaluation does not involve extrapolation to new environmental conditions. Performing a cross-validation is usually computationally expensive, as the calibration needs to be repeated for each set of hold-out data. Therefore, a suited validation method has to be chosen carefully. Alternatives include approximation to leave-one-out validation by WAIC (Vehtari et al., 2017).

The full red kite dSDM was evaluated based on its cross-validated abundance predictions using Harrell's c-index as a measure of predictive performance, which indicated excellent predictive accuracy (c-index: 0.88). In sites with highly fluctuating abundances performance dropped considerably, and only provided fair predictions (c-index: 0.66). A similar analysis was conducted by Briscoe et al. (2021) who compared the accuracy of correlative SDMs and dynamic occupancy models (Kéry et al., 2013) that were fitted to the MHB data of 69 Swiss birds, including the red kite. They found that predictive ability of occupancy was high for all examined model types when assessed across all sites (mean AUC > 0.8)

but much lower when specifically testing only sites that showed occupancy change (mean AUC 0.64-0.71). The AUC metric is based on predictions of occupancy only and therefore generally scores above the c-index, which ranks abundances. Collapsing our abundance predictions to occupancy and comparing them to Briscoe et al. (2021) in terms of the AUC, our calibrated IBM surpasses the mean of their red kite SDMs, both across all sites (mean AUC of 0.91 versus 0.85) and occupancy-switching sites only (0.80 versus 0.67). Especially in range shifting populations, such as the red kite in Switzerland, process-explicit dSDMs can outperform correlative approaches because they make no equilibrium assumption. Our model also showed clear advantages over the dynamic occupancy models in Briscoe et al. (2021), likely due to the explicit consideration of spatially-explicit processes such as density-dependence in population dynamics and dispersal.

The calibrated model was run forward under current environmental conditions in order to explore the potential population size and distribution. In the same way, it could be used to assess population trends under certain scenarios such as conservation measures involving habitat improvements or regulation of demographic rates. For predictions of future population dynamics, however, expected changes in land use and climate have to be taken into account. In our dSDM, these variables are only considered through the one-dimensional habitat suitability and thus can not impact demographic processes directly and independently, as ecological theory suggests. More complexity and mechanistic understanding could be incorporated by substituting the habitat model with direct relationships of species traits like demographic rates with environmental variables. Such a demographic range model is adequate for predictions under climate change (Schurr et al., 2012; Malchow et al., 2023). As a further limitation, the habitat map that underlies our model consists of a cSDM fitted to recent Atlas data. It is possible that suitable but not yet occupied parts of the red kite niche were missed in this data and therefore the future range would be underestimated by the predictions. This limitation can be circumvented by using a habitat model that does not rely on the equilibrium assumption, e.g. a rule-based model derived from knowledge about the species' habitat requirements or a eco-physiological SDM (Kearney & Porter, 2009). Moreover, the observed increases in range and density may in part be fueled by individuals that were not recruited in the study region but immigrated from surrounding high-density populations that were not considered in the model. More potential for model improvement lies in implementing additional processes such as mating systems, species interactions, or genetic and behavioural adaptation. Their successful parameterisation, however, will require adequate data.

The inverse calibration of dSDMs from observational data is also possible with other methods like pattern-oriented modelling (POM; V. Grimm et al., 2005; Mortensen et al.,

2021) or approximate Bayesian computation (ABC; Beaumont, 2010; Hauenstein et al., 2019), the latter of which has already been demonstrated in the RangeShifter model (Dominguez Almela et al., 2020). Independent of the chosen calibration method will the accurate parameterisation of dynamic and mechanistic SDMs remain a challenge until the paucity of high-quality ecological and monitoring data is alleviated (Oliver et al., 2012; Kissling, Ahumada, et al., 2018). Which parameters of a dSDM can be successfully calibrated depends on the available calibration data. Here, the type of data collected within monitoring programs plays an important role as all model output quantities can principally be used for inverse parameterisation. In our case study, for example, the abundances of juveniles and sub-adults were output from the IBM but could not be used for calibration because age classes are not distinguished in MHB surveys. Generally, the high uncertainties in parameter estimates caused by data limitations translate to large credibility intervals in model predictions, reducing the utility for conservation applications. Here, it is a clear advantage of the Bayesian framework that sources of prediction uncertainty are explicitly quantified and can thus be addressed, for example in targeted monitoring programs.

In conclusion, this case study shows how an individual-based dSDM can be built with RangeShiftR, calibrated using Bayesian inference, and validated by cross-validation. We demonstrated how the inclusion of monitoring data refined parameter estimates and greatly improved model fit and prediction accuracy. Well calibrated and validated process-based models offer compelling advantages over the currently most common static models. They are able to inform science-based management decisions and the design of proactive conservation measures (Zurell et al., 2022). Future progress in this field should be directed towards developing more flexible and accessible modelling tools, assessing their data requirements for effective parameterisation, and validating them against independent targets.

Chapter 4

Demography-environment relationships improve mechanistic understanding of range dynamics under climate change

4.1. Abstract

Species respond to climate change with range and abundance dynamics. To better explain and predict them, we need a mechanistic understanding of how the underlying demographic processes are shaped by climatic conditions. Here, we aim to infer demography-climate relationships from distribution and abundance data.

For this, we developed spatially-explicit, process-based models for eight Swiss breeding bird populations. These jointly consider dispersal, population dynamics and the climate-dependence of three demographic processes - juvenile survival, adult survival and fecundity. The models were calibrated to 267 nationwide abundance time-series in a Bayesian framework.

The fitted models showed moderate to excellent goodness-of-fit and discriminatory power. The most influential climatic predictors for population performance were the mean breeding-season temperature and the total winter precipitation. Contemporary climate change benefitted the population trends of typical mountain birds leading to lower population losses or even slight increases, whereas lowland birds were adversely affected.

Our results emphasise that generic process-based models embedded in a robust statistical framework can improve our predictions of range dynamics and may allow disentangling

the underlying processes. For future research, we advocate a stronger integration of experimental and empirical studies in order to gain more precise insights into the mechanisms by which climate affects populations.

4.2. Introduction

Changing climatic conditions are impacting natural systems around the globe, causing rapid biodiversity changes (Parmesan & Yohe, 2003; Hooper et al., 2012; Rosenzweig & Neofotis, 2013). Two of the most striking and commonly discussed impacts are distribution shifts (I.-C. Chen et al., 2011) (Thompson et al., this issue) and changes in population abundances (Martay et al., 2017) (Gregory et al., this issue). These range dynamics result from an interplay of key ecological processes such as local population dynamics and dispersal, which are widely considered to be influenced by the environment (Urban et al., 2016; Fei et al., 2017). An improved, model-based understanding of how climate affects range and population dynamics through these key processes may help to better explain and predict the observed responses (Urban et al., 2022; Ehrlén & W. F. Morris, 2015). Such insights are prerequisite for a quantitative, science-guided basis for deriving effective conservation measures to mitigate biodiversity loss (Zurell et al., 2022).

A process-based approach to species distribution modelling has been suggested repeatedly, going beyond purely correlative models (Guisan & Thuiller, 2005; Cuddington et al., 2013; Connolly et al., 2017; Briscoe et al., 2019). It is expected that process-based models can provide more reliable predictions under changing conditions by explicitly including causal eco-evolutionary mechanisms (Evans et al., 2015; Urban et al., 2016) and allowing for the representation of transient dynamics. Progress towards this goal was made with hybrid models that couple a phenomenological habitat model with processes like population dynamics and dispersal (Franklin, 2010). However, hybrid models do not allow to establish an explicit link between demographic processes and the environment. Instead, they assume that demography scales with a habitat suitability index, that is typically derived from a correlative model and may combine multiple land cover and climate variables (Singer et al., 2018). Yet, the relation of such suitability measures to abundance or growth rate has been questioned (Weber et al., 2017; Thuiller et al., 2014). Alternatively, a direct causal link can be established by considering explicit responses of processes, such as demography, to environmental predictors. For example, Schurr et al. (2012) proposed a spatially-explicit process-based model that considers parametric demography-environment relationships together with mechanistic dispersal effects.

Direct measurements of demography-environment relationships can be obtained by

measuring demographic rates over an environmental gradient, which requires large-scale and well-designed monitoring schemes (Paniw et al., 2021). This has been done for a number of plants (Housset et al., 2016; Treurnicht et al., 2016), but only rarely for animal species, for example fish (brown trout, (Cianfrani et al., 2015)), or birds (North-American forest birds, (Bonnot et al., 2018), and Arctic sea ducks, (Dunham et al., 2021)). As an alternative to direct measurements, Pagel & Schurr (2012) suggested an inverse modelling approach that simultaneously estimates the demography-environment relationships and all other process parameters from empirical data. In the original formulation, they assumed a logistic growth (as the Ricker model) to describe local population dynamics (Pagel & Schurr, 2012). Yet, a benchmarking study based on simulated data suggested that dynamic models with more complex life histories improved predictions of range dynamics (Zurell et al., 2016). Such an extension can be achieved with a refined population model that does not use a compound growth rate but considers explicit demographic sub-processes, such as survival and fecundity, together with their respective environmental responses.

Individual-based models (IBMs, Railsback & V. Grimm, 2019; DeAngelis & Mooij, 2005) provide a flexible modelling framework that can accommodate such complex life histories by considering relevant demographic processes at the scale of individuals. We thus regard IBMs as ideal candidate for achieving the necessary flexibility (Zurell et al., 2016). Here, we extend the statistical framework introduced by Pagel & Schurr (2012) to IBMs and jointly infer demography-environment relationships and dispersal for initially nine Swiss breeding

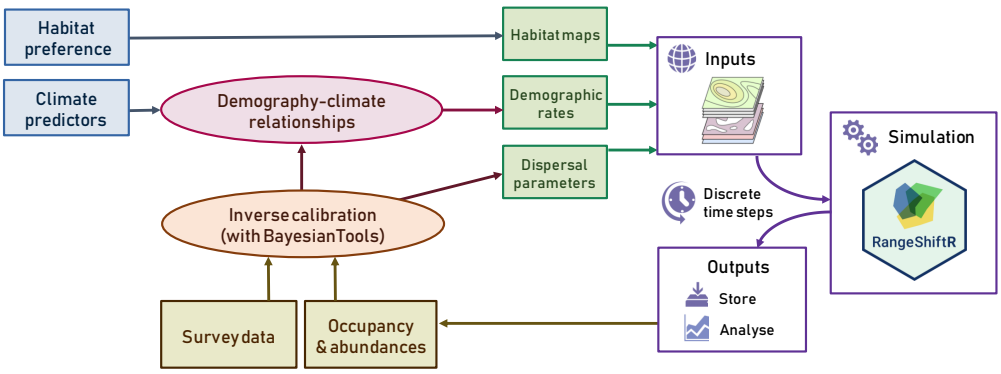

Figure 4.1.: Model workflow: The RangeShifter model (right) has several inputs (green boxes): (1) Habitat maps that are generated from habitat preferences (based on expert knowledge), (2) maps of demographic rates that are derived from demography-climate relationships (DCRs) and climate variables, and (3) dispersal parameters. The DCR parameters and dispersal parameters are estimated inversely in a Bayesian calibration, comparing observed survey data and simulated abundances (yellow boxes).

bird populations from long-term abundance data. To this end, we explicitly modelled the demographic sub-processes of juvenile survival, adult survival and fecundity together with dispersal by single-species IBMs. All our models were built using RangeShifter (Bocedi et al., 2021; Malchow et al., 2021), a modular individual-based modelling platform for simulating spatially-explicit, eco-evolutionary dynamics that can be generically applied to different species. Within a Bayesian framework, we calibrated the IBMs to abundance time series from 267 sites across Switzerland that are spanning the last two decades. In this period, complex range and population dynamics have been observed for Swiss birds (Briscoe et al., 2021; Maggini et al., 2011). Mountainous regions like the European Alps are particularly susceptible to current climate change, and altered temperature and precipitation patterns are already being observed (Gobiet et al., 2014). In Switzerland, the detected trend in air temperature increase over five decades (1959-2008) reached 0.35 K/decade, which amounts to about 1.6 times the northern hemispheric warming rate (Ceppi et al., 2012). We therefore expected that the observed range and population dynamics in Swiss birds are attributable to the climatic changes of the past decades.

Our goal was to assess if process-based models are able to provide useful predictions under changing climatic conditions and if they allow inference on the underlying mechanisms. For this, our models related different climate layers, which summarised key climatic variables during decisive periods of the year, directly to the spatio-temporal variation in demographic rates. We refer to these relationships as demography-climate relationships (DCRs), since we considered only climatic predictors. We examine the fitted DCRs for patterns across species and point out potential limitations in their causal interpretation, that originate from our data-driven calibration approach. To evaluate the DCRs, we map the demographic rates (juvenile survival, adult survival, fecundity) as well as the resulting local growth rate across Switzerland. Based on the calibrated model, we assess the impact of two decades of contemporary climate change on both the growth rate as well as on the abundance of each species. Such insights can facilitate the communication of severe consequences of climate change as well as the design of potential mitigation measures, targeting the specific demographic processes that are most impacted. Our approach is applicable to any population for which spatio-temporal abundance data are available. It can be flexibly extended to allow more detailed conclusions by incorporating more complex DCRs and using more fine-grained predictors.

4.3. Materials and Methods

4.3.1. Study area & data

Switzerland features strong elevational gradients, as large parts are located in the European Alps. The warming rates due to climate change show high spatial and seasonal variance, with their peak in summer at 0.46 K/decade and large values in the lowlands during autumn and in middle and high elevations in spring (Ceppi et al., 2012). To describe the climatic variation over this landscape, we used bioclimatic data from CHELSA v2.1 (Karger et al., 2017; Karger et al., 2018a). It provides monthly means of daily minimum, mean and maximum temperatures, as well as total precipitation for the years 1901-2019 at a spatial resolution of 30 arcsec ($\approx$ 1 km). These climate layers were averaged over several months for the breeding season (April-July), autumn (September-November) and winter (December-February), and standardised using the mean and standard deviation over the considered set of years (1997-2019). We further used land cover data from the CORINE project (European Union, 2022) for 2000, 2006, 2012, and 2018 at a resolution of 100 m to inform species-specific maps of suitable habitat (based on published information on habitat preferences, see below). Parameter inference was based on data from the standardised Swiss breeding bird survey (MHB) for the years 1999 to 2019. The MHB produces yearly time series at 267 sites selected in a systematic-random sampling design (Schmid et al., 2004). Each site comprises a 1 km^2 square in which the number of breeding pairs was counted during two to three repeat surveys per year using the so-called simplified territory mapping method (Schmid et al., 2004). To develop models of initial abundance, we further used Atlas data of the period 1993-96 (Schmid et al., 1998) that provides a snapshot of counts at 2318 sites randomly distributed across Switzerland.

4.3.2. Model building and calibration

We selected a list of bird species according to a set of common characteristics, which allowed us to use the same model structure for all. We chose passerines that prefer forests, shrubs and mountainous regions as their main habitats, are sedentary or short-distance migrants, have a similar life history in which 1-year-olds can be considered mature and able to reproduce, and show changes in spatial abundance between the two Atlas periods of 1993-96 and 2013-16. Focusing on forest and upland species meant that effects of land use change such as intensification of agriculture are less likely to contribute substantially to population dynamics (Barras, Braunisch, et al., 2021). By excluding long-distance migrants we could assume that local winter conditions are meaningful predictors of demographic

rates. These criteria allowed us to isolate the effects of climate on the population dynamics as much as possible. Further constraints were imposed in order to keep the parameter calibration feasible: The relatively simple life history was chosen to limit the number of demographic model parameters and a minimum number of 170 non-zero counts in the MHB data was required. Overall, the criteria related to the species' ecology and technical aspects of the parameterisation were fulfilled for nine species: Eurasian bullfinch, European crested tit, Eurasian treecreeper, Eurasian nuthatch, dunnock, goldcrest, common linnet, ring ouzel, and alpine accentor.

Table 4.1.: Aggregated climatic predictors and their responses as modelled by the demography-climate relationships. The climatic variables of mean temperature, minimum temperature, and total precipitation were averaged over a relevant season and, up to the given order, related to a demographic rate as response variable. These responses include fecundity ρ, juvenile survival s_j, and adult survival s_a.
()* - this effect was originally considered, but excluded due to high collinearity of T_{wn} and T_{at}.

climatic predictor	season	abbr.	order	response
mean temperature during breeding season	April-July	T_{br}	2	ρ
total precipitation during breeding season	April-July	P_{br}	2	ρ
mean temperature during autumn	Sept.-Nov.	T_{at}	2	s_j
minimum temperature during winter	Dec.-Feb.	T_{wn}	1	$(s_j)^*$, s_a
total precipitation during winter	Dec.-Feb.	P_{wn}	2	s_j, s_a

Despite their common characteristics, we expected that the demography of the species will respond differently to climate variation (Saether & Bakke, 2000; Cox et al., 2013). To understand these responses, we built species-specific IBMs with the RangeShifter modelling platform (Bocedi et al., 2021), operated via the RangeShiftR R package (Malchow et al., 2021). The IBMs simulate the population and dispersal dynamics of each species on a regularly gridded landscape of Switzerland. We modelled population dynamics with a female-only, 2-stage model comprising the stages "juvenile" and "breeding adult", with a transition time of one year between the two stages. The local population dynamics of this model are characterised by three demographic rates: juvenile and adult survival probability, s_j and s_a, and fecundity ρ. These demographic rates are considered to be directly and independently influenced by the local climatic conditions and are thus allowed to vary spatio-temporally, i.e. among cells and years. This link between demography and climate is described by six demography-climate relationships (DCRs, Table 4.1). The coefficients of the DCRs as well as all other model parameters are inversely estimated for each species

from MHB survey data within a Bayesian calibration (Fig. 4.1).

To formulate the DCRs, each demographic rate was related to relevant climate predictors using the structure of a generalised linear model, with a logarithmic link function for fecundity ρ and a logistic link for survival, s_j and s_a. As predictors, we considered mean or minimum temperature and total precipitation, averaged over the period of the year that was considered most relevant for the respective process (Table 4.1): Fecundity depended on the conditions during the breeding period (April-July); survival probabilities depended primarily on the winter conditions (December-February), with juvenile survival additionally affected by conditions in autumn (September-November) when juveniles are independent and are known to suffer from high mortality. All predictors were included with linear and quadratic polynomial effects, apart from minimum winter temperature, which was only included in linear form. Minimum winter temperature was highly correlated with autumn temperature (≈ 0.76), and was therefore excluded as predictor for s_j (but still included for s_a). Therefore, the DCR of temperature on juvenile survival should be interpreted as the combined effects from autumn and winter temperature. Within the IBM simulation, the realised values of all demographic rates are then obtained from the calibrated, species-specific DCRs, using only the climate layers as input (Fig. 4.1).

In our model, survival probability describes the annual mortality that primarily occurs during winter and additionally during autumn for juveniles. The modelled fecundity ρ includes all contributions to juvenile survival that occur before the juveniles are independent. Therefore, nestling mortality and early juvenile mortality are included in ρ. Fecundity was further assumed to be density-dependent, decreasing exponentially with the ratio $n_i b_i$ of local population density n_i and local resource availability $1/b_i$ (Neubert & Caswell, 2000). Resource availability was expressed as the overall strength of demographic density-dependence $1/b$, modulated by the local suitability h_i, as $b_i = b/h_i * 100$. This local suitability was determined from habitat preferences provided by Storchová & Horák (2018) (see Table C.2), which were used to determine habitat classes that coarsely delineate the typical habitat of each species. These habitat classes were mapped to CORINE land cover classes (see Table B.1), yielding binary habitat maps at a resolution of 100 m. Then, the maps were spatially aggregated to a resolution of 1 km by counting the number of (100-m)^2-habitat cells located within each 1-km^2-landscape cell i. The resulting index ranges from 0 to 100 and was used as suitability index h_i. A 10-km buffer around the Swiss border was retained to reduce boundary effects. To summarise, climatic variables determined all three demographic rates while habitat suitability only influenced the density-dependence effect on fecundity.

The process of natal dispersal was modelled in three explicit stages: emigration, transfer,

and settlement. The emigration probability p_e described the probability with which a juvenile embarks on a dispersal event. To identify the destination cell after transfer, an exponential dispersal kernel with mean dispersal distance $\bar{d}$ and uniformly distributed direction was evaluated individually. If the destination was a suitable cell, the juvenile settled in it. Else, if one of the eight directly neighbouring cells was suitable, the individual settled there and otherwise died. Hence, juveniles suffered a dispersal mortality that was additive to the annual mortality s_j. The order of processes in each simulation year was first reproduction, then dispersal, and lastly survival. We used stochastic initial conditions for each model run by drawing from an auto-regressive distribution model (Dormann et al., 2007) that was fitted to the Atlas data of the period 1993-96.

We estimated the parameters of each DCR simultaneously with all other model parameters ($1/b$, p_e, $\bar{d}$) inversely from MHB data using Bayesian inference (Hartig et al., 2011). As priors for the climate-independent parameters and the intercepts of the DCRs we assumed Gaussian distributions with means and standard deviations derived from the demographic traits provided by Storchová & Horák (2018) and the dispersal traits provided by Fandos et al. (2023) (all values listed in Table C.1). For the DCR coefficients, we used mildly regularising truncated normal priors with $\beta_{m,n} = 0 \pm 1$ and truncations at $[-5, 5]$. To link model predictions to observations, we compared the simulated abundance of adult breeding females with the observed breeding pair counts. For this, we assumed a negative-binomial likelihood with a truncated Gaussian prior of $\sigma = 50 \pm 50$, bounded between 0 and 500, on the dispersion parameter. To reduce the stochasticity in the likelihood stemming from the non-deterministic nature of the IBM, all counts were spatially aggregated to larger cells of $(25\ \text{km})^2$ and twenty IBM replicate runs were averaged for each sample. Posterior distributions were estimated using Markov chain Monte Carlo (MCMC) sampling with a differential evolution sampler (DEzs; Braak & Vrugt, 2008) implemented by the R package BayesianTools (Hartig et al., 2019). We ran three independent DEzs chains per species-specific calibration. Each chain had a length of 180 000 iterations, of which the first half was discarded as burn-in period. The MCMCs converged for eight out of the nine selected species. Based on this, the goldcrest was excluded from further analysis.

4.3.3. Evaluation and analyses

To validate and evaluate model predictions, we examined both the full IBM simulations and the extracted DCRs. All evaluations were based on a sample of 400 draws taken from the joint posterior of each species. The full simulations provided spatio-temporal projections of adult abundance, which were used to validate the model fit to MHB counts and to the

Swiss breeding bird index (Knaus et al., 2022).

The goodness-of-fit of spatio-temporal projections was evaluated with RMSE (root mean squared error; Table C.3) and Harrell's c-index (Newson, 2006; Table 4.2). The c-index is a rank correlation index that generalises the AUC index to non-binary response variables and we used its implementation in the Hmisc R package (Tikhonov et al., 2020). It quantifies the probability that the ranking of a pair of model-projected abundances matches the respective ranking of MHB counts in a given site and year. We henceforth refer to this measure as spatio-temporal c-index. For further validation, we generated model projections of total adult abundance time series relative to the year 1999 (Figures Fig. 4.2 and Fig. C.1, left panel). They were compared to the Swiss breeding bird index, which directly estimates the same quantity from MHB data and was thus considered as reference (Figures Fig. 4.2 and Fig. C.1, right panel). Additionally, we quantified spatial and temporal prediction accuracy separately with a spatial AUC and a temporal c-index. These followed the procedures presented in Briscoe et al. (2021), who compared correlative species distribution models (SDMs) and dynamic occupancy models (DOMs) for 69 Swiss breeding bird species. Specifically, we compressed the abundance predictions to presence-absence data and averaged these across replicate runs to obtain per-cell occupancy probabilities. We then computed the spatial AUC achieved for each year and averaged these across all years to obtain a mean yearly spatial AUC. The temporal c-index (called temporal AUC in Briscoe et al., 2021) was calculated by comparing the model projections of abundance time series relative to the year 1999 with the Swiss breeding bird index (Briscoe et al., 2021). We used both spatial AUC and temporal c-index for a direct comparison with the performances of the SDMs and DOMs presented in Briscoe et al. (2021).

As a second step, we visually inspected the conditional response curves of all six DCRs within the range of observed climatic predictors for each species. This range spanned the 10th and 90th percentile of climate values occupied by a species, while the respective second predictor is held constant at its median. We then extracted the median and credible intervals for each demographic rate, as shown in Figures Fig. 4.3 and Fig. C.2. The relationship for fecundity included density-dependence and thus had an additional parameter ($1/b$), describing the strength of density-dependence, and two additional predictors (local habitat suitability h_i and density n_i). For deriving the response curves, h_i was held constant at its species-specific median and n_i was set to one breeding pair per 1-km^2 cell, yielding the fecundity that is realised at low densities.

Lastly, we quantified the effects on predicted population performance that could be attributed to climatic trends over the observed time period. From the three demographic rates, we derived a local, low-density growth rate r as an overall measure of population

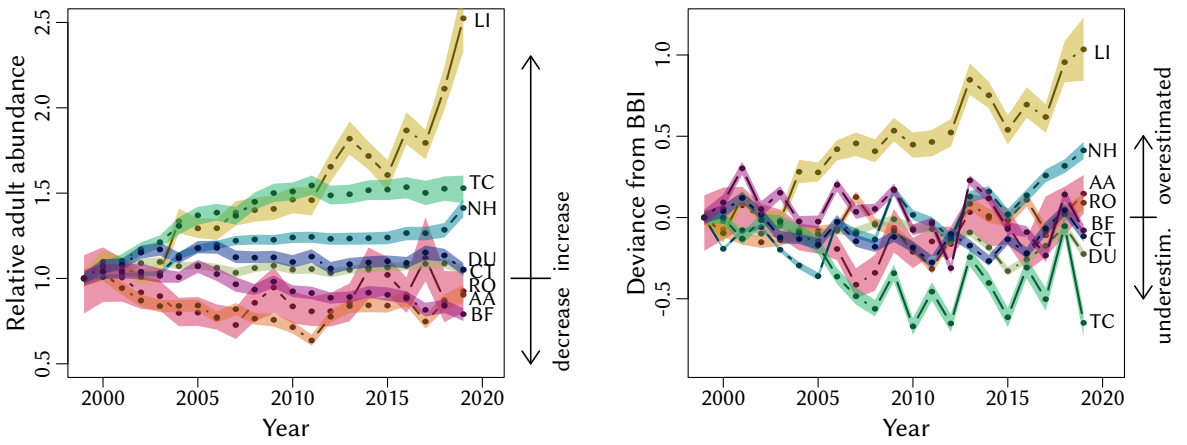

Figure 4.2.: Time series of simulated relative adult abundance (left) and their deviation from the Swiss breeding bird index (BBI, right), with 1999 (the first year of MHB data) as reference year. Shown are the median and the 80% credible interval. BF - Bullfinch (pink); CT - Crested tit (dark blue); TC - Eurasian treecreeper (dark green); NH - Eurasian nuthatch (light blue); DU - Dunnock (light green); LI - Common linnet (yellow); RO - Ring ouzel (orange); AA - Alpine accentor (red). Fig. C.1 shows the 95% credible intervals.

performance. It was given by the leading eigenvalue of the transition matrix (as the population-based equivalent to our IBM), $r = s_a/2 + (s_a^2/4 + s_j\,\rho)^{-1/2}$. As a measure of vulnerability to climate change, we assessed the partial response of r to the observed changes in each climate variable individually (Table 4.2). For this, we compared a base growth rate, given as the value predicted at the median value of all predictors, with those for which a single predictor was changed. The amount of considered climatic change was determined from the linear trend in each predictor, accumulated over the twenty years of survey data (1999-2019). Thus, the vulnerability indicator combines the effects from both the sensitivity of the growth rate to climate change and the amount of exposure. However, it takes into account only the isolated effect from one predictor, while there are likely interactions between the impacts of different aspects of climate change. As an overall indicator of climate change impact, that simultaneously considers all predictors as well as their interactions, we used the full IBM to generate abundance projections under two scenarios: The factual, observed climate scenario and a counter-factual no-climate-change scenario, which consisted of trend-corrected predictors to simulate a stationary climate. The impact measure was then given by the ratio of projected mean adult abundance over the years 2017-2019 under the scenarios of actual versus stationary climate.

4.4. Results

The goodness-of-fit and discriminatory power of the posterior predictions was assessed using RMSE and the spatio-temporal c-index for all species. The RMSE ranged from 1.3 to 5.7 (Table C.3). The spatio-temporal c-index ranged from 72% to 88% (Table 4.2), indicating moderate to excellent model fit depending on the species. The two measures ranked models in a different order but the model for alpine accentor scored best in both. Separately considering the spatial and temporal predictive accuracy (Table C.3) showed that all models had good to excellent accuracy in the spatial predictions, as the spatial AUC ranged from 74% to 89%, but less and more variable temporal predictive accuracy, with the temporal c-index ranging from 42% to 80% (Table C.3). The IBM projections of total adult abundance are shown in Fig. 4.2 (left), relative to the initial year when the MHB was launched (1999). The models for linnet, treecreeper, and nuthatch predicted increasing trends, while stable or slightly declining trends were predicted for the remaining species. Those three models also showed the largest deviations from the Swiss breeding bird index, which indicated under-predicted abundance for the treecreeper and over-predicted abundances for linnet and nuthatch (Fig. 4.2, right). Interestingly, the temporal c-index, which considers the local abundance time series at all sites instead of the total Swiss abundance time series, is highest for these three models. Comparing to the SDMs and DOMs presented in Briscoe et al. (2021), our IBMs showed lower spatial predictive accuracy in terms of spatial AUC (Table C.3). By contrast, the IBMs exhibited consistently higher temporal predictive accuracy than SDMs in terms of temporal c-index. Considering DOMs, our IBMs improved the temporal c-index by more than 20% for nuthatch and linnet, and achieved similar or slightly lower temporal predictive accuracy for the other species (Table C.3).

The conditional response plots of all six demography-climate relationships (DCRs) are shown in Fig. 4.3, with the three response rates in rows and their respective temperature and precipitation predictors in columns (separate DCRs per species are shown in Fig. C.2). For each species, the DCRs were evaluated over their core occupied climatic range (given as the central 80% quantiles), while the respective second predictor is held constant at its median. The fecundity-temperature DCR indicated a trend of lower fecundity with increasing breeding season temperatures. Most species showed a monotonically decreasing relationship, though for the treecreeper and nuthatch it was almost constant, and only the linnet exhibited a clear unimodal response with an optimum at around 10°C. The fecundity-precipitation DCR showed weak unimodal responses for bullfinch, crested tit and ring ouzel with optima around 150 mm, and a pronounced unimodal response for

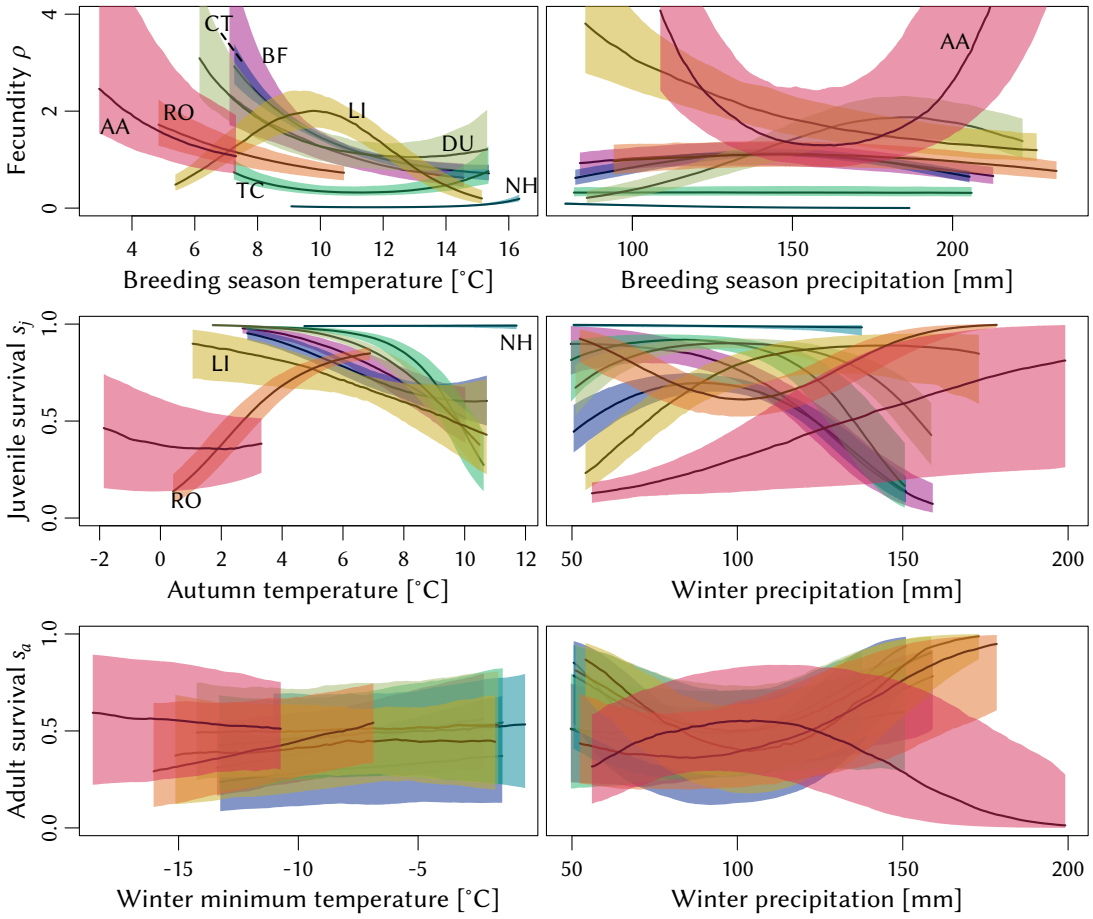

Figure 4.3.: Demography-climate relationships for all species, evaluated over their respective typical climatic ranges. Shown are the median and 80% credible interval. BF - Bullfinch (pink); CT - Crested tit (dark blue); TC - Eurasian treecreeper (dark green); NH - Eurasian nuthatch (light blue); DU - Dunnock (light green); LI - Common linnet (yellow); RO - Ring ouzel (orange); AA - Alpine accentor (red). Fig. C.2 shows the single DCRs with both 80% and 95% credible intervals.

the dunnock with an optimum around 190 mm. Surprisingly, for the alpine accentor this relationship was bimodal (two optima at the boundaries of a steep inverted parabola), which is physiologically implausible. The DCRs for juvenile survival exhibited high values around 6°C mean autumn temperature for all species apart from the alpine accentor and around 100 mm total winter precipitation for all species apart from the alpine accentor and linnet. We found a monotonically decreasing response of juvenile survival to mean autumn temperature for most species except the nuthatch and ring ouzel. Its response to

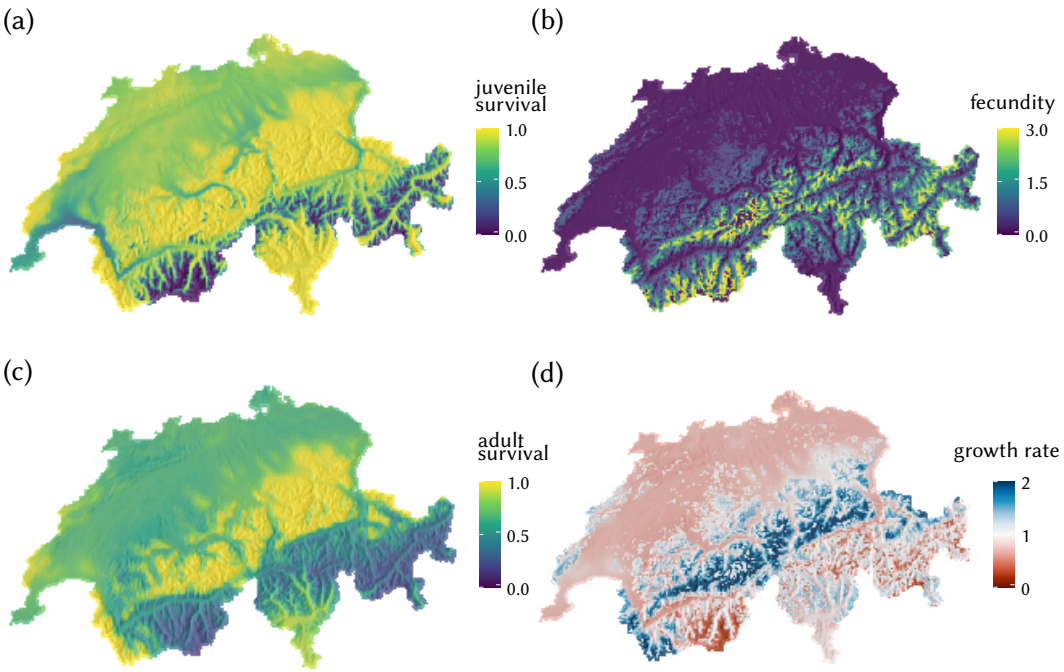

Figure 4.4.: The three demographic rates juvenile survival (a), fecundity (b), adult survival (c), and the resulting growth rate at low densities (d) for the ring ouzel in year 2018. In (d), red/blue shades indicate growth rates below/above unity (the value indicating population stability).

winter precipitation was strong and monotonically decreasing for the bullfinch, unimodal for the crested tit, treecreeper, and dunnock, and monotonically increasing for the linnet and alpine accentor. The ring ouzel exhibited a bimodal response. The DCRs for adult survival were overall weaker and more uncertain than those for fecundity and juvenile survival. The relationship between adult survival and minimum winter temperature was fitted with only a first-order polynomial (Table 4.1) and results indicated a weak but consistent positive trend for most species. Only the alpine accentor, a typical mountain bird, exhibited a constant or slightly decreasing relationship with temperature, which may be attributed to its adaptation to low temperatures. The DCR of adult survival with winter precipitation showed slight bimodal responses for the crested tit, nuthatch, dunnock and linnet that could be deemed physiologically implausible. The alpine accentor showed a unimodal response with an optimum at around 100 mm, and bullfinch, treecreeper and ring ouzel showed slightly increasing adult survival with winter precipitation. We discuss possible explanations for these physiologically implausible DCRs and give remarks on their interpretation in the discussion.

To better understand the interplay of the different demographic processes, we summarised the three demographic rates obtained from the DCRs to a density-dependent growth rate *r*. A species can persist only in regions where the climatic conditions allow for sufficient growth. Fig. 4.4 (a-c) show illustrative maps of each demographic rate and Fig. 4.4 (d) presents the resulting growth rate at low density (i.e., at one breeding pair per 1 km^2) for the ring ouzel in 2018. The map of growth rates highlights areas of negative population growth ($r < 1$) and those of positive growth ($r > 1$), thus providing an assessment of demographically suitable areas. For example, in the northern Alps all three demographic rates largely coincided in exhibiting high values, which resulted in positive growth of ring ouzel. In contrast, some areas in the southern Alps showed high fecundity but low survival probabilities, which resulted in a negative population growth.

To assess the impact of the observed climate change on the study populations, we examined two measures of population response (Table 4.2): First, we calculated the change in low-density growth rate caused by the change of individual climate predictors that was observed over the survey period (second row in Table 4.2). According to this analysis, the most influential climate predictors were the mean temperature during breeding season, T_{br}, which tended to decrease population growth, and precipitation during winter, P_{wn}, which tended to increase population growth. The bullfinch and crested tit were consistently disadvantaged by the change in climate predictors, while the nuthatch benefitted. Other species experienced mixed effects from the changed climate predictors on their growth rates, such as alpine accentor and ring ouzel which were adversely affected by the observed trends in T_{br}, but gained from increases in P_{wn}. Secondly, we compared abundance predictions for the years 2017-2019 under the scenarios of observed climate versus no-climate change (last column in Table 4.2). According to this analysis, some species showed lower current abundances than would have been expected under a no-climate change scenario (bullfinch, crested tit, treecreeper, dunnock). The remaining species exhibited higher predicted current abundances (nuthatch, linnet, ring ouzel, alpine accentor) indicating that these species profited from climate change. Presumably, this benefit was primarily driven by increased winter precipitation. However, a predicted positive effect of climate change on abundance did not necessarily result in increasing populations. For example the ring ouzel and alpine accentor showed slight negative trends even under the more favourable scenario of observed climate change (Fig. 4.2).

4.5. Discussion

Spatio-temporal changes in species abundance result from a complex interplay of multiple ecological processes and environmental drivers. In this study, we analysed the range and population dynamics of Swiss breeding birds using spatially explicit, individual-based models (IBMs) that included demographic and dispersal processes. We used a generic modelling framework and Bayesian calibration to jointly infer these processes and their demography-climate relationships (DCRs) from survey data. This procedure allowed us to disentangle the effects of recent climate change on observed range and population dynamics and to determine if population trends were positively or negatively affected. Yet, results also indicated that care must be taken when interpreting the fitted DCRs as they need to be investigated closely for physiological plausibility. Implausible response shapes can indicate missing or misrepresented ecological processes, missing environmental predictors, or a lack of data to confidently separate the processes. Overall, our framework shows great promise for fitting process-based models to survey data and for attributing observed population trends to ecological and environmental processes (Gonzalez et al., 2023). It thus helps improving our mechanistic understanding of range dynamics under climate change and pinpointing missing knowledge.

The increasing availability of long-term monitoring data allows fitting and validating complex process-based population models (Briscoe et al., 2021; Fordham et al., 2018). In this study, we inversely parameterised IBMs based on long-term, nation-wide survey data in Switzerland. Importantly, our framework extends previous approaches (Pagel & Schurr, 2012) by allowing higher flexibility in the representation of demographic processes. Our models explicitly included crucial factors such as density-dependence and climatic impacts on demographic rates (Ehrlén & W. F. Morris, 2015). At the same time, simplifying assumptions were made to obtain parsimonious models that were able to broadly capture the observed abundance patterns. This included describing the transfer phase with a dispersal kernel and employing a relatively simple stage-structured, female-only population model (Caswell, 2000). Modelling only the female part of the population was justified by assuming that reproduction is not limited by adult male abundance, considering that the modelled species breed in pairs and birds show a balanced or even male-skewed adult sex ratio (Donald, 2007). Apart from this, a female-only model does not explicitly consider Allee effects and can be thus expected to perform better for populations with high rather than low densities. The presented framework, however, can accommodate other modelling assumptions than those exemplified here, since it is generic and flexible. It uses openly available tools and can thus be readily applied to other populations.

Table 4.2.: Model evaluation results for each species (column 1). The spatio-temporal c-index (a rank correlation index, column 2) measures prediction accuracy in terms of discriminatory power. Column 3 states the low-density growth rate at median predictor values and columns 4 to 8 give its partial response to the observed trend in each climate variable. Details are given in the methods section. Colours code for strength of response, where grey denote little to no effect (less than 5% change), light red/blue denote small decrease/increase (more than 5% change), and dark red/blue denote strong decrease/increase (more than 10% change) in growth rate. The last column gives the ratio of simulated adult abundance under scenarios of observed and missing climate change. Given are the median and 80% credible interval.

	c-index	r_{med}	T_{br}	P_{br}	T_{at}	T_{wn}	P_{wn}	abund. change
absolute change			+1.0 K	−11.6 mm	+1.1 K	+1.5 K	+29 mm	
Bullfinch	0.80	1.20	0.93	1.00	0.96	1.02	0.89	0.85 (0.83-0.90)
Crested tit	0.75	1.05	0.94	0.97	0.97	1.01	0.98	0.80 (0.79-0.80)
E. treecreeper	0.77	0.84	1.02	1.00	0.97	1.01	0.98	0.94 (0.90-0.99)
E. nuthatch	0.74	0.56	1.07	1.04	1.00	1.03	1.10	1.07 (1.07-1.08)
Dunnock	0.73	1.32	0.97	0.90	0.96	1.00	1.02	0.90 (0.89-0.91)
Common linnet	0.72	1.43	1.03	1.05	0.97	1.01	1.10	1.24 (1.24-1.25)
Ring ouzel	0.82	1.05	0.95	1.00	1.07	1.02	1.21	1.13 (1.10-1.20)
Alpine accentor	0.88	1.05	0.95	0.97	1.00	0.99	1.04	1.10 (1.05-1.13)

When validating our spatio-temporal predictions against observations, our models achieved moderate to excellent predictive accuracy, with the highest performance for the alpine accentor. We also evaluated the ability of our models to predict the adult abundance time-series against the independently derived Swiss breeding bird index and found adequate fit of the temporal dynamics for most species. We compared our results to the findings of a recent study (Briscoe et al., 2021), that evaluated the performance of correlative species distribution models (SDMs) and dynamic occupancy models (DOMs) for predicting range dynamics of Swiss breeding birds. DOMs represent local occurrence as a result from colonisation and extinction dynamics, but do not explicitly consider dispersal. Briscoe et al. (2021) found that SDMs made more reliable spatial predictions, but DOMs provided superior temporal predictions of occupancy dynamics. Our results corroborate and generalise these findings, showing that dynamic population models which explicitly consider demography and dispersal can provide more accurate predictions of range and population dynamics than other currently used approaches. Still, SDMs provided better spatial predictions of occupancy and our IBMs improved the temporal predictions over DOMs only for a few but not all species. In part, this can be explained by the fact that our IBMs used fewer predictors and instead imposed structure through specific assumptions

on the causal demographic-ecological processes. Its predictions are therefore expected to fit less closely to training data and in turn perform better on extrapolation. Further, the underlying heuristic habitat maps were based only on published trait data of main habitat preferences and may be overestimating the amount of suitable habitat. The preferences were given in terms of coarse habitat classes, such as deciduous or coniferous forest, while the true habitat preferences may be much more specific and met in only a smaller subset of the identified habitat areas. Lower predictive accuracy compared to DOMs could also be related to structural uncertainty in our models. For example, the fecundity DCRs of nuthatch and treecreeper were mostly constant in both predictors such that all spatial variation in fecundity originated from the habitat maps, possibly indicating missing environmental predictors. Overall, our results demonstrate that dynamic models that are sufficiently flexible to reflect main abundance patterns can improve predictions of range dynamics.

The calibrated DCRs allow to investigate how demographic processes vary with climate. When interpreting the individual DCRs, it is important to consider the specific role of the respective demographic rate within the model. In our IBMs, juvenile and adult survival rates represent primarily winter and autumn mortality but do not account for dispersal mortality. The latter is instead represented by failed dispersal events and was modelled as climate-independent. Thus, effective annual survival is lower than suggested by the DCRs and resulting local population dynamics alone. Further, fecundity described the number of independent juveniles produced per breeding pair and year. It therefore subsumes factors such as the number of broods per year and early juvenile mortality. Most fitted DCRs showed monotonous or unimodal relationships. For example, fecundity decreased with above-median temperatures during breeding season for all species. Maximum juvenile survival was surprisingly high, approaching 100% for some species. This seems unrealistic even under favourable climatic conditions as juveniles of most species typically experience higher mortality in their first winter compared to adults. In the context of our model structure, however, high apparent juvenile survival rates could be compensating for high simulated dispersal mortality. Thus, in order to compare survival rates of our models against empirical estimates, the number of juveniles lost during dispersal needs to be discounted. With respect to parameter uncertainty, DCRs of fecundity and juvenile survival were more certain and had smaller credible intervals than DCRs for adult survival. This suggests that fecundity and juvenile survival indeed depended strongly on climate, while adult survival may be mediated by additional processes.

Explicit consideration of demographic responses to environmental factors can improve our mechanistic understanding of species niche and range dynamics Schurr et al., 2012;

Pagel & Schurr, 2012. Despite the advantages of mechanistic models, however, they are often difficult to parameterise. For this, inverse parametrisation can make use of commonly available data such as abundance and occurrence data. Here, all DCRs were calibrated to observed abundance data, and population dynamics emerged from the combined effect of the three demographic processes together with dispersal. Their interactions can entail limited identifiability of parameters from the available data, if the same abundance patterns arise from different combinations of survival and fecundity values. This increases the uncertainty of parameter estimates (Oberpriller et al., 2021), leading to uncertain DCRs, and additional data may be needed for successful calibration. Further, structural model error can be present where the modelled processes do not correspond to the true ecological processes. In such cases, the calibration may compensate for flawed modelling assumptions and lead to unexpected DCR shapes (Oberpriller et al., 2021). The inversely fitted DCRs are therefore still phenomenological and their transferability should be interpreted carefully. For instance, some fitted DCRs were bimodal with two optima at the extremes of their climatic range. This was found for the fecundity-precipitation DCR of the alpine accentor and the juvenile survival-precipitation DCR of the ring ouzel. Such a relationship is physiologically implausible as demographic rates typically peak within certain climatic limits. A possible explanation for the alpine accentor is that the assumed fecundity-habitat relationship may not hold and the DCR attempts to compensate for low realised fecundities at the range margins, where low habitat suitability is projected. With respect to the ring ouzel, the local winter conditions may be poor predictors of survival since large parts of their Swiss population migrates during winter. Also, for most species, the relationships of adult survival with winter precipitation was slightly bimodal. This can be a result from interactions among adult survival and juvenile survival, which shared minimum winter temperature as a common predictor. These two DCRs tended to be negatively correlated for most species, apart from ring ouzel and alpine accentor, which supports this hypothesis. Such a negative correlation was also found by Dybala et al. (2013), who modelled the impact of climate change on the demography of song sparrows in California. Tavecchia et al. (2016) showed that climate-driven vital rates do not necessarily imply climate-driven population dynamics, especially in highly mobile species, as trade-offs can mask the changes in underlying processes. Further, an example for a potential missing mechanism are negative species interactions (Schultz et al., 2022), which can confound the value of a DCR, especially towards the range margins. Therefore, we advise that extrapolation to non-analogue climatic conditions outside the sampled range of training data should only be attempted if the fitted DCRs appear plausible. Importantly, despite limitations in interpretability and transferability of individual DCRs, their combined effects within

the full model simulations were still able to reproduce the observed abundances and yield moderate to excellent model predictions. Thereby, DCRs facilitate an improved mechanistic understanding of the underlying processes and potentially missing information, which offers substantial advantages over simple hybrid models (Pagel & Schurr, 2012; Zurell et al., 2016).

Our presented model framework allows complex assessments of the factors and mechanisms that underlie model predictions. By combining the demographic rates to an overall growth rate, we can better understand the causes for demographic suitability of different geographic regions and compare interpretations across different model frameworks. For example, we found that the ring ouzel was predicted to generally persist in high altitudes where fecundity is high enough, but that some of these high-altitude areas are climatically unsuitable due to high winter mortality. According to Barras, Braunisch, et al. (2021), future losses in abundance are expected especially in the northern Alps, where we predicted highest current growth rates, and gains in abundance are expected in the central Alps, where we predicted lowest current growth rates. To assess the impacts of observed climatic changes on the demographic performance of the studied species, we considered two measures of climate vulnerability. First, evaluating the conditional impact of each climatic predictor identified breeding-season temperature and winter precipitation as the most influential variables. This impact is a combined effect of the magnitude of already observed climate change and the sensitivity of the growth rate to them. However, more targeted investigations are needed to understand the biological pathways by which a given abiotic factor controls an ecological process. For example, Barras, Niffenegger, et al. (2021) explained for ring ouzel that elevated temperatures during breeding negatively impacted the feeding of chicks by parents. Indeed, our model confirms a negative effect of breeding-season temperature on growth rate for this species. Also, our predicted current growth rate (1.05) coincides with the one measured by Barras, Blache, et al. (2021) (1.04). Second, comparing the simulated abundances under observed climate with a no-climate change scenario, we were able to estimate the degree to which predicted abundance trends could be attributed to recent climate change. Such analyses are useful to understand the overall direction of the combined effects of climate change on populations. For example, ring ouzel and alpine accentor show slightly declining population trends, both in the breeding bird index and in our projections. However, our models indicated that predicted abundance was still higher then in the no-climate change scenario, implying that both species would experience even stronger population declines without recent climate change. Overall, our models suggested that typical mountain species tend to benefit from recent climate change (without necessarily amounting to positive population trends), while lowland species are

already negatively affected by climate change. We do not expect the positive effects for mountain species to last far into the future, as climatic changes become more pronounced. In fact, while we assessed the effect of contemporary climate change only, the vulnerability of Swiss breeding birds to future climate change was investigated previously by comparing current climatic conditions with those in 2100 (Maggini et al., 2014). According to their predictions, alpine accentor and ring ouzel will suffer strong range contractions until the end of this century. Here, correctly identified DCRs can help to identify promising avenues for effective management. By explicitly investigating how individual demographic rates are affected by climate change, targeted measures can be designed to support these vulnerable processes and mitigate climate change effects.

Given the broad impact of climate change on ecological processes, we urgently need better predictions. Our study demonstrates that calibrating detailed, process-based models from survey data is feasible and can improve predictions of spatio-temporal range and population dynamics over other modelling approaches. Further, explicitly modelling the responses of separate demographic rates to climate allows to develop a mechanistic understanding of the differential effects of contemporary climate change. Yet, it is important to acknowledge that our model framework relies on confining modelling assumptions and inverse parameterisation. It is therefore still phenomenological to a certain extent and the resulting demography-climate relationships need to be interpreted cautiously. Specifically, they should be inspected for plausibility before making predictions into the future or drawing conclusions for targeted conservation management. For future research, we advocate a stronger integration of experimentally or empirically measured DCRs, for example by adding such information as strong informative prior in the Bayesian calibration. In order to determine appropriate model structures for modelling climate change responses, more abiotic and biotic mechanisms should be tested for example by considering additional environmental predictors and alternative model structures. Ultimately, this will increase our confidence for drawing conclusions on the mechanisms underlying complex range and population dynamics and making predictions into the future.

Chapter 5

Discussion

5.1. Spatial models for decision making

Significance

As the impacts of human activities on Earth's ecosystems are accumulating, our awareness grows that the planet's resources are finite. The limits of a safe operating space for humanity, within which sustainable and just human development is possible, are explored by the planetary boundaries framework (Rockström et al., 2009; O'Neill et al., 2018). The boundary on biosphere integrity is still difficult to delineate, but research suggests that anthropogenic impacts have already caused a persistent loss in biodiversity and ecosystem productivity (Steffen, Richardson, et al., 2015). To counter this development, global efforts are being conducted to protect and recover biodiversity and thus to "bend the curve" away from continued biodiversity loss (IPBES, 2019). Examples include the UN decades on biodiversity (2011-2020) and ecosystem restoration (2021–2030) and the 2050 Vision for Biodiversity by the Convention on Biological Diversity (CBD, 2020).

The design of efficient conservation actions is dependent on reliable prediction of the current and future state of biodiversity. This encompasses the aspects of biodiversity on all ecological levels, from genes to communities, as they are considered to be crucial determinants of biosphere resilience (Folke et al., 2004; Oliver et al., 2015). To be able to provide such comprehensive and reliable predictions, cross-scale and process-based models as well as the data required for their parameterisation are urgently needed (Purves et al., 2013).

The work documented in this thesis provides a step towards this goal; a step that can appear small compared to the size of the overall objective, but not an insignificant one. I have made a contribution to promote the use of process-based species distribution models

(SDMs) for population assessments in a way that is efficient and provides meaningful outcomes. To this end, I have co-developed an individual-based modelling platform that jointly simulates three key ecological processes – population dynamics, dispersal, and heritable adaptation – and made it available for the widely-used programming language R. Thanks to its modular structure, the platform is readily used to compose individual-based models (IBMs) of given specifications. I have further provided a comprehensive case study that demonstrates how the platform can be used to build, calibrate and validate an IBM using literature and monitoring data. It discusses the interpretation of calibrated parameters and shows how the fitted model can be applied to make projections that include quantified uncertainties. The presented modelling workflow can be adopted for other species for which heterogeneous data sources are available. Finally, I showed that the modelling platform can be used to assess climatic suitability for a species and to detect climate change effects on current populations that can be attributed to specific climatic drivers. Such assessments can help to identify potential conservation pathways to mitigate climate change impacts.

The methods presented in this thesis are widely applicable. They constitute a complete modelling workflow for process-based models from specification, parametrisation, and calibration to validation, interpretation, and attribution. However, further advancements and generalisations are possible and needed. Yet, they have the potential to support the proposed shift towards process-based modelling for informing spatial conservation planning in an uncertain future.

Towards dynamic modelling

Currently, the models used for spatial predictions mostly rely on the detection and extrapolation of statistical correlations between observed current species distributions and their abiotic environment. In a recent review (Zurell et al., 2022; Appendix A.1), we found that the large majority (79%) of published studies with a clear management application used static models, most of which were correlative SDMs. However, static models in general are unfit to model the dynamic responses of species' to global change. Specifically, correlative static models are expected to become unreliable under future, changing conditions, as the fitted correlation structure is unlikely to be conserved.

In view of this discrepancy, we tested whether dynamic models can improve the prediction of species range dynamics (Briscoe et al., 2021; Appendix A.2). To this end, we compared dynamic occupancy models with static correlative models, using long-term monitoring data for 69 Swiss breeding birds (Schmid et al., 2004). Dynamic occupancy models represent the colonisation-extinction dynamics on a spatially-implicit patch-matrix land-

scape and can account for imperfect detection. In our test study, these models significantly outperformed static correlative models in predictive performance of future occupancy (Briscoe et al., 2021).

Recommendations for practical modelling

To address further typical shortcomings in current modelling practice, we compiled five recommendations to enhance the use of spatially-explicit models for decision making in animal conservation and restoration (Zurell et al., 2022; Appendix A.1). In this thesis, I attended to the first three recommendations: "1) developing a toolbox with multiple, easier-to-use methods, 2) improving calibration and validation of dynamic modelling approaches and 3) developing best-practise guidelines for applying these models" (Zurell et al., 2022). With RangeShifter 2.0 (Bocedi et al., 2021; Appendix A.3) we have developed an accessible software for individual-based eco-evolutionary modelling, that extends the toolbox of open-source software developed by the ecological research community. To make it integrable into workflows in R, I developed the RangeShiftR package that implements an interface to the RangeShifter 2.0 model and contains auxiliary functionality (Malchow et al., 2021). My case study of the red kite addresses recommendations 2 and 3, as it demonstrates an integrated workflow for the application of RangeShiftR to a conservation-relevant population (Malchow et al., 2022). It combines Bayesian calibration to monitoring data and a spatial-block cross-validation. With this, the workflow can provide transparent assessments of prediction uncertainty and predictive performance by consistently propagating uncertainties from the input data to the model predictions and subsequent validation with independent data. These assessments form the basis to producing trustworthy predictions, which are urgently needed to support decision-making. The RangeShifter IBM (Bocedi et al., 2014; Bocedi et al., 2021) has already been successfully applied in many theoretical and empirical studies (e.g. Henry et al., 2017; Ovenden et al., 2019; Hunter-Ayad & Hassall, 2020; Bleyhl et al., 2021), providing proof of its practicability.

5.2. Extending the model

RangeShifter as a hybrid model

The original RangeShifter model runs on gridded landscapes that contain values of habitat suitability for the study species. These habitat landscapes can be derived from correlative SDMs or from habitat preferences. Within each cell, RangeShifter stochastically models local population dynamics that can consider complex stage-structures and density-dependencies on each demographic process (fecundity, survival and development).

Modelling local abundance instead of only occurrence has significant advantages, as abundance determines the strength of density-dependent effects (e.g. on dispersal) and mediates the function a species assumes in its local community through inter-specific interactions (Ehrlén & W. F. Morris, 2015; Johnston et al., 2015). Additionally, RangeShifter explicitly models a detailed dispersal process that is organised in three phases: emigration, transfer and settlement (J. M. J. Travis et al., 2012), where the transfer phase can be represented by a complex movement model. Since range shifts are understood to arise from an interplay of demography and dispersal, this setup is adequate to model them (Hastings et al., 2005; J. M. J. Travis et al., 2013). In this form, RangeShifter can be seen as a type of hybrid model (Franklin, 2010), though these are usually implemented as population-based models (Fordham et al., 2013) and can not include individual behaviour such as in movement processes.

Multiple predictors

By considering a one-layered landscape of habitat suitabilities to drive the simulated population and dispersal dynamics, RangeShiftR assumes that these processes are influenced by the environment in a common way. The suitability values are often derived from multiple environmental predictors, e.g. via a correlative SDM, and hence reflect a fixed combination of effects. Because of this dimension reduction, differential effects of predictors on the various ecological processes can not be represented. However, fundamental demographic processes such as fecundity, growth, and survival can have specific responses to various aspects of local environmental conditions (Selwood et al., 2015). For example, Bonnot et al. (2018) detected a response of breeding productivity to temperature in north-american forest birds and Dybala et al. (2013) found that in song sparrows adult and juvenile survival responded differently to temperature and precipitation. To investigate such demography-environment relationships, I extended the RangeShifter model so that multiple, climatic predictors could independently influence each demographic rate via a linear model (Malchow et al., 2023, Chapter 4). The established functional relationships between climate and demography allow to disentangle the constituent processes that determine local species persistence and link them to climatic variables (Ehrlén & W. F. Morris, 2015; Hansen et al., 2016).

Individual-based adaptation

RangeShifter additionally models a process that requires to resolve a population at the individual level: intra-specific variation (in dispersal traits) that is heritable and thus allows for local adaptation (Henry et al., 2013). This additional component can be crucial to realistically model range dynamics (DeMarche et al., 2019), as species are understood

to have three options for responding to changing conditions: ”move, adapt or die”. The first and last are commonly considered in models by including local population dynamics and dispersal, but adaptation mechanisms are often missing. Adaptation can happen behaviourally (Beever et al., 2017) or genetically by evolution (Diamond, 2018), where behaviour tends to change on smaller time scales, but also cases of rapid evolution have been observed. For example, local adaptation in life-history traits can buffer negative effects on population dynamics (Jensen et al., 2008). Expanding or invasive populations that can show accelerating spread caused by local adaptations (Whitney & Gabler, 2008). A prominent example is the invasion of cane toad in Australia, where individuals at the leading range edge exhibited higher dispersal rates due to rapid evolution of dispersal and life history traits (Perkins et al., 2013). This shows that not only the effects of single ecological processes are important to consider, but that their interplay can give rise to observed spatial dynamics.

RangeShifter offers the technical capability to represent such interactions, but individual trait variation is difficult to parameterise because the required data is rare and costly to obtain. For this reason, I did not apply the genetics module of RangeShifter in my study on demography-climate relationships (Chapter 4), although the demographic response to climate variation is assumed to be shaped by adaptation, especially at the trailing range edge (Sunday et al., 2012; Comte et al., 2014). Including this effect in the model would allow to infer dynamic demography-climate relationships, which would further improve our mechanistic understanding of range shifts.

Missing interactions

RangeShifter integrates many key eco-evolutionary processes that are considered to be crucial for modelling range dynamics (Urban et al., 2016). An important process that is still missing, however, are species interactions (Araújo & Luoto, 2007; Brooker et al., 2007; Zurell, 2017). Empirical evidence for competition in plants, for example, was found by Sanczuk et al. (2022) and Schultz et al. (2022). Multi-species extensions to correlative SDMs, so-called joint SDMs (Pollock et al., 2014), already exist and are increasingly applied. Further, community models that consider population dynamics in complex interaction networks have been investigated (Carrara et al., 2015). In a theoretical study, for instance, we showed that the ratio of mutualistic to antagonistic interactions can determine the demographic stability of an interaction network (Emary & Malchow, 2022, Appendix A.4). Such models are usually non-spatial, however, and spatially-explicit process-based models that incorporate inter-specific interactions are still rare. Individual-based models are a promising tool for this (J. Travis et al., 2005), as species interactions are considered to take

effect on small scales and can be trait-dependent.

Inter-specific interactions do also interact with other ecological processes such as adaptation (Gandon & Michalakis, 2002) and dispersal (Ettinger & HilleRisLambers, 2017), as species interaction networks can be disrupted due to mismatches in species responses. For example, differences in range shifts can cause spatial mismatch while differential phenology shifts entail temporal mismatches (Both et al., 2006).

A full model

The complexities that arise from multiple interacting mechanisms can only be resolved by a model that jointly represents all relevant processes on their respective ecological and spatio-temporal scales. In an article that originated from a workshop on biodiversity modelling at the McGill University in Montreal, Canada, we conceptualised a platform for global biodiversity modelling (Urban et al., 2022; Appendix A.5), that harmonises existing modelling frameworks and allows concerted model building efforts by the ecological research community. Such a platform would be dependent on the collaboration of practitioners and researchers around the world to compile the necessary data, codes and analyses, but it would provide us with a powerful tool to project and protect global biodiversity.

5.3. Accessibility

Modelling tools

The models that are designed and developed are only useful if they are applied. A major determinant of applicability is accessibility. This encompasses both the availability of the software itself and its usability.

Software availability is greatly increased by the growing use of free open-source licensing (and especially copyleft licensing, which preserves the openness even for derivatives of a software). It makes the software available to anyone for free and allows for public collaboration. This has also been facilitated by the wide-spread use of the programming language R (R Core Team, 2023) in ecology, which follows the copyleft philosophy and only accepts copyleft software on its package archive CRAN. Many packages for spatially-explicit ecological modelling are published there, such as the pioneering bioclim for bioclimatic envelope models (Booth et al., 2014), sdm and zoon for correlative SDMs (Naimi & Araújo, 2016; Golding et al., 2018), hmsc for joint SDMs (Tikhonov et al., 2020), migclim for a hybrid model (Engler et al., 2012), and steps for a flexible spatially-explicit population model (Visintin et al., 2020). RangeShiftR is the only R-package that implements a modular,

eco-evolutionary IBM for R.

With NetLogo and HexSim, other, stand-alone and closed, software platforms for individual-based modelling exist, but they are not specific to ecological modelling. Both have a companion R-package to facilitate model building and analysis of outputs in R.

As a ready-to-use ecological modelling platform, RangeShiftR puts a large emphasis on its usability. The package comes with extensive built-in help pages. The web page hosts a number of extensive, step-by-step tutorials that guide through the RangeShiftR functionality and provide an easy start. Further, a comprehensive user manual is provided, in English and Spanish language. Within the RangeShifter team, we have designed and conducted workshops to help students, researchers and practitioners to apply the model for their case study. Further, we are planning to prepare a how-to guide that covers the necessary considerations and practical steps to build an adequate RangeShifter model.

Data accessibility

The need for accessibility also extends to data sources. Complex, process-based models require diverse and reliable data for their parameterisation. This can include data from experiments, monitoring schemes, or citizen science initiatives, but too often there are high barriers in terms of accessibility and effort needed for data cleaning and harmonisation. A framework for scientific data management, that addresses these issues, is given by the FAIR principles - Findable, Accessible, Interoperable and Reusable (Wilkinson et al., 2016). Good examples for this are given by the COMPADRE and COMADRE databases of demographic rates for many plant and animal species. They provide a valuable data source for process-based population models.

5.4. Bayesian calibration

Creating a model encompasses not only the specification of the modelled processes, but also their parametrisation. With my case study of the red kite (Chapter 3), I have provided a workflow for the integrated parameterisation from direct and indirect knowledge using Bayesian calibration.

The likelihood function

The likelihood function is a central element in a Bayesian calibration as it links direct and indirect knowledge via a data-generating model. For complex processes, this data-generating model can usually not be expressed in a closed mathematical form, because the correlation between stochastic sub-processes and hidden states can not be tracked. Instead, the data-generating model can be expressed by a stochastic simulation model,

that explicitly evaluates all sub-processes (Hartig et al., 2011). Here, individual-based models are powerful tools, because the sub-processes can be resolved to a level where the intrinsic uncertainties are assumed to be known. For example, in RangeShifter, the survival process is modelled by a Bernoulli trial and reproduction by a draw from a Poisson model. The resulting uncertainties and their correlations are propagated through to model projections by the IBM. This also means that a Bayesian inference is conditional on the specified likelihood function, and the efficiency by which information is extracted from the data depends on the adequateness of the data-generating model.

Sensitivity analysis

A vital step in the modelling workflow is sensitivity analysis (Saltelli et al., 2006; Christopher Frey & Patil, 2002). A local, one-factor-at-a-time sensitivity analysis should be performed first. It can act as a check of the model setup as it shows whether the model responds reasonably to changes in single parameters. The local should be followed by a global sensitivity analysis that can take correlations between sensitivities into account. In the context of calibration, specifically, a sensitivity analysis of the likelihood function using simulated data is recommendable. The sensitivity of likelihood translates to identifiability of the parameter in the inverse setting, so that parameters, to which the likelihood is sensitive, can be expected to be informed by the data. However, it is important to note that the may be significant differences in parameter identifiability between the simulated data used for sensitivity analysis and the calibration data.

Calibration interpretation

In my case study, the RangeShiftR red kite model could be successfully calibrated from the utilised data. The information for the direct parameterisation was gleaned from published and unpublished data and consolidated with expert knowledge. The data for inverse parameterisation was taken from the Swiss breeding bird survey. The inclusion of this indirect knowledge considerably strengthened the parametrisation, as shown by a comparison of prior and posterior predictions: The posterior predictions replicated independent validation data and had much smaller uncertainties.

The results of a successful calibration can be used to draw conclusions from the difference of posterior and prior estimates, i.e. from the information that was extracted from the calibration data. However, care must be taken when interpreting such parameter corrections as a modelled processes can take an unintended role within the model under calibration, for example when it compensates for unrepresented processes.

Additional considerations

An important advantage of Bayesian parameter inference is that it works consistently even with small amounts of calibration data. The less informative the data is, the more weight will the direct parametrisation have in the final calibration. Further, this property makes it possible to quantify the amount of data needed to reach a given maximum level of uncertainty (Leung & Steele, 2013). A considerable disadvantage can be presented by the technical implementation of a Bayesian calibration. Most applied cases will use one of the many Markov Chain Monte Carlo (MCMC) algorithms to sample from the posterior distribution (Luengo et al., 2020). These methods require a large number of repeat runs of the data-generating model, which can amount to significant computational costs. When using MCMC approximations, the result should always be checked for convergence using multiple methods (Conn et al., 2018).

5.5. Validation, Prediction, and Attribution

Model validation

Before basing management decisions on a model, it is crucial to assess its reliability by validating it with independent data (Araújo et al., 2005). However, this step is often skipped in applications of process-based models. If the validation data has autocorrelation, it is crucial to account for them in the data splitting, since emaining correlations will likely result in over-confident performance assessments (D. R. Roberts et al., 2017). In my case study of the red kite (Chapter 3), I demonstrated a spatial-block cross-validation scheme to assess model performance. Alternative methods include random k-fold cross-validation or leave-p-out cross-validation. Leave-one-out cross-validation can be approximated by WAIC (Vehtari et al., 2017). All these methods, however, entail additional computations, which can exacerbate the challenge of high computational costs in process-based modelling.

Cross-validation techniques always set aside a portion of the calibration data for later validation, thus reducing the information content that is available for parametrisation. Ideally, other types of independent validation data should be used for validation, e.g. from another monitoring scheme with a different spatio-temporal structure.

Model predictions

A central property of the Bayesian framework is that uncertainties are consistently propagated throughout, while taking the internal correlation structure into account. This allows to quantify how input and parameter uncertainties contribute to outcome uncertainty in model predictions. In Chapter 3, I used this to predict the potential current

distribution and size of the Swiss population of the red kite together with the attached uncertainties, by running the model forweard under a constant environment. With such predictions, it is also possible to assess the effect of alternative management scenarios, such as habitat restoration or reintroductions.

Since environmental conditions are expected to change in the future, the assumption of a constant environment introduces a discrepancy for future predictions. To make valid predictions of species responses to climate change, such as range shifts, it is necessary to model the underlying causal structure.

Attribution

When the causal drivers of species responses and their relationship with the mediating ecological process is explicitly included in the model, the observed responses can be directly attributed to these drivers. To this end, I modelled and calibrated the demography-climate relationships of eight Swiss breeding birds in (Malchow et al., 2023; Chapter 4). With this, I could attribute their current population trends to recent climate change and identify the differential effects of climatic variables on the population growth rate. Such assessments provide vital knowledge to design climate change mitigation measures and improve our understanding of the mechanisms behind species responses to climate change.

A model can only successfully disentangle the causal structure, if all relevant drivers and processes are included. Only then can also valid attributions be derived (Rosenzweig & Neofotis, 2013). Many attribution studies describe climate (change) with only few predictors, often mean temperature. It has been suggested, however, that other aspects like precipitation as well as increased variances and risks of extreme events are influential and must be considered (Garcia et al., 2014; Vázquez et al., 2017). For example, Jørgensen et al. (2016) attribute abundance shits in European birds to both climate change and land-use change and Skagen & Adams (2012) attributed increased nest failure to extreme weather events during breeding seasons.

5.6. Conclusion

Much work is being directed towards making ecological models adequate for application to highly complex ecological systems and thus useful for decision making (Cuddington et al., 2013; Getz et al., 2018; Schuwirth et al., 2019; Araújo et al., 2019). A complete modelling workflow comprises many steps from conceptualisation to prediction and attribution (Hansen et al., 2016). Many of these steps depend on ecological theory and expert knowledge, such as model building and selecting validation targets. However,

modelling efforts are often restricted by the low availability of ecological data, especially at the gene and community level. Therefore, in order to reach the goal of a global biodiversity model, we need not only to advance modelling techniques, but also collect and manage the data that is required for their complete parametrisation (Kissling, Walls, et al., 2018).

My work provides a contribution towards the more widespread use of individual-based models. It can help to use existing data more efficiently, make better predictions of species distributions under future conditions, and improve our understanding of the mechanisms that underlie species responses to global change. As such, it is meant to form a part of the ambitious effort that is needed in order to bend the curve on biodiversity.

Bibliography

Aben, J., Bocedi, G., Palmer, S. C. F., Pellikka, P., Strubbe, D., Hallmann, C., Travis, J. M. J., Lens, L., and Matthysen, E. (2016). „The importance of realistic dispersal models in conservation planning: application of a novel modelling platform to evaluate management scenarios in an Afrotropical biodiversity hotspot". *Journal of Applied Ecology* 53.4, pp. 1055–1065. DOI: 10.1111/1365-2664.12643.

Aebischer, A. and Scherler, P. (2021). *Der Rotmilan - Ein Greifvogel im Aufwind*. 1st ed. Bern: Haupt Verlag. 232 pp. ISBN: 978-3-258-08249-3.

Andrieu, C. and Roberts, G. O. (2009). „The pseudo-marginal approach for efficient Monte Carlo computations". *The Annals of Statistics* 37.2, pp. 697–725. DOI: 10.1214/07-AOS574.

Araújo, M. B., Anderson, R. P., Barbosa, A. M., Beale, C. M., Dormann, C. F., Early, R., Garcia, R. A., Guisan, A., Maiorano, L., Naimi, B., O'Hara, R. B., Zimmermann, N. E., and Rahbek, C. (2019). „Standards for distribution models in biodiversity assessments". *Science Advances* 5.1, eaat4858. DOI: 10.1126/sciadv.aat4858.

Araújo, M. B. and Luoto, M. (2007). „The importance of biotic interactions for modelling species distributions under climate change". *Global Ecology and Biogeography* 16.6, pp. 743–753. DOI: 10.1111/j.1466-8238.2007.00359.x.

Araújo, M. B., Pearson, R. G., Thuiller, W., and Erhard, M. (2005). „Validation of species–climate impact models under climate change". *Global Change Biology* 11.9, pp. 1504–1513. DOI: 10.1111/j.1365-2486.2005.01000.x.

Araújo, M. B. and Peterson, A. T. (2012). „Uses and misuses of bioclimatic envelope modeling". *Ecology* 93.7, pp. 1527–1539. DOI: 10.1890/11-1930.1.

Arlot, S. and Celisse, A. (2010). „A survey of cross-validation procedures for model selection". *Statistics Surveys* 4, pp. 40–79. DOI: 10.1214/09-SS054.

Austin, M. (2007). „Species distribution models and ecological theory: A critical assessment and some possible new approaches". *Ecological Modelling* 200.1, pp. 1–19. DOI: 10.1016/j.ecolmodel.2006.07.005.

Balvanera, P., Pfaff, A., Viña, A., Garcia Frapolli, E., Hussain, S. A., Merino, L., Minang, P. A., Nagabhatla, N., and Sidorovich, A. (2019). *Chapter 2.1 Status and Trends –Drivers of Change*. Zenodo. DOI: 10.5281/zenodo.5517423.

Barber-O'Malley, B., Lassalle, G., Chust, G., Diaz, E., O'Malley, A., Paradinas Blázquez, C., Pórtoles Marquina, J., and Lambert, P. (2022). „HyDiaD: A hybrid species distribution model combining dispersal, multi-habitat suitability, and population dynamics for diadromous species under climate change scenarios". *Ecological Modelling* 470, p. 109997. DOI: 10.1016/j.ecolmodel.2022.109997.

Barras, A. G., Blache, S., Schaub, M., and Arlettaz, R. (2021). „Variation in Demography and Life-History Strategies Across the Range of a Declining Mountain Bird Species". *Frontiers in Ecology and Evolution* 9. DOI: 10.3389/fevo.2021.780706.

Barras, A. G., Braunisch, V., and Arlettaz, R. (2021). „Predictive models of distribution and abundance of a threatened mountain species show that impacts of climate change overrule those of land use change". en. *Diversity and Distributions* 27.6. Ed. by L. Maiorano, pp. 989–1004. DOI: 10.1111/ddi.13247.

Barras, A. G., Niffenegger, C. A., Candolfi, I., Hunziker, Y. A., and Arlettaz, R. (2021). „Nestling diet and parental food provisioning in a declining mountain passerine reveal high sensitivity to climate change". en. *Journal of Avian Biology* 52.2. DOI: 10.1111/jav.02649.

Baucks, C. (2018). „The effect of food supplementation on range use of breeding red kites (Milvus milvus) in Switzerland". Master thesis. Swiss Ornithological Institute Sempach.

Beaumont, M. A. (2010). „Approximate Bayesian Computation in Evolution and Ecology". *Annual Review of Ecology, Evolution, and Systematics* 41.1, pp. 379–406. DOI: 10.1146/annurev-ecolsys-102209-144621.

Beever, E. A., Hall, L. E., Varner, J., Loosen, A. E., Dunham, J. B., Gahl, M. K., Smith, F. A., and Lawler, J. J. (2017). „Behavioral flexibility as a mechanism for coping with climate change". *Frontiers in Ecology and the Environment* 15.6, pp. 299–308. DOI: 10.1002/fee.1502.

Bell, D. M. and Schlaepfer, D. R. (2016). „On the dangers of model complexity without ecological justification in species distribution modeling". *Ecological Modelling* 330, pp. 50–59. DOI: 10.1016/j.ecolmodel.2016.03.012.

Bleyhl, B., Ghoddousi, A., Askerov, E., Bocedi, G., Breitenmoser, U., Manvelyan, K., Palmer, S. C. F., Soofi, M., Weinberg, P., Zazanashvili, N., Shmunk, V., Zurell, D., and Kuemmerle, T. (2021). „Reducing persecution is more effective for restoring large carnivores than restoring their prey". *Ecological Applications* 31.5, e02338. DOI: 10.1002/eap.2338.

Bocedi, G., Palmer, S. C. F., Malchow, A.-K., Zurell, D., Watts, K., and Travis, J. M. J. (2021). „RangeShifter 2.0: an extended and enhanced platform for modelling spatial eco-evolutionary dynamics and species' responses to environmental changes". *Ecography* 44.10, pp. 1453–1462. DOI: 10.1111/ecog.05687.

Bocedi, G., Palmer, S. C. F., Pe'er, G., Heikkinen, R. K., Matsinos, Y. G., Watts, K., and Travis, J. M. J. (2014). „RangeShifter: a platform for modelling spatial eco-evolutionary dynamics and species' responses to environmental changes". *Methods in Ecology and Evolution* 5.4, pp. 388–396. DOI: 10.1111/2041-210X.12162.

Bolam, F. C. et al. (2021). „How many bird and mammal extinctions has recent conservation action prevented?" *Conservation Letters* 14.1, e12762. DOI: 10.1111/conl.12762.

Bonnot, T. W., Cox, W. A., Thompson, F. R., and Millspaugh, J. J. (2018). „Threat of climate change on a songbird population through its impacts on breeding". *Nature Climate Change* 8.8, pp. 718–722. DOI: 10.1038/s41558-018-0232-8.

Booth, T. H., Nix, H. A., Busby, J. R., and Hutchinson, M. F. (2014). „bioclim: the first species distribution modelling package, its early applications and relevance to most current MaxEnt studies". *Diversity and Distributions* 20.1, pp. 1–9. DOI: 10.1111/ddi.12144.

Both, C., Bouwhuis, S., Lessells, C. M., and Visser, M. E. (2006). „Climate change and population declines in a long-distance migratory bird". *Nature* 441.7089, pp. 81–83. DOI: 10.1038/nature04539.

Braak, C. J. F. ter and Vrugt, J. A. (2008). „Differential Evolution Markov Chain with snooker updater and fewer chains". *Statistics and Computing* 18.4, pp. 435–446. DOI: 10.1007/s11222-008-9104-9.

Briscoe, N. J., Zurell, D., Elith, J., König, C., Fandos, G., Malchow, A.-K., Kéry, M., Schmid, H., and Guillera-Arroita, G. (2021). „Can dynamic occupancy models improve predictions of species' range dynamics? A test using Swiss birds". *Global Change Biology* 27.18, pp. 4269–4282. DOI: 10.1111/gcb.15723.

Briscoe, N. J. et al. (2019). „Forecasting species range dynamics with process-explicit models: matching methods to applications". *Ecology Letters* 22.11, pp. 1940–1956. DOI: 10.1111/ele.13348.

Brommer, J. E., Lehikoinen, A., and Valkama, J. (2012). „The Breeding Ranges of Central European and Arctic Bird Species Move Poleward". en. *PLOS ONE* 7.9, e43648. DOI: 10.1371/journal.pone.0043648.

Broms, K. M., Hooten, M. B., Johnson, D. S., Altwegg, R., and Conquest, L. L. (2016). „Dynamic occupancy models for explicit colonization processes". *Ecology* 97.1, pp. 194–204. DOI: 10.1890/15-0416.1.

Brooker, R. W., Travis, J. M. J., Clark, E. J., and Dytham, C. (2007). „Modelling species' range shifts in a changing climate: The impacts of biotic interactions, dispersal distance and the rate of climate change". *Journal of Theoretical Biology* 245.1, pp. 59–65. DOI: 10.1016/j.jtbi.2006.09.033.

Brotons, L., De Cáceres, M., Fall, A., and Fortin, M.-J. (2012). „Modeling bird species distribution change in fire prone Mediterranean landscapes: incorporating species dispersal and landscape dynamics". *Ecography* 35.5, pp. 458–467. DOI: 10.1111/j.1600-0587.2011.06878.x.

Buckley, L. B., Urban, M. C., Angilletta, M. J., Crozier, L. G., Rissler, L. J., and Sears, M. W. (2010). „Can mechanism inform species' distribution models?" *Ecology Letters* 13.8, pp. 1041–1054. DOI: 10.1111/j.1461-0248.2010.01479.x.

Cabral, J. S., Valente, L., and Hartig, F. (2017). „Mechanistic simulation models in macroecology and biogeography: state-of-art and prospects". *Ecography* 40.2, pp. 267–280. DOI: 10.1111/ecog.02480.

Cailleret, M., Bircher, N., Hartig, F., Hülsmann, L., and Bugmann, H. (2020). „Bayesian calibration of a growth-dependent tree mortality model to simulate the dynamics of European temperate forests". *Ecological Applications* 30.1, e02021. DOI: 10.1002/eap.2021.

Carrara, F., Giometto, A., Seymour, M., Rinaldo, A., and Altermatt, F. (2015). „Inferring species interactions in ecological communities: a comparison of methods at different levels of complexity". *Methods in Ecology and Evolution* 6.8, pp. 895–906. DOI: 10.1111/2041-210X.12363.

Caswell, H. (2000). *Matrix population models*. Vol. 1. Sinauer Sunderland, MA.

CBD (2020). *Global Biodiversity Outlook 5*. Montreal: Secretariat of the Convention on Biological Diversity. ISBN: 978-92-9225-688-3.

Ceppi, P., Scherrer, S. C., Fischer, A. M., and Appenzeller, C. (2012). „Revisiting Swiss temperature trends 1959–2008". *International Journal of Climatology* 32.2, pp. 203–213. DOI: 10.1002/joc.2260.

Cereghetti, E., Scherler, P., Fattebert, J., and Grüebler, M. U. (2019). „Quantification of anthropogenic food subsidies to an avian facultative scavenger in urban and rural habitats". *Landscape and Urban Planning* 190, p. 103606. DOI: 10.1016/j.landurbplan.2019.103606.

Chase, J. M. and Leibold, M. A. (2009). *Ecological Niches: Linking Classical and Contemporary Approaches*. University of Chicago Press. 224 pp. ISBN: 978-0-226-10181-1.

Chen, I.-C., Hill, J. K., Ohlemüller, R., Roy, D. B., and Thomas, C. D. (2011). „Rapid Range Shifts of Species Associated with High Levels of Climate Warming". *Science* 333.6045, pp. 1024–1026. DOI: 10.1126/science.1206432.

Chen, Q., Han, R., Ye, F., and Li, W. (2011). „Spatio-temporal ecological models". *Ecological Informatics*. Special Issue: 5th Anniversary 6.1, pp. 37–43. DOI: 10.1016/j.ecoinf.2010.07.006.

Christopher Frey, H. and Patil, S. R. (2002). „Identification and Review of Sensitivity Analysis Methods". *Risk Analysis* 22.3, pp. 553–578. DOI: 10.1111/0272-4332.00039.

Chubaty, A. M., Roitberg, B. D., and Li, C. (2009). „A dynamic host selection model for mountain pine beetle, Dendroctonus ponderosae Hopkins". *Ecological Modelling* 220.9, pp. 1241–1250. DOI: 10.1016/j.ecolmodel.2009.01.039.

Cianfrani, C., Satizábal, H. F., and Randin, C. (2015). „A spatial modelling framework for assessing climate change impacts on freshwater ecosystems: Response of brown trout (Salmo trutta L.) biomass to warming water temperature". en. *Ecological Modelling* 313, pp. 1–12. DOI: 10.1016/j.ecolmodel.2015.06.023.

Comte, L., Murienne, J., and Grenouillet, G. (2014). „Species traits and phylogenetic conservatism of climate-induced range shifts in stream fishes". *Nature Communications* 5.1, p. 5053. DOI: 10.1038/ncomms6053.

Conn, P. B., Johnson, D. S., Williams, P. J., Melin, S. R., and Hooten, M. B. (2018). „A guide to Bayesian model checking for ecologists". *Ecological Monographs* 88.4, pp. 526–542. DOI: 10.1002/ecm.1314.

Connolly, S. R., Keith, S. A., Colwell, R. K., and Rahbek, C. (2017). „Process, Mechanism, and Modeling in Macroecology". *Trends in Ecology & Evolution* 32.11, pp. 835–844. DOI: 10.1016/j.tree.2017.08.011.

Cox, W. A., Thompson III, F. R., Reidy, J. L., and Faaborg, J. (2013). „Temperature can interact with landscape factors to affect songbird productivity". en. *Global Change Biology* 19.4, pp. 1064–1074. DOI: 10.1111/gcb.12117.

Csilléry, K., François, O., and Blum, M. G. (2012). „abc: an R package for approximate Bayesian computation (ABC)“. *Methods in Ecology and Evolution* 3.3, pp. 475–479. DOI: 10.1111/j.2041-210X.2011.00179.x.

Cuddington, K., Fortin, M.-J., Gerber, L. R., Hastings, A., Liebhold, A., O'Connor, M., and Ray, C. (2013). „Process-based models are required to manage ecological systems in a changing world“. *Ecosphere* 4.2, art20. DOI: 10.1890/ES12-00178.1.

DeAngelis, D. L. and Mooij, W. M. (2005). „Individual-Based Modeling of Ecological and Evolutionary Processes“. *Annual Review of Ecology, Evolution, and Systematics* 36.1, pp. 147–168. DOI: 10.1146/annurev.ecolsys.36.102003.152644.

DeMarche, M. L., Doak, D. F., and Morris, W. F. (2019). „Incorporating local adaptation into forecasts of species' distribution and abundance under climate change“. *Global Change Biology* 25.3, pp. 775–793. DOI: 10.1111/gcb.14562.

Diamond, S. E. (2018). „Contemporary climate-driven range shifts: Putting evolution back on the table“. *Functional Ecology* 32.7, pp. 1652–1665. DOI: 10.1111/1365-2435.13095.

Díaz, S. et al. (2019). „Pervasive human-driven decline of life on Earth points to the need for transformative change“. *Science* 366.6471, eaax3100. DOI: 10.1126/science.aax3100.

Dominguez Almela, V., Palmer, S. C. F., Gillingham, P. K., Travis, J. M. J., and Britton, J. R. (2020). „Integrating an individual-based model with approximate Bayesian computation to predict the invasion of a freshwater fish provides insights into dispersal and range expansion dynamics“. *Biological Invasions* 22.4, pp. 1461–1480. DOI: 10.1007/s10530-020-02197-6.

Donald, P. F. (2007). „Adult sex ratios in wild bird populations“. *Ibis* 149.4, pp. 671–692. DOI: https://doi.org/10.1111/j.1474-919X.2007.00724.x.

Dormann, C. F., Schymanski, S. J., Cabral, J., Chuine, I., Graham, C., Hartig, F., Kearney, M., Morin, X., Römermann, C., Schröder, B., and Singer, A. (2012). „Correlation and process in species distribution models: bridging a dichotomy“. *Journal of Biogeography* 39.12, pp. 2119–2131. DOI: 10.1111/j.1365-2699.2011.02659.x.

Dormann, C. F. et al. (2007). „Methods to account for spatial autocorrelation in the analysis of species distributional data: a review“. *Ecography* 30.5, pp. 609–628. DOI: 10.1111/j.2007.0906-7590.05171.x.

Dormann, C. F. et al. (2013). „Collinearity: a review of methods to deal with it and a simulation study evaluating their performance“. *Ecography* 36.1, pp. 27–46. DOI: 10.1111/j.1600-0587.2012.07348.x.

Dornelas, M., Gotelli, N. J., McGill, B., Shimadzu, H., Moyes, F., Sievers, C., and Magurran, A. E. (2014). „Assemblage Time Series Reveal Biodiversity Change but Not Systematic Loss". *Science* 344.6181, pp. 296–299. DOI: 10.1126/science.1248484.

Duarte, C. M., Agusti, S., Barbier, E., Britten, G. L., Castilla, J. C., Gattuso, J.-P., Fulweiler, R. W., Hughes, T. P., Knowlton, N., Lovelock, C. E., Lotze, H. K., Predragovic, M., Poloczanska, E., Roberts, C., and Worm, B. (2020). „Rebuilding marine life". *Nature* 580.7801, pp. 39–51. DOI: 10.1038/s41586-020-2146-7.

Dunham, K. D., Tucker, A. M., Koons, D. N., Abebe, A., Dobson, F. S., and Grand, J. B. (2021). „Demographic responses to climate change in a threatened Arctic species". *Ecology and Evolution* 11.15, pp. 10627–10643. DOI: 10.1002/ece3.7873.

Dybala, K. E., Eadie, J. M., Gardali, T., Seavy, N. E., and Herzog, M. P. (2013). „Projecting demographic responses to climate change: adult and juvenile survival respond differently to direct and indirect effects of weather in a passerine population". en. *Global Change Biology* 19.9, pp. 2688–2697. DOI: 10.1111/gcb.12228.

Eddelbuettel, D., François, R., Allaire, J., Ushey, K., Kou, Q., Russel, N., Chambers, J., and Bates, D. (2011). „Rcpp: Seamless R and C++ integration". *Journal of Statistical Software* 40.8, pp. 1–18. DOI: 10.18637/jss.v040.i08.

Ehrlén, J. and Morris, W. F. (2015). „Predicting changes in the distribution and abundance of species under environmental change". *Ecology Letters* 18.3, pp. 303–314. DOI: https://doi.org/10.1111/ele.12410.

Elith, J., Leathwick, J. R., and Hastie, T. (2008). „A working guide to boosted regression trees". *Journal of Animal Ecology* 77.4, pp. 802–813. DOI: 10.1111/j.1365-2656.2008.01390.x.

Elith, J., Kearney, M., and Phillips, S. (2010). „The art of modelling range-shifting species". *Methods in Ecology and Evolution* 1.4, pp. 330–342. DOI: 10.1111/j.2041-210X.2010.00036.x.

Elith, J. and Leathwick, J. R. (2009). „Species Distribution Models: Ecological Explanation and Prediction Across Space and Time". *Annual Review of Ecology, Evolution, and Systematics* 40.1, pp. 677–697. DOI: 10.1146/annurev.ecolsys.110308.120159.

Ellison, A. M. (2004). „Bayesian inference in ecology". *Ecology Letters* 7.6, pp. 509–520. DOI: 10.1111/j.1461-0248.2004.00603.x.

Emary, C. and Malchow, A.-K. (2022). „Stability-instability transition in tripartite merged ecological networks". *Journal of Mathematical Biology* 85.3, p. 20. DOI: 10.1007/s00285-022-01783-7.

Engler, R., Hordijk, W., and Guisan, A. (2012). „The MIGCLIM R package – seamless integration of dispersal constraints into projections of species distribution models". *Ecography* 35.10, pp. 872–878. DOI: 10.1111/j.1600-0587.2012.07608.x.

Ettinger, A. and HilleRisLambers, J. (2017). „Competition and facilitation may lead to asymmetric range shift dynamics with climate change". *Global Change Biology* 23.9, pp. 3921–3933. DOI: 10.1111/gcb.13649.

European Union (2022). *Copernicus Land Monitoring Service*. https://land.copernicus.eu/. European Environment Agency (EEA).

Evans, T. G., Diamond, S. E., and Kelly, M. W. (2015). „Mechanistic species distribution modelling as a link between physiology and conservation". *Conservation Physiology* 3.1. DOI: 10.1093/conphys/cov056.

Fandos, G., Talluto, M., Fiedler, W., Robinson, R. A., Thorup, K., and Zurell, D. (2023). „Standardised empirical dispersal kernels emphasise the pervasiveness of long-distance dispersal in European birds". *Journal of Animal Ecology* 92.1, pp. 158–170. DOI: 10.1111/1365-2656.13838.

Fei, S., Desprez, J. M., Potter, K. M., Jo, I., Knott, J. A., and Oswalt, C. M. (2017). „Divergence of species responses to climate change". *Science Advances* 3.5, e1603055. DOI: 10.1126/sciadv.1603055.

Folke, C., Carpenter, S., Walker, B., Scheffer, M., Elmqvist, T., Gunderson, L., and Holling, C. S. (2004). „Regime Shifts, Resilience, and Biodiversity in Ecosystem Management". *Annual Review of Ecology, Evolution, and Systematics* 35, pp. 557–581.

Fordham, D. A., Akçakaya, H. R., Araújo, M. B., Keith, D. A., and Brook, B. W. (2013). „Tools for integrating range change, extinction risk and climate change information into conservation management". *Ecography* 36.9, pp. 956–964. DOI: 10.1111/j.1600-0587.2013.00147.x.

Fordham, D. A., Bertelsmeier, C., Brook, B. W., Early, R., Neto, D., Brown, S. C., Ollier, S., and Araújo, M. B. (2018). „How complex should models be? Comparing correlative and mechanistic range dynamics models". *Global Change Biology* 24.3, pp. 1357–1370. DOI: 10.1111/gcb.13935.

Fordham, D. A., Haythorne, S., Brown, S. C., Buettel, J. C., and Brook, B. W. (2021). „poems: R package for simulating species' range dynamics using pattern-oriented validation". *Methods in Ecology and Evolution* 12.12, pp. 2364–2371. DOI: 10.1111/2041-210X.13720.

Fourcade, Y., Besnard, A. G., and Secondi, J. (2018). „Paintings predict the distribution of species, or the challenge of selecting environmental predictors and evaluation statistics". *Global Ecology and Biogeography* 27.2, pp. 245–256. DOI: 10.1111/geb.12684.

Franklin, J. (2010). „Moving beyond static species distribution models in support of conservation biogeography". *Diversity and Distributions* 16.3, pp. 321–330. DOI: 10.1111/j.1472-4642.2010.00641.x.

– (2013). „Species distribution models in conservation biogeography: developments and challenges". *Diversity and Distributions* 19.10, pp. 1217–1223. DOI: 10.1111/ddi.12125.

Gallien, L., Münkemüller, T., Albert, C. H., Boulangeat, I., and Thuiller, W. (2010). „Predicting potential distributions of invasive species: where to go from here?" *Diversity and Distributions* 16.3, pp. 331–342. DOI: 10.1111/j.1472-4642.2010.00652.x.

Gandon, S. and Michalakis, Y. (2002). „Local adaptation, evolutionary potential and host–parasite coevolution: interactions between migration, mutation, population size and generation time". *Journal of Evolutionary Biology* 15.3, pp. 451–462. DOI: 10.1046/j.1420-9101.2002.00402.x.

Garcia, R. A., Cabeza, M., Rahbek, C., and Araújo, M. B. (2014). „Multiple Dimensions of Climate Change and Their Implications for Biodiversity". *Science* 344.6183. DOI: 10.1126/science.1247579.

Gelman, A., Carlin, J. B., Stern, H. S., Dunson, D. B., Vehtaki, A., and Rubin, D. B. (2013). *Bayesian data analysis*. 3rd ed. Chapman and Hall. ISBN: 9781439840955.

Gelman, A. and Rubin, D. B. (1992). „Inference from Iterative Simulation Using Multiple Sequences". *Statistical Science* 7.4, pp. 457–472. DOI: 10.1214/ss/1177011136.

Getz, W. M., Marshall, C. R., Carlson, C. J., Giuggioli, L., Ryan, S. J., Romañach, S. S., Boettiger, C., Chamberlain, S. D., Larsen, L., D'Odorico, P., and O'Sullivan, D. (2018). „Making ecological models adequate". *Ecology Letters* 21.2, pp. 153–166. DOI: 10.1111/ele.12893.

Gillespie, C. S. and Golightly, A. (2010). „Bayesian inference for generalized stochastic population growth models with application to aphids". *Journal of the Royal Statistical Society: Series C (Applied Statistics)* 59.2, pp. 341–357.

Gilroy, J. J. and Edwards, D. P. (2017). „Source-sink dynamics: a neglected problem for landscape-scale biodiversity conservation in the tropics". *Current Landscape Ecology Reports* 2.1, pp. 51–60.

Gobiet, A., Kotlarski, S., Beniston, M., Heinrich, G., Rajczak, J., and Stoffel, M. (2014). „21st century climate change in the European Alps—A review". *Science of The Total Environment* 493, pp. 1138–1151. DOI: 10.1016/j.scitotenv.2013.07.050.

Golding, N., August, T. A., Lucas, T. C. D., Gavaghan, D. J., Loon, E. E. van, and McInerny, G. (2018). „The zoon r package for reproducible and shareable species distribution modelling". *Methods in Ecology and Evolution* 9.2, pp. 260–268. DOI: 10.1111/2041-210X.12858.

Gonzalez, A., Chase, J. M., and O'Connor, M. I. (2023). „A framework for the detection and attribution of biodiversity change". *Philosophical Transactions of the Royal Society B: Biological Sciences* 378.1881, p. 20220182. DOI: 10.1098/rstb.2022.0182.

Grimm, N. B., Chapin III, F. S., Bierwagen, B., Gonzalez, P., Groffman, P. M., Luo, Y., Melton, F., Nadelhoffer, K., Pairis, A., Raymond, P. A., Schimel, J., and Williamson, C. E. (2013). „The impacts of climate change on ecosystem structure and function". *Frontiers in Ecology and the Environment* 11.9, pp. 474–482. DOI: 10.1890/120282.

Grimm, V. et al. (2020). „The ODD protocol for describing agent-based and other simulation models: A second update to improve clarity, replication, and structural realism". *Journal of Artificial Societies and Social Simulation* 23.2.

Grimm, V., Berger, U., Bastiansen, F., Eliassen, S., Ginot, V., Giske, J., Goss-Custard, J., Grand, T., Heinz, S. K., Huse, G., et al. (2006). „A standard protocol for describing individual-based and agent-based models". *Ecological modelling* 198.1, pp. 115–126.

Grimm, V., Berger, U., DeAngelis, D. L., Polhill, J. G., Giske, J., and Railsback, S. F. (2010). „The ODD protocol: A review and first update". *Ecological Modelling* 221.23, pp. 2760–2768. DOI: 10.1016/j.ecolmodel.2010.08.019.

Grimm, V., Revilla, E., Berger, U., Jeltsch, F., Mooij, W. M., Railsback, S. F., Thulke, H.-H., Weiner, J., Wiegand, T., and DeAngelis, D. L. (2005). „Pattern-Oriented Modeling of Agent-Based Complex Systems: Lessons from Ecology". *Science* 310.5750, pp. 987–991. DOI: 10.1126/science.1116681.

Guisan, A. and Thuiller, W. (2005). „Predicting species distribution: offering more than simple habitat models". *Ecology Letters* 8.9, pp. 993–1009. DOI: 10.1111/j.1461-0248.2005.00792.x.

Guisan, A. and Zimmermann, N. E. (2000). „Predictive habitat distribution models in ecology". *Ecological Modelling* 135.2, pp. 147–186. DOI: 10.1016/S0304-3800(00)00354-9.

Guisan, A. et al. (2013). „Predicting species distributions for conservation decisions". *Ecology Letters* 16.12. Ed. by H. Arita, pp. 1424–1435. DOI: 10.1111/ele.12189.

Hagen, O., Flück, B., Fopp, F., Cabral, J. S., Hartig, F., Pontarp, M., Rangel, T. F., and Pellissier, L. (2021). „gen3sis: A general engine for eco-evolutionary simulations of the processes that shape Earth's biodiversity". *PLOS Biology* 19.7, e3001340. DOI: 10.1371/journal.pbio.3001340.

Hansen, G., Stone, D., Auffhammer, M., Huggel, C., and Cramer, W. (2016). „Linking local impacts to changes in climate: a guide to attribution". *Regional Environmental Change* 16.2, pp. 527–541. DOI: 10.1007/s10113-015-0760-y.

Hanski, I. (1994). „A practical model of metapopulation dynamics". *Journal of animal ecology*, pp. 151–162.

Harfoot, M. B. J., Newbold, T., Tittensor, D. P., Emmott, S., Hutton, J., Lyutsarev, V., Smith, M. J., Scharlemann, J. P. W., and Purves, D. W. (2014). „Emergent Global Patterns of Ecosystem Structure and Function from a Mechanistic General Ecosystem Model". *PLOS Biology* 12.4, e1001841. DOI: 10.1371/journal.pbio.1001841.

Hartig, F., Calabrese, J. M., Reineking, B., Wiegand, T., and Huth, A. (2011). „Statistical inference for stochastic simulation models – theory and application". *Ecology Letters* 14.8, pp. 816–827. DOI: 10.1111/j.1461-0248.2011.01640.x.

Hartig, F., Dyke, J., Hickler, T., Higgins, S. I., O'Hara, R. B., Scheiter, S., and Huth, A. (2012). „Connecting dynamic vegetation models to data – an inverse perspective". *Journal of Biogeography* 39.12, pp. 2240–2252. DOI: 10.1111/j.1365-2699.2012.02745.x.

Hartig, F., Minunno, F., and Paul, S. (2019). „BayesianTools: General-purpose MCMC and SMC Samplers and Tools for Bayesian Statistics". *R package version 0.1.7.*

Hastings, A., Cuddington, K., Davies, K. F., Dugaw, C. J., Elmendorf, S., Freestone, A., Harrison, S., Holland, M., Lambrinos, J., Malvadkar, U., Melbourne, B. A., Moore, K., Taylor, C., and Thomson, D. (2005). „The spatial spread of invasions: new developments in theory and evidence". *Ecology Letters* 8.1, pp. 91–101. DOI: 10.1111/j.1461-0248.2004.00687.x.

Hauenstein, S., Fattebert, J., Grüebler, M. U., Naef-Daenzer, B., Pe'er, G., and Hartig, F. (2019). „Calibrating an individual-based movement model to predict functional connectivity for little owls". *Ecological Applications* 29.4, e01873. DOI: 10.1002/eap.1873.

Hedger, R. D., Sundt-Hansen, L. E., Forseth, T., Ugedal, O., Diserud, O. H., Kvambekk, Å. S., and Finstad, A. G. (2013). „Predicting climate change effects on subarctic–Arctic

populations of Atlantic salmon (Salmo salar)". *Canadian Journal of Fisheries and Aquatic Sciences* 70.2, pp. 159–168. DOI: 10.1139/cjfas-2012-0205.

Henry, R. C., Bocedi, G., and Travis, J. M. J. (2013). „Eco-evolutionary dynamics of range shifts: Elastic margins and critical thresholds". *Journal of Theoretical Biology* 321, pp. 1–7. DOI: 10.1016/j.jtbi.2012.12.004.

Henry, R. C., Palmer, S. C. F., Watts, K., Mitchell, R. J., Atkinson, N., and Travis, J. M. J. (2017). „Tree loss impacts on ecological connectivity: Developing models for assessment". *Ecological Informatics* 42, pp. 90–99. DOI: 10.1016/j.ecoinf.2017.10.010.

Higgins, S. I., O'Hara, R. B., and Römermann, C. (2012). „A niche for biology in species distribution models". *Journal of Biogeography* 39.12, pp. 2091–2095. DOI: 10.1111/jbi.12029.

Hijmans, R. J. and Etten, J. van (2016). „raster: Geographic data analysis and modeling". *R package version* 2.8.

Hijmans, R. J., Phillips, S., Leathwick, J., and Elith, J. (2017). „dismo: Species distribution modeling". *R package version* 1.4, pp. 1–1.

Hoffmann, M. et al. (2010). „The Impact of Conservation on the Status of the World's Vertebrates". *Science* 330.6010, pp. 1503–1509. DOI: 10.1126/science.1194442.

Hooper, D. U., Adair, E. C., Cardinale, B. J., Byrnes, J. E. K., Hungate, B. A., Matulich, K. L., Gonzalez, A., Duffy, J. E., Gamfeldt, L., and O'Connor, M. I. (2012). „A global synthesis reveals biodiversity loss as a major driver of ecosystem change". *Nature* 486.7401, pp. 105–108. DOI: 10.1038/nature11118.

Housset, J. M., Carcaillet, C., Girardin, M. P., Xu, H., Tremblay, F., and Bergeron, Y. (2016). „In situ Comparison of Tree-Ring Responses to Climate and Population Genetics: The Need to Control for Local Climate and Site Variables". *Frontiers in Ecology and Evolution* 4.

Hunter-Ayad, J. and Hassall, C. (2020). „An empirical, cross-taxon evaluation of landscape-scale connectivity". *Biodiversity and Conservation* 29.4, pp. 1339–1359. DOI: 10.1007/s10531-020-01938-2.

Hutchinson, G. E. (1957). „Concluding remarks". *Cold spring harbor symposium on quantitative biology* 22, pp. 415–427.

IPBES (2019). *The global assessment report on biodiversity and ecosystem services: Summary for policy makers.* Paris: Intergovernmental Science-Policy Platform on Biodiversity and Ecosystem Services.

Jaatinen, K., Westerbom, M., Norkko, A., Mustonen, O., and Koons, D. N. (2021). „Detrimental impacts of climate change may be exacerbated by density-dependent population regulation in blue mussels". *Journal of Animal Ecology* 90.3, pp. 562–573. DOI: 10.1111/1365-2656.13377.

Jackson, S. T. and Overpeck, J. T. (2000). „Responses of plant populations and communities to environmental changes of the late Quaternary". *Paleobiology* 26 (S4), pp. 194–220. DOI: 10.1017/S0094837300026932.

Jarnevich, C. S., Stohlgren, T. J., Kumar, S., Morisette, J. T., and Holcombe, T. R. (2015). „Caveats for correlative species distribution modeling". *Ecological Informatics* 29, pp. 6–15. DOI: 10.1016/j.ecoinf.2015.06.007.

Jensen, L. F., Hansen, M. M., Pertoldi, C., Holdensgaard, G., Mensberg, K.-L. D., and Loeschcke, V. (2008). „Local adaptation in brown trout early life-history traits: implications for climate change adaptability". *Proceedings of the Royal Society B: Biological Sciences* 275.1653, pp. 2859–2868. DOI: 10.1098/rspb.2008.0870.

Jiménez-Valverde, A., Lobo, J. M., and Hortal, J. (2008). „Not as good as they seem: the importance of concepts in species distribution modelling". *Diversity and Distributions* 14.6, pp. 885–890. DOI: 10.1111/j.1472-4642.2008.00496.x.

Johnson, L. R. and Briggs, C. J. (2011). „Parameter inference for an individual based model of chytridiomycosis in frogs". *Journal of Theoretical Biology* 277.1, pp. 90–98. DOI: 10.1016/j.jtbi.2011.02.010.

Johnston, A., Fink, D., Reynolds, M. D., Hochachka, W. M., Sullivan, B. L., Bruns, N. E., Hallstein, E., Merrifield, M. S., Matsumoto, S., and Kelling, S. (2015). „Abundance models improve spatial and temporal prioritization of conservation resources". *Ecological Applications* 25.7, pp. 1749–1756. DOI: 10.1890/14-1826.1.

Jørgensen, P. S. et al. (2016). „Continent-scale global change attribution in European birds - combining annual and decadal time scales". en. *Global Change Biology* 22.2, pp. 530–543. DOI: 10.1111/gcb.13097.

Kampichler, C., Turnhout, C. A. M. v., Devictor, V., and Jeugd, H. P. v. d. (2012). „Large-Scale Changes in Community Composition: Determining Land Use and Climate Change Signals". *PLOS ONE* 7.4, e35272. DOI: 10.1371/journal.pone.0035272.

Karger, D. N., Conrad, O., Böhner, J., Kawohl, T., Kreft, H., Soria-Auza, R. W., Zimmermann, N. E., Linder, H. P., and Kessler, M. (2018a). „Data from: Climatologies at high resolution for the earth's land surface areas". *EnviDat*. DOI: 10.16904/envidat.228.v2.1.

Karger, D. N., Conrad, O., Böhner, J., Kawohl, T., Kreft, H., Soria-Auza, R. W., Zimmermann, N. E., Linder, H. P., and Kessler, M. (2017). „Climatologies at high resolution for the earth's land surface areas". *Scientific Data* 4, p. 170122. DOI: 10.1038/sdata.2017.122.

– (2018b). *Data from: Climatologies at high resolution for the earth's land surface areas.* DOI: 10.5061/dryad.kd1d4.

Kattwinkel, M. and Reichert, P. (2017). „Bayesian parameter inference for individual-based models using a Particle Markov Chain Monte Carlo method". *Environmental Modelling & Software* 87, pp. 110–119. DOI: 10.1016/j.envsoft.2016.11.001.

Katzenberger, J., Gottschalk, E., Balkenhol, N., and Waltert, M. (2019). „Long-term decline of juvenile survival in German Red Kites". *Journal of Ornithology* 160.2, pp. 337–349. DOI: 10.1007/s10336-018-1619-z.

Kearney, M. (2006). „Habitat, environment and niche: what are we modelling?" *Oikos* 115.1, pp. 186–191. DOI: 10.1111/j.2006.0030-1299.14908.x.

Kearney, M. and Porter, W. (2009). „Mechanistic niche modelling: combining physiological and spatial data to predict species' ranges". *Ecology Letters* 12.4, pp. 334–350. DOI: 10.1111/j.1461-0248.2008.01277.x.

Keith, D. A., Akçakaya, H. R., Thuiller, W., Midgley, G. F., Pearson, R. G., Phillips, S. J., Regan, H. M., Araújo, M. B., and Rebelo, T. G. (2008). „Predicting extinction risks under climate change: coupling stochastic population models with dynamic bioclimatic habitat models". *Biology Letters* 4.5, pp. 560–563. DOI: 10.1098/rsbl.2008.0049.

Kéry, M., Guillera-Arroita, G., and Lahoz-Monfort, J. J. (2013). „Analysing and mapping species range dynamics using occupancy models". *Journal of Biogeography* 40.8, pp. 1463–1474. DOI: 10.1111/jbi.12087.

Kissling, W. D., Ahumada, J. A., et al. (2018). „Building essential biodiversity variables (EBVs) of species distribution and abundance at a global scale". *Biological Reviews* 93.1, pp. 600–625. DOI: 10.1111/brv.12359.

Kissling, W. D. and Schleuning, M. (2015). „Multispecies interactions across trophic levels at macroscales: retrospective and future directions". *Ecography* 38.4, pp. 346–357. DOI: 10.1111/ecog.00819.

Kissling, W. D., Walls, R., et al. (2018). „Towards global data products of Essential Biodiversity Variables on species traits". *Nature Ecology & Evolution* 2.10, pp. 1531–1540. DOI: 10.1038/s41559-018-0667-3.

Knaus, P., Strebel, N., and Sattler, T. (2022). *The State of Birds in Switzerland 2022*. Sempach: Swiss Ornithological Institute.

Knaus, P., Jérôme, G., Sattler, T., Wechsler, S., Kéry, M., Strebel, N., and Antoniazza, S. (2018). *Schweizer Brutvogelatlas 2013-2016*. Sempach, Schweiz: Schweizerische Vogelwarte. ISBN: 978-3-85949-009-3.

Lacy, R. C. (1993). „VORTEX: a computer simulation model for population viability analysis". *Wildlife Research* 20.1, pp. 45–65. DOI: 10.1071/wr9930045.

Landguth, E. L., Bearlin, A., Day, C. C., and Dunham, J. (2017). „CDMetaPOP: an individual-based, eco-evolutionary model for spatially explicit simulation of landscape demogenetics". *Methods in Ecology and Evolution* 8.1, pp. 4–11. DOI: 10.1111/2041-210X.12608.

Lenoir, J. and Svenning, J.-C. (2015). „Climate-related range shifts – a global multidimensional synthesis and new research directions". *Ecography* 38.1, pp. 15–28. DOI: 10.1111/ecog.00967.

Leung, B. and Steele, R. J. (2013). „The value of a datum – how little data do we need for a quantitative risk analysis?" *Diversity and Distributions* 19.5, pp. 617–628. DOI: 10.1111/ddi.12062.

Lewis, S. L. and Maslin, M. A. (2015). „Defining the Anthropocene". *Nature* 519.7542, pp. 171–180. DOI: 10.1038/nature14258.

Luengo, D., Martino, L., Bugallo, M., Elvira, V., and Särkkä, S. (2020). „A survey of Monte Carlo methods for parameter estimation". *EURASIP Journal on Advances in Signal Processing* 2020.1, p. 25. DOI: 10.1186/s13634-020-00675-6.

Lurgi, M., Brook, B. W., Saltré, F., and Fordham, D. A. (2015). „Modelling range dynamics under global change: which framework and why?" *Methods in Ecology and Evolution* 6.3, pp. 247–256. DOI: 10.1111/2041-210X.12315.

MacArthur, R. H. (1968). „The theory of the niche". *Population biology and evolution*. New York: Syracuse University Press, pp. 159–176.

Maggini, R., Lehmann, A., Kéry, M., Schmid, H., Beniston, M., Jenni, L., and Zbinden, N. (2011). „Are Swiss birds tracking climate change?: Detecting elevational shifts using response curve shapes". en. *Ecological Modelling* 222.1, pp. 21–32. DOI: 10.1016/j.ecolmodel.2010.09.010.

Maggini, R., Lehmann, A., Zbinden, N., Zimmermann, N. E., Bolliger, J., Schröder, B., Foppen, R., Schmid, H., Beniston, M., and Jenni, L. (2014). „Assessing species vulnerability to

climate and land use change: the case of the Swiss breeding birds". en. *Diversity and Distributions* 20.6, pp. 708–719. DOI: 10.1111/ddi.12207.

Malchow, A.-K., Hartig, F., Reeg, J., Kéry, M., and Zurell, D. (2023). „Demography–environment relationships improve mechanistic understanding of range dynamics under climate change". *Philosophical Transactions of the Royal Society B: Biological Sciences* 378.1881, p. 20220194. DOI: 10.1098/rstb.2022.0194.

Malchow, A.-K., Bocedi, G., Palmer, S. C. F., Travis, J. M. J., and Zurell, D. (2021). „RangeShiftR: an R package for individual-based simulation of spatial eco-evolutionary dynamics and species' responses to environmental changes". *Ecography* 44.10, pp. 1443–1452. DOI: 10.1111/ecog.05689.

Malchow, A.-K., Fandos, G., Kormann, U., Grüebler, M., Kéry, M., Hartig, F., and Zurell, D. (2022). *Fitting an individual-based model of spatial population dynamics to long-term monitoring data*. DOI: 10.1101/2022.09.26.509574.

Manel, S., Schwartz, M. K., Luikart, G., and Taberlet, P. (2003). „Landscape genetics: combining landscape ecology and population genetics". *Trends in Ecology & Evolution* 18.4, pp. 189–197. DOI: 10.1016/S0169-5347(03)00008-9.

Manson, S., An, L., Clarke, K. C., Heppenstall, A., Koch, J., Krzyzanowski, B., Morgan, F., O'Sullivan, D., Runck, B. C., Shook, E., and Tesfatsion, L. (2020). „Methodological Issues of Spatial Agent-Based Models". *Journal of Artificial Societies and Social Simulation* 23.1, p. 3.

Marion, G., McInerny, G. J., Pagel, J., Catterall, S., Cook, A. R., Hartig, F., and O'Hara, R. B. (2012). „Parameter and uncertainty estimation for process-oriented population and distribution models: data, statistics and the niche". *Journal of Biogeography* 39.12, pp. 2225–2239. DOI: 10.1111/j.1365-2699.2012.02772.x.

Martay, B., Brewer, M. J., Elston, D. A., Bell, J. R., Harrington, R., Brereton, T. M., Barlow, K. E., Botham, M. S., and Pearce-Higgins, J. W. (2017). „Impacts of climate change on national biodiversity population trends". en. *Ecography* 40.10, pp. 1139–1151. DOI: 10.1111/ecog.02411.

Martínez-Minaya, J., Cameletti, M., Conesa, D., and Pennino, M. G. (2018). „Species distribution modeling: a statistical review with focus in spatio-temporal issues". *Stochastic Environmental Research and Risk Assessment* 32.11, pp. 3227–3244. DOI: 10.1007/s00477-018-1548-7.

McFarland, T. M., Mathewson, H. A., Groce, J. E., Morrison, M. L., Newnam, J. C., Snelgrove, R. T., Skow, K. L., Collier, B. A., and Wilkins, R. N. (2012). „Utilization of a species

occupancy model for management and conservation". *Wildlife Society Bulletin* 36.3, pp. 432–439. DOI: 10.1002/wsb.106.

McGill, B. J., Dornelas, M., Gotelli, N. J., and Magurran, A. E. (2015). „Fifteen forms of biodiversity trend in the Anthropocene". *Trends in Ecology & Evolution* 30.2, pp. 104–113. DOI: 10.1016/j.tree.2014.11.006.

Menzel, A., Yuan, Y., Matiu, M., Sparks, T., Scheifinger, H., Gehrig, R., and Estrella, N. (2020). „Climate change fingerprints in recent European plant phenology". *Global Change Biology* 26.4, pp. 2599–2612. DOI: 10.1111/gcb.15000.

Moran, E. V., Hartig, F., and Bell, D. M. (2016). „Intraspecific trait variation across scales: implications for understanding global change responses". *Global Change Biology* 22.1, pp. 137–150. DOI: 10.1111/gcb.13000.

Morris, M. D. (1991). „Factorial Sampling Plans for Preliminary Computational Experiments". *Technometrics* 33.2, pp. 161–174. DOI: 10.1080/00401706.1991.10484804.

Mortensen, L. O., Chudzinska, M. E., Slabbekoorn, H., and Thomsen, F. (2021). „Agent-based models to investigate sound impact on marine animals: bridging the gap between effects on individual behaviour and population level consequences". *Oikos* 130.7, pp. 1074–1086. DOI: 10.1111/oik.08078.

Moulin, T., Perasso, A., Calanca, P., and Gillet, F. (2021). „DynaGraM: A process-based model to simulate multi-species plant community dynamics in managed grasslands". *Ecological Modelling* 439, p. 109345. DOI: 10.1016/j.ecolmodel.2020.109345.

Murray-Rust, D., Brown, C., Vliet, J. van, Alam, S. J., Robinson, D. T., Verburg, P. H., and Rounsevell, M. (2014). „Combining agent functional types, capitals and services to model land use dynamics". *Environmental Modelling & Software* 59, pp. 187–201. DOI: 10.1016/j.envsoft.2014.05.019.

Nachtigall, W. (2008). „Der Rotmilan (Milvus milvus, L. 1758) in Sachsen und Südbrandenburg–Untersuchungen zu Verbreitung und Ökologie". *Diss., Univ. Halle-Wittenberg*.

Nägeli, M., Scherler, P., Witczak, S., Catitti, B., Aebischer, A., Bergen, V. van, Kormann, U., and Grüebler, M. U. (2021). „Weather and food availability additively affect reproductive output in an expanding raptor population". *Oecologia*. DOI: 10.1007/s00442-021-05076-6.

Naimi, B. and Araújo, M. B. (2016). „sdm: a reproducible and extensible R platform for species distribution modelling". *Ecography* 39.4, pp. 368–375. DOI: 10.1111/ecog.01881.

Nenzén, H. K., Swab, R. M., Keith, D. A., and Araújo, M. B. (2012). „demoniche – an R-package for simulating spatially-explicit population dynamics". *Ecography* 35.7, pp. 577–580. DOI: 10.1111/j.1600-0587.2012.07378.x.

Neubert, M. G. and Caswell, H. (2000). „Density-dependent vital rates and their population dynamic consequences". *Journal of Mathematical Biology* 41.2, pp. 103–121.

Newbold, T. et al. (2015). „Global effects of land use on local terrestrial biodiversity". *Nature* 520.7545, pp. 45–50. DOI: 10.1038/nature14324.

Newson, R. (2006). „Confidence Intervals for Rank Statistics: Somers' D and Extensions". *The Stata Journal* 6.3, pp. 309–334. DOI: 10.1177/1536867X0600600302.

Newton, I., Davis, P., and Davis, J. (1989). „Age of first breeding, dispersal and survival of Red Kites Milvus milvus in Wales". *Ibis* 131.1, pp. 16–21.

O'Neill, D. W., Fanning, A. L., Lamb, W. F., and Steinberger, J. K. (2018). „A good life for all within planetary boundaries". *Nature Sustainability* 1.2, pp. 88–95. DOI: 10.1038/s41893-018-0021-4.

Oberpriller, J., Cameron, D. R., Dietze, M. C., and Hartig, F. (2021). „Towards robust statistical inference for complex computer models". *Ecology Letters* 24.6, pp. 1251–1261.

Oliver, T. H., Gillings, S., Girardello, M., Rapacciuolo, G., Brereton, T. M., Siriwardena, G. M., Roy, D. B., Pywell, R., and Fuller, R. J. (2012). „Population density but not stability can be predicted from species distribution models". *Journal of Applied Ecology* 49.3, pp. 581–590. DOI: 10.1111/j.1365-2664.2012.02138.x.

Oliver, T. H. et al. (2015). „Biodiversity and Resilience of Ecosystem Functions". *Trends in Ecology & Evolution* 30.11, pp. 673–684. DOI: 10.1016/j.tree.2015.08.009.

Osipova, E., Emslie-Smith, M., Osti, M., Murai, M., Åberg, U., and Shadie, P. (2020). *IUCN World Heritage Outlook 3*. IUCN. ISBN: 978-2-8317-2086-9.

Ovaskainen, O., Finkelshtein, D., Kutoviy, O., Cornell, S., Bolker, B., and Kondratiev, Y. (2014). „A general mathematical framework for the analysis of spatiotemporal point processes". *Theoretical Ecology* 7.1, pp. 101–113. DOI: 10.1007/s12080-013-0202-8.

Ovenden, T. S., Palmer, S. C. F., Travis, J. M. J., and Healey, J. R. (2019). „Improving reintroduction success in large carnivores through individual-based modelling: How to reintroduce Eurasian lynx (Lynx lynx) to Scotland". *Biological Conservation* 234, pp. 140–153. DOI: 10.1016/j.biocon.2019.03.035.

Pacioni, C. and Mayer, F. (2017). „vortexR: an R package for post Vortex simulation analysis". *Methods in Ecology and Evolution* 8.11, pp. 1477–1481. DOI: 10.1111/2041-210X.12786.

Pagel, J. and Schurr, F. M. (2012). „Forecasting species ranges by statistical estimation of ecological niches and spatial population dynamics". *Global Ecology and Biogeography* 21.2, pp. 293–304. DOI: 10.1111/j.1466-8238.2011.00663.x.

Palmer, S. C. F., Coulon, A., and Travis, J. M. J. (2011). „Introducing a 'stochastic movement simulator' for estimating habitat connectivity". *Methods in Ecology and Evolution* 2.3, pp. 258–268. DOI: 10.1111/j.2041-210X.2010.00073.x.

Paniw, M. et al. (2021). „The myriad of complex demographic responses of terrestrial mammals to climate change and gaps of knowledge: A global analysis". en. *Journal of Animal Ecology* 90.6, pp. 1398–1407. DOI: 10.1111/1365-2656.13467.

Parmesan, C. (2006). „Ecological and Evolutionary Responses to Recent Climate Change". *Annual Review of Ecology, Evolution, and Systematics* 37.1, pp. 637–669. DOI: 10.1146/annurev.ecolsys.37.091305.110100.

Parmesan, C. and Yohe, G. (2003). „A globally coherent fingerprint of climate change impacts across natural systems". *Nature* 421.6918, pp. 37–42. DOI: 10.1038/nature01286.

Pearson, R. G. and Dawson, T. P. (2003). „Predicting the impacts of climate change on the distribution of species: are bioclimate envelope models useful?" *Global Ecology and Biogeography* 12.5, pp. 361–371. DOI: 10.1046/j.1466-822X.2003.00042.x.

Pellissier, L., Rohr, R. P., Ndiribe, C., Pradervand, J.-N., Salamin, N., Guisan, A., and Wisz, M. (2013). „Combining food web and species distribution models for improved community projections". *Ecology and Evolution* 3.13, pp. 4572–4583. DOI: 10.1002/ece3.843.

Perkins, T. A., Phillips, B. L., Baskett, M. L., and Hastings, A. (2013). „Evolution of dispersal and life history interact to drive accelerating spread of an invasive species". *Ecology Letters* 16.8, pp. 1079–1087. DOI: 10.1111/ele.12136.

Pfeiffer, T. and Schaub, M. (2023). „Productivity drives the dynamics of a red kite source population that depends on immigration". *Journal of Avian Biology* 2023.1-2, e02984.

Phillips, S. J., Anderson, R. P., Dudík, M., Schapire, R. E., and Blair, M. E. (2017). „Opening the black box: an open-source release of Maxent". *Ecography* 40.7, pp. 887–893. DOI: 10.1111/ecog.03049.

Pollock, L. J., Tingley, R., Morris, W. K., Golding, N., O'Hara, R. B., Parris, K. M., Vesk, P. A., and McCarthy, M. A. (2014). „Understanding co-occurrence by modelling species simultaneously with a Joint Species Distribution Model (JSDM)". *Methods in Ecology and Evolution* 5.5, pp. 397–406. DOI: 10.1111/2041-210X.12180.

Pulliam, H. R. (2000). „On the relationship between niche and distribution“. *Ecology Letters* 3.4, pp. 349–361. DOI: 10.1046/j.1461-0248.2000.00143.x.

Purves, D., Scharlemann, J. P. W., Harfoot, M., Newbold, T., Tittensor, D. P., Hutton, J., and Emmott, S. (2013). „Time to model all life on Earth“. *Nature* 493.7432, pp. 295–297. DOI: 10.1038/493295a.

Qiao, H., Soberón, J., and Peterson, A. T. (2015). „No silver bullets in correlative ecological niche modelling: insights from testing among many potential algorithms for niche estimation“. *Methods in Ecology and Evolution* 6.10, pp. 1126–1136. DOI: 10.1111/2041-210X.12397.

R Core Team (2023). *R: A Language and Environment for Statistical Computing*. Vienna, Austria: R Foundation for Statistical Computing.

Railsback, S. F. and Grimm, V. (2019). *Agent-Based and Individual-Based Modeling: A Practical Introduction, Second Edition*. Princeton University Press. 359 pp. ISBN: 978-0-691-19004-4.

Risk, B. B., Valpine, P. de, and Beissinger, S. R. (2011). „A robust-design formulation of the incidence function model of metapopulation dynamics applied to two species of rails“. *Ecology* 92.2, pp. 462–474. DOI: 10.1890/09-2402.1.

Roberts, D. R., Bahn, V., Ciuti, S., Boyce, M. S., Elith, J., Guillera-Arroita, G., Hauenstein, S., Lahoz-Monfort, J. J., Schröder, B., Thuiller, W., Warton, D. I., Wintle, B. A., Hartig, F., and Dormann, C. F. (2017). „Cross-validation strategies for data with temporal, spatial, hierarchical, or phylogenetic structure“. *Ecography* 40.8, pp. 913–929. DOI: 10.1111/ecog.02881.

Rockström, J. et al. (2009). „Planetary Boundaries: Exploring the Safe Operating Space for Humanity“. *Ecology and Society* 14.2.

Rodríguez, L., García, J. J., Carreño, F., and Martínez, B. (2019). „Integration of physiological knowledge into hybrid species distribution modelling to improve forecast of distributional shifts of tropical corals“. *Diversity and Distributions* 25.5, pp. 715–728. DOI: 10.1111/ddi.12883.

Rosenbaum, B., Raatz, M., Weithoff, G., Fussmann, G. F., and Gaedke, U. (2019). „Estimating Parameters From Multiple Time Series of Population Dynamics Using Bayesian Inference“. *Frontiers in Ecology and Evolution* 6. DOI: 10.3389/fevo.2018.00234.

Rosenzweig, C. and Neofotis, P. (2013). „Detection and attribution of anthropogenic climate change impacts“. en. *WIREs Climate Change* 4.2, pp. 121–150. DOI: 10.1002/wcc.209.

Saether, B.-E. and Bakke, O. (2000). „Avian Life History Variation and Contribution of Demographic Traits to the Population Growth Rate“. en. *Ecology* 81.3, pp. 642–653. DOI: 10.1890/0012-9658(2000)081[0642:ALHVAC]2.0.CO;2.

Saltelli, A., Ratto, M., Tarantola, S., and Campolongo, F. (2006). „Sensitivity analysis practices: Strategies for model-based inference“. *Reliability Engineering & System Safety*. The Fourth International Conference on Sensitivity Analysis of Model Output (SAMO 2004) 91.10, pp. 1109–1125. DOI: 10.1016/j.ress.2005.11.014.

Sanczuk, P., De Lombaerde, E., Haesen, S., Van Meerbeek, K., Luoto, M., Van der Veken, B., Van Beek, E., Hermy, M., Verheyen, K., Vangansbeke, P., et al. (2022). „Competition mediates understorey species range shifts under climate change“. *Journal of Ecology*.

Santos, E. P., Wagner, H. H., Ferraz, S. F. B., and Siqueira, T. (2020). „Interactive persistent effects of past land-cover and its trajectory on tropical freshwater biodiversity“. *Journal of Applied Ecology* 57.11, pp. 2149–2158. DOI: 10.1111/1365-2664.13717.

Sarukhan, J. et al. (2005). *Millenium Ecosystem Assessment: Ecosystems and human well-being*. Island Press.

Schaub, M. (2012). „Spatial distribution of wind turbines is crucial for the survival of red kite populations“. *Biological Conservation* 155, pp. 111–118. DOI: 10.1016/j.biocon.2012.06.021.

Scheffers, B. R. et al. (2016). „The broad footprint of climate change from genes to biomes to people“. *Science* 354.6313, aaf7671. DOI: 10.1126/science.aaf7671.

Schmid, H., Luder, R., Naef-Daenzer, B., Graf, R., and Zbinden, N. (1998). *Schweizer Brutvogelatlas 1993–1996*. Sempach, Schweiz: Schweizerische Vogelwarte. ISBN: 978-3-9521064-5-7.

Schmid, H., Zbinden, N., and Keller, V. (2004). *Überwachung der Bestandsentwicklung häufiger Brutvögel in der Schweiz*. Sempach: Schweizerische Vogelwarte.

Schmolke, A., Thorbek, P., DeAngelis, D. L., and Grimm, V. (2010). „Ecological models supporting environmental decision making: a strategy for the future“. *Trends in Ecology & Evolution* 25.8, pp. 479–486. DOI: 10.1016/j.tree.2010.05.001.

Schultz, E. L., Hülsmann, L., Pillet, M. D., Hartig, F., Breshears, D. D., Record, S., Shaw, J. D., DeRose, R. J., Zuidema, P. A., and Evans, M. E. (2022). „Climate-driven, but dynamic and complex? A reconciliation of competing hypotheses for species' distributions“. *Ecology letters* 25.1, pp. 38–51. DOI: 10.1111/ele.13902.

Schurr, F. M., Pagel, J., Cabral, J. S., Groeneveld, J., Bykova, O., O'Hara, R. B., Hartig, F., Kissling, W. D., Linder, H. P., Midgley, G. F., Schröder, B., Singer, A., and Zimmermann, N. E. (2012). „How to understand species' niches and range dynamics: a demographic

research agenda for biogeography". *Journal of Biogeography* 39.12, pp. 2146–2162. DOI: 10.1111/j.1365-2699.2012.02737.x.

Schuwirth, N., Borgwardt, F., Domisch, S., Friedrichs, M., Kattwinkel, M., Kneis, D., Kuemmerlen, M., Langhans, S. D., Martínez-López, J., and Vermeiren, P. (2019). „How to make ecological models useful for environmental management". *Ecological Modelling* 411, p. 108784. DOI: 10.1016/j.ecolmodel.2019.108784.

Schweiger, O., Heikkinen, R. K., Harpke, A., Hickler, T., Klotz, S., Kudrna, O., Kühn, I., Pöyry, J., and Settele, J. (2012). „Increasing range mismatching of interacting species under global change is related to their ecological characteristics". *Global Ecology and Biogeography* 21.1, pp. 88–99. DOI: 10.1111/j.1466-8238.2010.00607.x.

Selwood, K. E., McGeoch, M. A., and Mac Nally, R. (2015). „The effects of climate change and land-use change on demographic rates and population viability". *Biological Reviews* 90.3, pp. 837–853. DOI: 10.1111/brv.12136.

Semper-Pascual, A., Burton, C., Baumann, M., Decarre, J., Gavier-Pizarro, G., Gómez-Valencia, B., Macchi, L., Mastrangelo, M. E., Pötzschner, F., Zelaya, P. V., and Kuemmerle, T. (2021). „How do habitat amount and habitat fragmentation drive time-delayed responses of biodiversity to land-use change?" *Proceedings of the Royal Society B: Biological Sciences* 288.1942, p. 20202466. DOI: 10.1098/rspb.2020.2466.

Sergio, F., Tavecchia, G., Blas, J., Tanferna, A., and Hiraldo, F. (2021). „Demographic modeling to fine-tune conservation targets: importance of pre-adults for the decline of an endangered raptor". *Ecological Applications* 31.3, e2266. DOI: 10.1002/eap.2266.

Sillero, N. (2011). „What does ecological modelling model? A proposed classification of ecological niche models based on their underlying methods". *Ecological Modelling* 222.8, pp. 1343–1346. DOI: 10.1016/j.ecolmodel.2011.01.018.

Sillero, N., Arenas-Castro, S., Enriquez-Urzelai, U., Vale, C. G., Sousa-Guedes, D., Martínez-Freiría, F., Real, R., and Barbosa, A. M. (2021). „Want to model a species niche? A step-by-step guideline on correlative ecological niche modelling". *Ecological Modelling* 456, p. 109671. DOI: 10.1016/j.ecolmodel.2021.109671.

Singer, A., Johst, K., Banitz, T., Fowler, M. S., Groeneveld, J., Gutiérrez, A. G., Hartig, F., Krug, R. M., Liess, M., Matlack, G., Meyer, K. M., Pe'er, G., Radchuk, V., Voinopol-Sassu, A.-J., and Travis, J. M. J. (2016). „Community dynamics under environmental change: How can next generation mechanistic models improve projections of species distributions?" *Ecological Modelling*. Next generation ecological modelling, concepts,

and theory: structural realism, emergence, and predictions 326, pp. 63–74. DOI: 10.1016/j.ecolmodel.2015.11.007.

Singer, A., Schweiger, O., Kühn, I., and Johst, K. (2018). „Constructing a hybrid species distribution model from standard large-scale distribution data". *Ecological Modelling* 373, pp. 39–52. DOI: 10.1016/j.ecolmodel.2018.02.002.

Singer, A., Travis, J. M. J., and Johst, K. (2013). „Interspecific interactions affect species and community responses to climate shifts". *Oikos* 122.3, pp. 358–366. DOI: 10.1111/j.1600-0706.2012.20465.x.

Skagen, S. K. and Adams, A. A. Y. (2012). „Weather effects on avian breeding performance and implications of climate change". en. *Ecological Applications* 22.4, pp. 1131–1145. DOI: 10.1890/11-0291.1.

Smolik, M., Dullinger, S., Essl, F., Kleinbauer, I., Leitner, M., Peterseil, J., Stadler, L.-M., and Vogl, G. (2010). „Integrating species distribution models and interacting particle systems to predict the spread of an invasive alien plant". *Journal of Biogeography* 37.3, pp. 411–422. DOI: 10.1111/j.1365-2699.2009.02227.x.

Soberón, J. (2007). „Grinnellian and Eltonian niches and geographic distributions of species". *Ecology Letters* 10.12, pp. 1115–1123. DOI: 10.1111/j.1461-0248.2007.01107.x.

Soberón, J. and Nakamura, M. (2009). „Niches and distributional areas: Concepts, methods, and assumptions". *Proceedings of the National Academy of Sciences* 106 (Supplement 2), pp. 19644–19650. DOI: 10.1073/pnas.0901637106.

Steffen, W., Broadgate, W., Deutsch, L., Gaffney, O., and Ludwig, C. (2015). „The trajectory of the Anthropocene: The Great Acceleration". *The Anthropocene Review* 2.1, pp. 81–98. DOI: 10.1177/2053019614564785.

Steffen, W., Richardson, K., et al. (2015). „Planetary boundaries: Guiding human development on a changing planet". *Science* 347.6223. DOI: 10.1126/science.1259855.

Storchová, L. and Horák, D. (2018). „Life-history characteristics of European birds". *Global Ecology and Biogeography* 27.4, pp. 400–406. DOI: 10.1111/geb.12709.

Sunday, J. M., Bates, A. E., and Dulvy, N. K. (2012). „Thermal tolerance and the global redistribution of animals". *Nature Climate Change* 2.9, pp. 686–690. DOI: 10.1038/nclimate1539.

Synes, N. W., Brown, C., Palmer, S. C. F., Bocedi, G., Osborne, P. E., Watts, K., Franklin, J., and Travis, J. M. J. (2019). „Coupled land use and ecological models reveal emergence and feedbacks in socio-ecological systems". *Ecography* 42.4, pp. 814–825. DOI: 10.1111/ecog.04039.

Tavecchia, G., Tenan, S., Pradel, R., Igual, J.-M., Genovart, M., and Oro, D. (2016). „Climate-driven vital rates do not always mean climate-driven population". *Global Change Biology* 22.12, pp. 3960–3966. DOI: 10.1111/gcb.13330.

Thomas, C. D. and Lennon, J. J. (1999). „Birds extend their ranges northwards". en. *Nature* 399.6733, pp. 213–213. DOI: 10.1038/20335.

Thompson, B. K., Olden, J. D., and Converse, S. J. (2021). „Mechanistic invasive species management models and their application in conservation". *Conservation Science and Practice* 3.11, e533. DOI: 10.1111/csp2.533.

Thuiller, W., Lafourcade, B., Engler, R., and Araújo, M. B. (2009). „BIOMOD – a platform for ensemble forecasting of species distributions". *Ecography* 32.3, pp. 369–373. DOI: 10.1111/j.1600-0587.2008.05742.x.

Thuiller, W. et al. (2014). „Does probability of occurrence relate to population dynamics?" *Ecography* 37.12, pp. 1155–1166. DOI: 10.1111/ecog.00836.

Tikhonov, G., Opedal, Ø. H., Abrego, N., Lehikoinen, A., Jonge, M. M. J. de, Oksanen, J., and Ovaskainen, O. (2020). „Joint species distribution modelling with the r-package Hmsc". *Methods in Ecology and Evolution* 11.3, pp. 442–447. DOI: 10.1111/2041-210X.13345.

Tilman, D., Clark, M., Williams, D. R., Kimmel, K., Polasky, S., and Packer, C. (2017). „Future threats to biodiversity and pathways to their prevention". *Nature* 546.7656, pp. 73–81. DOI: 10.1038/nature22900.

Travis, J., Brooker, R., and Dytham, C. (2005). „The interplay of positive and negative species interactions across an environmental gradient: insights from an individual-based simulation model". *Biology Letters* 1.1, pp. 5–8. DOI: 10.1098/rsbl.2004.0236.

Travis, J. M. J., Delgado, M., Bocedi, G., Baguette, M., Bartoń, K., Bonte, D., Boulangeat, I., Hodgson, J. A., Kubisch, A., Penteriani, V., Saastamoinen, M., Stevens, V. M., and Bullock, J. M. (2013). „Dispersal and species' responses to climate change". *Oikos* 122.11, pp. 1532–1540. DOI: 10.1111/j.1600-0706.2013.00399.x.

Travis, J. M. J., Mustin, K., Bartoń, K. A., Benton, T. G., Clobert, J., Delgado, M. M., Dytham, C., Hovestadt, T., Palmer, S. C. F., Dyck, H. V., and Bonte, D. (2012). „Modelling dispersal: an eco-evolutionary framework incorporating emigration, movement, settlement behaviour and the multiple costs involved". *Methods in Ecology and Evolution* 3.4, pp. 628–641. DOI: 10.1111/j.2041-210X.2012.00193.x.

Treurnicht, M., Pagel, J., Esler, K. J., Schutte-Vlok, A., Nottebrock, H., Kraaij, T., Rebelo, A. G., and Schurr, F. M. (2016). „Environmental drivers of demographic variation across the

global geographical range of 26 plant species". en. *Journal of Ecology* 104.2, pp. 331–342. DOI: 10.1111/1365-2745.12508.

Urban, M. C. et al. (2016). „Improving the forecast for biodiversity under climate change". *Science* 353.6304. DOI: 10.1126/science.aad8466.

Urban, M. C. et al. (2022). „Coding for Life: Designing a Platform for Projecting and Protecting Global Biodiversity". *BioScience* 72.1, pp. 91–104. DOI: 10.1093/biosci/biab099.

Valavi, R., Elith, J., Lahoz-Monfort, J. J., and Guillera-Arroita, G. (2019). „blockCV: An r package for generating spatially or environmentally separated folds for k-fold cross-validation of species distribution models". *Methods in Ecology and Evolution* 10.2, pp. 225–232. DOI: 10.1111/2041-210X.13107.

Vázquez, D. P., Gianoli, E., Morris, W. F., and Bozinovic, F. (2017). „Ecological and evolutionary impacts of changing climatic variability". *Biological Reviews* 92.1, pp. 22–42. DOI: 10.1111/brv.12216.

Vehtari, A., Gelman, A., and Gabry, J. (2017). „Practical Bayesian model evaluation using leave-one-out cross-validation and WAIC". *Statistics and Computing* 27.5, pp. 1413–1432. DOI: 10.1007/s11222-016-9696-4.

Vehtari, A., Gelman, A., Simpson, D., Carpenter, B., and Bürkner, P.-C. (2021). „Rank-Normalization, Folding, and Localization: An Improved R^ for Assessing Convergence of MCMC (with Discussion)". *Bayesian Analysis* 16.2, pp. 667–718. DOI: 10.1214/20-BA1221.

Visintin, C., Briscoe, N. J., Woolley, S. N. C., Lentini, P. E., Tingley, R., Wintle, B. A., and Golding, N. (2020). „steps: Software for spatially and temporally explicit population simulations". *Methods in Ecology and Evolution* 11.4, pp. 596–603. DOI: 10.1111/2041-210X.13354.

Warne, D. J., Baker, R. E., and Simpson, M. J. (2020). „A practical guide to pseudo-marginal methods for computational inference in systems biology". *Journal of Theoretical Biology* 496, p. 110255. DOI: 10.1016/j.jtbi.2020.110255.

Watts, K., Whytock, R. C., Park, K. J., Fuentes-Montemayor, E., Macgregor, N. A., Duffield, S., and McGowan, P. J. K. (2020). „Ecological time lags and the journey towards conservation success". *Nature Ecology & Evolution* 4.3, pp. 304–311. DOI: 10.1038/s41559-019-1087-8.

Weber, M. M., Stevens, R. D., Diniz-Filho, J. A. F., and Grelle, C. E. V. (2017). „Is there a correlation between abundance and environmental suitability derived from ecological niche modelling? A meta-analysis". en. *Ecography* 40.7, pp. 817–828. DOI: 10.1111/ecog.02125.

Wenger, S. J. and Olden, J. D. (2012). „Assessing transferability of ecological models: an underappreciated aspect of statistical validation". *Methods in Ecology and Evolution* 3.2, pp. 260–267. DOI: 10.1111/j.2041-210X.2011.00170.x.

Whitney, K. D. and Gabler, C. A. (2008). „Rapid evolution in introduced species, 'invasive traits' and recipient communities: challenges for predicting invasive potential". *Diversity and Distributions* 14.4, pp. 569–580. DOI: 10.1111/j.1472-4642.2008.00473.x.

Wiens, J. J. (2016). „Climate-Related Local Extinctions Are Already Widespread among Plant and Animal Species". *PLOS Biology* 14.12, e2001104. DOI: 10.1371/journal.pbio.2001104.

Wiens, J. J. and Graham, C. H. (2005). „Niche Conservatism: Integrating Evolution, Ecology, and Conservation Biology". *Annual Review of Ecology, Evolution, and Systematics* 36.1, pp. 519–539. DOI: 10.1146/annurev.ecolsys.36.102803.095431.

Wilkinson, M. D. et al. (2016). „The FAIR Guiding Principles for scientific data management and stewardship". *Scientific Data* 3.1, p. 160018. DOI: 10.1038/sdata.2016.18.

WWF (2020). *Living Planet Report 2020 - Bending the curve of biodiversity loss.* Gland, Switzerland: Almond, R.E.A., Grooten M. and Petersen, T. (Eds).

Yin, D. and He, F. (2014). „A simple method for estimating species abundance from occurrence maps". *Methods in Ecology and Evolution* 5.4, pp. 336–343. DOI: 10.1111/2041-210X.12159.

Zurell, D. (2017). „Integrating demography, dispersal and interspecific interactions into bird distribution models". *Journal of Avian Biology* 48.12, pp. 1505–1516. DOI: 10.1111/jav.01225.

Zurell, D., König, C., Malchow, A.-K., Kapitza, S., Bocedi, G., Travis, J., and Fandos, G. (2022). „Spatially explicit models for decision-making in animal conservation and restoration". *Ecography* 2022.4. DOI: 10.1111/ecog.05787.

Zurell, D., Thuiller, W., Pagel, J., Cabral, J. S., Münkemüller, T., Gravel, D., Dullinger, S., Normand, S., Schiffers, K. H., Moore, K. A., and Zimmermann, N. E. (2016). „Benchmarking novel approaches for modelling species range dynamics". *Global Change Biology* 22.8, pp. 2651–2664. DOI: 10.1111/gcb.13251.

Zylstra, E. R. and Zipkin, E. F. (2021). „Accounting for sources of uncertainty when forecasting population responses to climate change". *Journal of Animal Ecology* 90.3, pp. 558–561. DOI: 10.1111/1365-2656.13443.

Appendix A

Coauthorships

This appendix lists the publications that I have coauthored and are relevant to the field.

A.1. Spatially explicit models for decision-making in animal conservation and restoration

Zurell, D., König, C., **Malchow, A.-K.**, Kapitza, S., Bocedi, G., Travis, J., and Fandos, G. (2022). Spatially explicit models for decision-making in animal conservation and restoration. *Ecography*, 2022(4). https://doi.org/10.1111/ecog.05787

Abstract. Models are useful tools for understanding and predicting ecological patterns and processes. Under ongoing climate and biodiversity change, they can greatly facilitate decision-making in conservation and restoration and help designing adequate management strategies for an uncertain future. Here, we review the use of spatially explicit models for decision support and to identify key gaps in current modelling in conservation and restoration. Of 650 reviewed publications, 217 publications had a clear management application and were included in our quantitative analyses. Overall, modelling studies were biased towards static models (79%), towards the species and population level (80%) and towards conservation (rather than restoration) applications (71%). Correlative niche models were the most widely used model type. Dynamic models as well as the gene-to-individual level and the community-to-ecosystem level were under-represented, and explicit cost optimisation approaches were only used in 10% of the studies. We present a new model typology for selecting models for animal conservation and restoration, characterising model types according to organisational levels, biological processes of interest and desired management applications. This typology will help to more closely link models to management goals. Additionally, future efforts need to overcome important challenges related to data integration, model integration and decision-making. We conclude with five key recommendations, suggesting that wider usage of spatially explicit models for decision support can be achieved by 1) developing a toolbox with multiple, easier-to-use methods, 2) improving calibration and validation of dynamic modelling approaches and 3) developing best-practise guidelines for applying these models. Further, more robust decision-making can be achieved by 4) combining multiple modelling approaches to assess uncertainty, and 5) placing models at the core of adaptive management. These efforts must be accompanied by long-term funding for modelling and monitoring, and improved communication between research and practise to ensure optimal conservation and restoration outcomes.

A.2. Can dynamic occupancy models improve predictions of species' range dynamics? A test using Swiss birds

Briscoe, N. J., Zurell, D., Elith, J., König, C., Fandos, G., **Malchow, A.-K.**, Kéry, M., Schmid, H., and Guillera-Arroita, G. (2021). Can dynamic occupancy models improve predictions of species' range dynamics? A test using Swiss birds. *Global Change Biology*, 27(18), 4269–4282. https://doi.org/10.1111/gcb.15723

Abstract. Predictions of species' current and future ranges are needed to effectively manage species under environmental change. Species ranges are typically estimated using correlative species distribution models (SDMs), which have been criticized for their static nature. In contrast, dynamic occupancy models (DOMs) explicitily describe temporal changes in species' occupancy via colonization and local extinction probabilities, estimated from time series of occurrence data. Yet, tests of whether these models improve predictive accuracy under current or future conditions are rare. Using a long-term data set on 69 Swiss birds, we tested whether DOMs improve the predictions of distribution changes over time compared to SDMs. We evaluated the accuracy of spatial predictions and their ability to detect population trends. We also explored how predictions differed when we accounted for imperfect detection and parameterized models using calibration data sets of different time series lengths. All model types had high spatial predictive performance when assessed across all sites (mean AUC > 0.8), with flexible machine learning SDM algorithms outperforming parametric static and DOMs. However, none of the models performed well at identifying sites where range changes are likely to occur. In terms of estimating population trends, DOMs performed best, particularly for species with strong population changes and when fit with sufficient data, while static SDMs performed very poorly. Overall, our study highlights the importance of considering what aspects of performance matter most when selecting a modelling method for a particular application and the need for further research to improve model utility. While DOMs show promise for capturing range dynamics and inferring population trends when fitted with sufficient data, computational constraints on variable selection and model fitting can lead to reduced spatial accuracy of predictions, an area warranting more attention.

A.3. RangeShifter 2.0: An extended and enhanced platform for modelling spatial eco-evolutionary dynamics and species' responses to environmental changes

Bocedi, G., Palmer, S. C. F., **Malchow, A.-K.**, Zurell, D., Watts, K., and Travis, J. M. J. (2021). RangeShifter 2.0: An extended and enhanced platform for modelling spatial eco-evolutionary dynamics and species' responses to environmental changes. *Ecography*, 44(10), 1453–1462. https://doi.org/10.1111/ecog.05687

Abstract. Process-based models are becoming increasingly used tools for understanding how species are likely to respond to environmental changes and to potential management options. RangeShifter is one such modelling platform, which has been used to address a range of questions including identifying effective reintroduction strategies, understanding patterns of range expansion and assessing population viability of species across complex landscapes. Here we introduce a new version, RangeShifter 2.0, which incorporates important new functionality. It is now possible to simulate dynamics over user-specified, temporally changing landscapes. Additionally, we integrated a new genetic module, notably introducing an explicit genetic modelling architecture, which allows for simulation of neutral and adaptive genetic processes. Furthermore, emigration, transfer and settlement traits can now all evolve, allowing for sophisticated simulation of the evolution of dispersal. We illustrate the potential application of RangeShifter 2.0's new functionality by two examples. The first illustrates the range expansion of a virtual species across a dynamically changing UK landscape. The second demonstrates how the software can be used to explore the concept of evolving connectivity in response to land-use modification, by examining how movement rules come under selection over landscapes of different structure and composition. RangeShifter 2.0 is built using object-oriented C++ providing computationally efficient simulation of complex individual-based, eco-evolutionary models. The code has been redeveloped to enable use across operating systems, including on high performance computing clusters, and the Windows graphical user interface has been enhanced. RangeShifter 2.0 will facilitate the development of in-silico assessments of how species will respond to environmental changes and to potential management options for conserving or controlling them. By making the code available open source, we hope to inspire further collaborations and extensions by the ecological community.

A.4. Stability-instability transition in tripartite merged ecological networks

Emary, C., and **Malchow, A.-K.** (2022). Stability-instability transition in tripartite merged ecological networks. *Journal of Mathematical Biology*, 85(3), 20. https://doi.org/10.1007/s00285-022-01783-7

Abstract. Although ecological networks are typically constructed based on a single type of interaction, e.g. trophic interactions in a food web, a more complete picture of ecosystem composition and functioning arises from merging networks of multiple interaction types. In this work, we consider tripartite networks constructed by merging two bipartite networks, one mutualistic and one antagonistic. Taking the interactions within each sub-network to be distributed randomly, we consider the stability of the dynamics of the network based on the spectrum of its community matrix. In the asymptotic limit of a large number of species, we show that the spectrum undergoes an eigenvalue phase transition, which leads to an abrupt destabilisation of the network as the ratio of mutualists to antagonists is increased. We also derive results that show how this transition is manifest in networks of finite size, as well as when disorder is introduced in the segregation of the two interaction types. Our random-matrix results will serve as a baseline for understanding the behaviour of merged networks with more realistic structures and/or more detailed dynamics.

A.5. Coding for Life: Designing a Platform for Projecting and Protecting Global Biodiversity

Urban, M. C., Travis, J. M. J., Zurell, D., Thompson, P. L., Synes, N. W., Scarpa, A., Peres-Neto, P. R., **Malchow, A.-K.**, James, P. M. A., Gravel, D., De Meester, L., Brown, C., Bocedi, G., Albert, C. H., Gonzalez, A., and Hendry, A. P. (2022). Coding for Life: Designing a Platform for Projecting and Protecting Global Biodiversity. *BioScience*, 72(1), 91–104. https://doi.org/10.1093/biosci/biab099

Abstract. Time is running out to limit further devastating losses of biodiversity and nature's contributions to humans. Addressing this crisis requires accurate predictions about which species and ecosystems are most at risk to ensure efficient use of limited conservation and management resources. We review existing biodiversity projection models and discover problematic gaps. Current models usually cannot easily be reconfigured for other species or systems, omit key biological processes, and cannot accommodate feedbacks with Earth system dynamics. To fill these gaps, we envision an adaptable, accessible, and universal biodiversity modeling platform that can project essential biodiversity variables, explore the implications of divergent socioeconomic scenarios, and compare conservation and management strategies. We design a roadmap for implementing this vision and demonstrate that building this biodiversity forecasting platform is possible and practical.

Appendix B

Supporting information: Fitting an individual-based model of spatial population dynamics to long-term monitoring data

B.1. Supplementary figures and tables

Table B.1.: The CORINE land cover classes (column 3) were aggregated to the land-use variables (column 2) that were considered as predictors in the habitat suitability model (HSM). The asterisks in column 1 mark those aggregated variables that remained after the variable selection process and were used as predictors in the HSM.

HSM var	Aggregated land cover type	Corine classes
	artificial surfaces	111-142
	arable land	211-213
*	orchards, pastures, heterogeneous agricultural areas	221-223, 231, 241-244
*	forests	311-313
	natural grassland, moors and heathland	321-324
	no vegetation	331-335
*	wetlands, water bodies	411-423, 511-523

Table B.2.: Overview of all data sources used to parameterise and calibrate the dynamic SDM.

Usage	Data type	Data source
Direct parametrisation		
Initial distribution	Abundance snapshot	Breeding bird Atlas II (1993-96) (Schmid et al., 1998)
Static habitat model (cSDM)	Presence/absence	Breeding bird Atlas III (2013-16) (Knaus et al., 2018)
	Bioclimatic variables	CHELSA Bioclim v1.2: WorldClim (1979-2013) (Karger et al., 2017; Karger et al., 2018)
	Land cover	CORINE (2012) (European Union, 2022)
Habitat suitability maps (cSDM projections)	Bioclimatic variables - same as for fitting	CHELSA Bioclim v1.2: WorldClim (1979-2013)
	Land cover - varying	CORINE (2000, 2006, 2012, 2018) (European Union, 2022)
Individual-based model	Stage structure	Sergio et al. (2021) and Newton et al. (1989)
	Survival probabilities	Katzenberger et al. (2019) (also Schaub (2012) and Newton et al. (1989))
	Fecundity	Nägeli et al. (2021) (also Schaub (2012) and Nachtigall (2008))
	Emigration probability	own unpublished data
	Dispersal distance	Nachtigall (2008) (also Newton et al. (1989) and own unpublished data)
Indirect parametrisation		
Calibration (likelihood input)	Abundance time series	Swiss breeding bird survey (1999-2019) (Schmid & Volet, 2004)
Validation		
Internal validation (cross-validation)	Abundance time series (folds of calibration data set)	Swiss breeding bird survey (1999-2019) (Schmid & Volet, 2004)
External validation	Relative abundance time series	Swiss breeding bird index (1999-2019) (Knaus et al., 2022)

Table B.3.: All nineteen WorldClim Bioclimatic variables (column 2 and 3) were considered as predictors in the habitat suitability model (HSM). The asterisks in column 1 mark those variables that remained after the variable selection process and were used as predictors in the HSM.

HSM var	Name	Description
	BIO1	Annual Mean Temperature
*	BIO2	Mean Diurnal Range (monthly Mean(max_{temp} - min_{temp}))
*	BIO3	Isothermality (BIO2/BIO7) (* 100)
*	BIO4	Temperature Seasonality (standard deviation *100)
*	BIO5	Max Temperature of Warmest Month
	BIO6	Min Temperature of Coldest Month
	BIO7	Mean Temperature of Wettest Quarter
*	BIO9	Mean Temperature of Driest Quarter
	BIO10	Mean Temperature of Warmest Quarter
	BIO11	Mean Temperature of Coldest Quarter
	BIO12	Annual Precipitation
*	BIO13	Precipitation of Wettest Month
*	BIO14	Precipitation of Driest Month
*	BIO15	Precipitation Seasonality (Coefficient of Variation)
	BIO16	Precipitation of Wettest Quarter
	BIO17	Precipitation of Driest Quarter
	BIO18	Precipitation of Warmest Quarter
	BIO19	Precipitation of Coldest Quarter

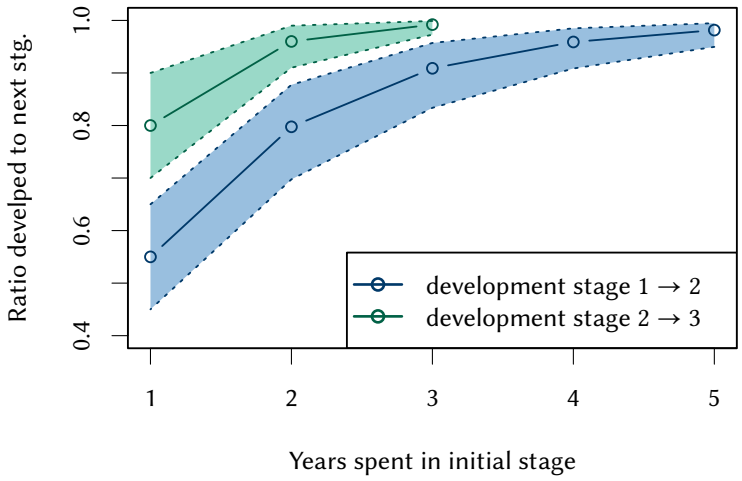

Figure B.1.: Ratio of individuals of an initial stage (1 or 2) that have developed to the next stage (2 or 3) after a number of years x have passed.

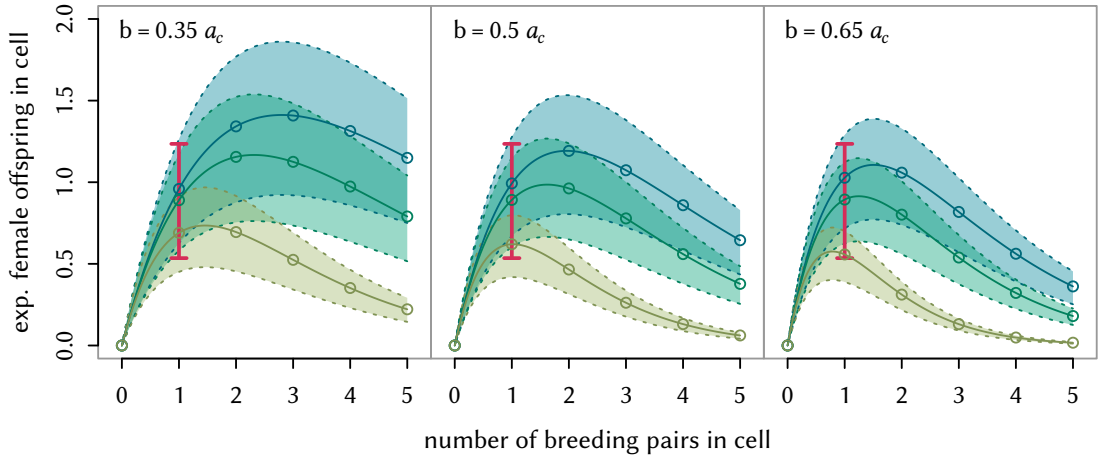

Figure B.2.: Mean and standard deviation of the number of expected female offspring per cell over the number of breeding pairs in that cell for different values of the parameter that controls the strength of demographic density-dependence $b = (0.50 \pm 0.15)\, a_c$. Blue, turquoise and green show this relation for a cell of 98, 81, and 51% habitat suitability (the maximum, median and minimum HSI over all habitat cells). The red bar indicates the range of observed fecundities $\phi_1 = 0.88 \pm 0.35$.

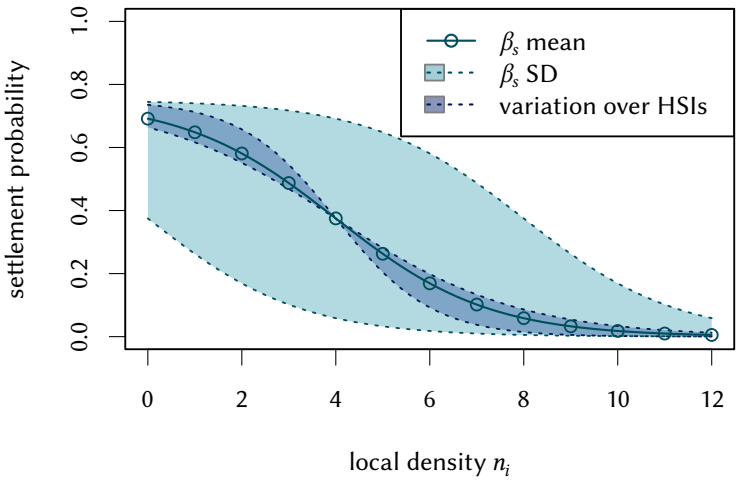

Figure B.3.: Mean and standard deviation of settlement probability $p_s = p_{s,0}\,(1 + e^{-\alpha_s\,(b_i n_i - \beta_s)})^{-1}$. The inflection point β_s is a calibrated parameter and is estimated as $\hat{\beta}_s = \beta_s / b = (4 \pm 4)\,a_c^{-1}$. The maximum settlement probability $s_0 = 0.75$ and slope parameter $\alpha_s = -1$ are fixed parameters.

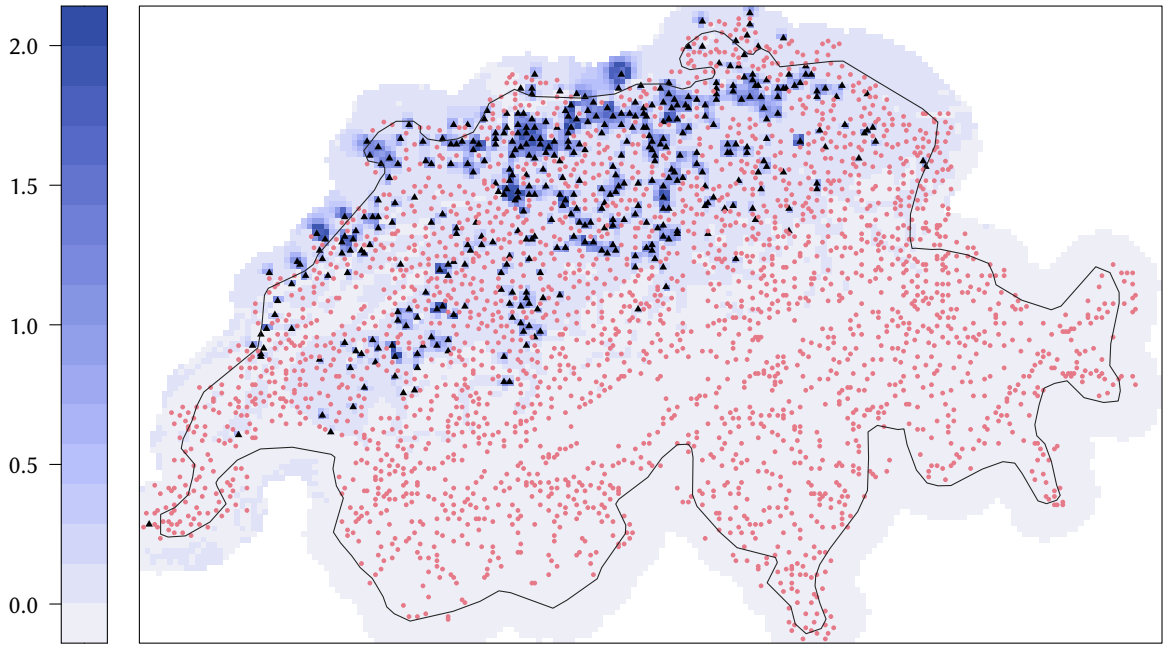

Figure B.4.: The initial distribution of stage-3 individuals in each simulation is drawn from a joint Poisson distribution. The map shows the respective means for each cell on the colour scale. The underlying Poisson model is based on the Atlas data from 1993-'96; their absences and presences are shown as red circles and black triangles, respectively.

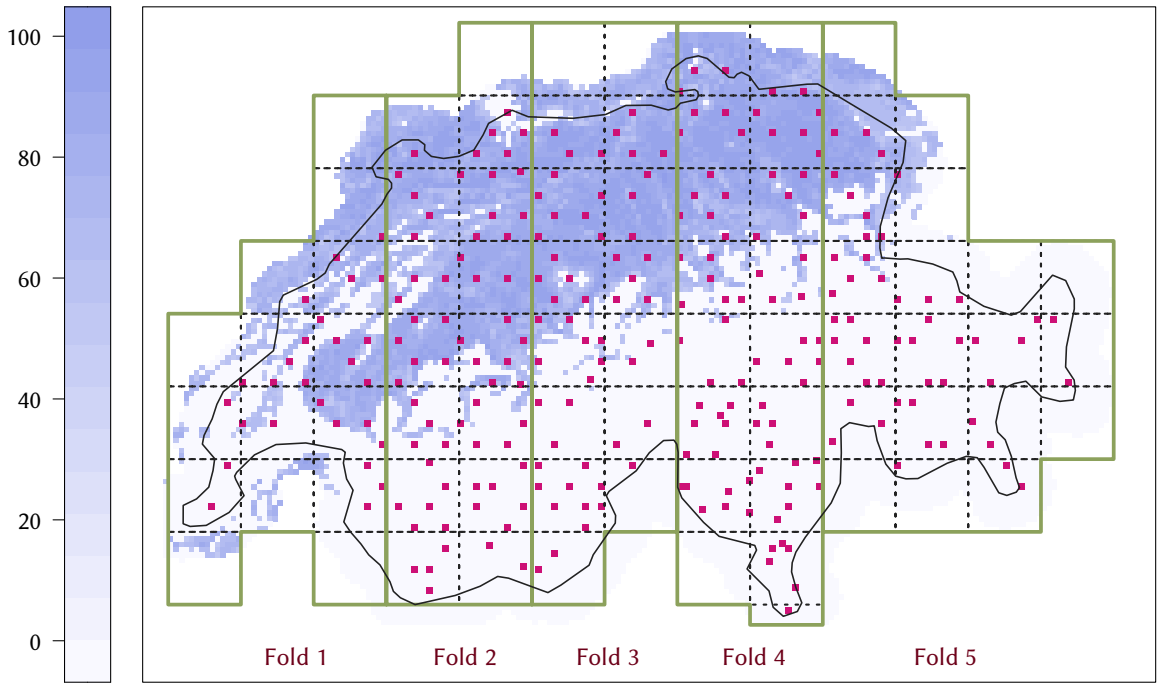

Figure B.5.: Spatial aggregation of observed and simulated abundance data: The solid green line delineates the spatial folds used for model evaluation. The broken blue line shows the spatial blocks within which the abundance data are aggregated. The map shows the simulation grid with the habitat suitability in year 2018 of each 2×2 km^2 cell (blue colour scale) and the locations of MHB sites (pink squares) for reference.

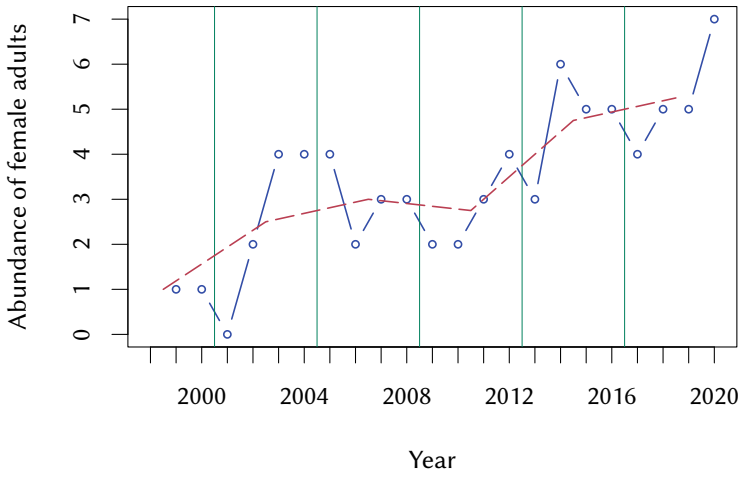

Figure B.6.: Temporal aggregation of observed and simulated abundance data: The vertical lines delineate the temporal blocks within which the abundance data are aggregated. The blue line and circles show an exemplary time series of total female abundance within a given spatial block, the broken red line shows their means within each temporal block.

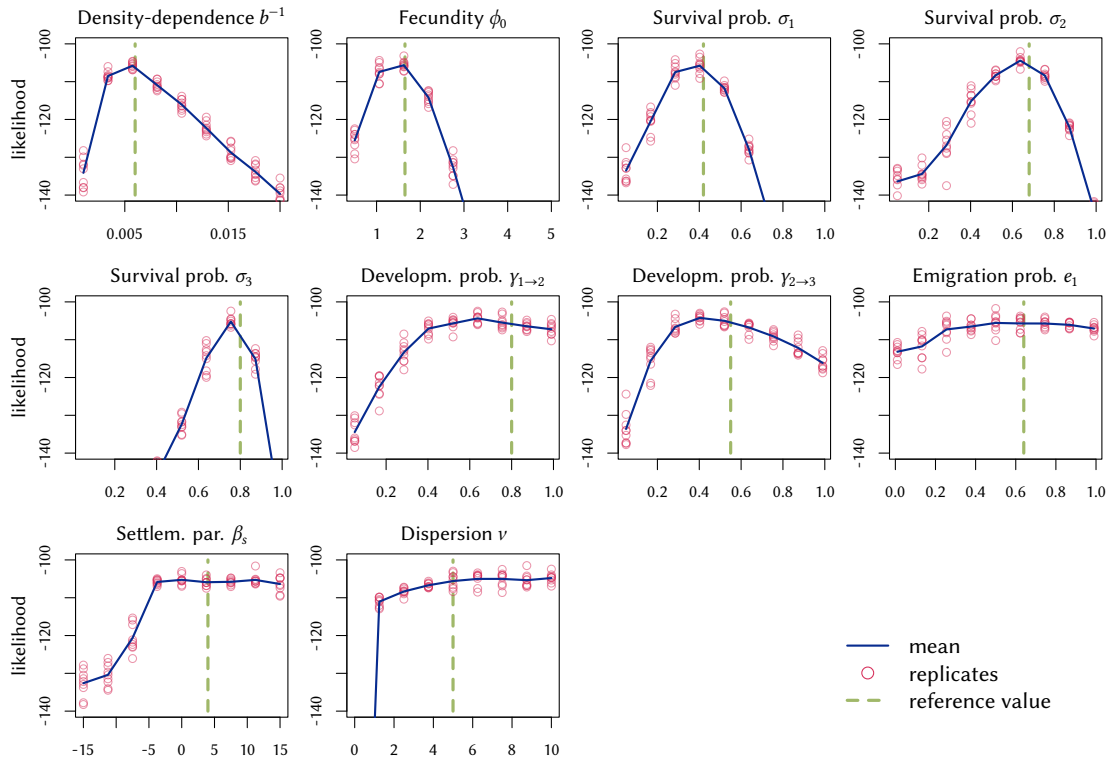

Figure B.7.: One-factor-at-a-time sensitivity analysis. The green broken vertical lines mark the reference values, with which the reference data D_{ref} was simulated. To evaluate the sensitivity of each single parameter θ_i on the likelihood $l(\theta) = p(D_{\text{sim}} \mid \theta, M)$, it is varied within the boundaries of its prior while keeping all other parameters constant and its likelihood with respect to D_{ref} is evaluated.

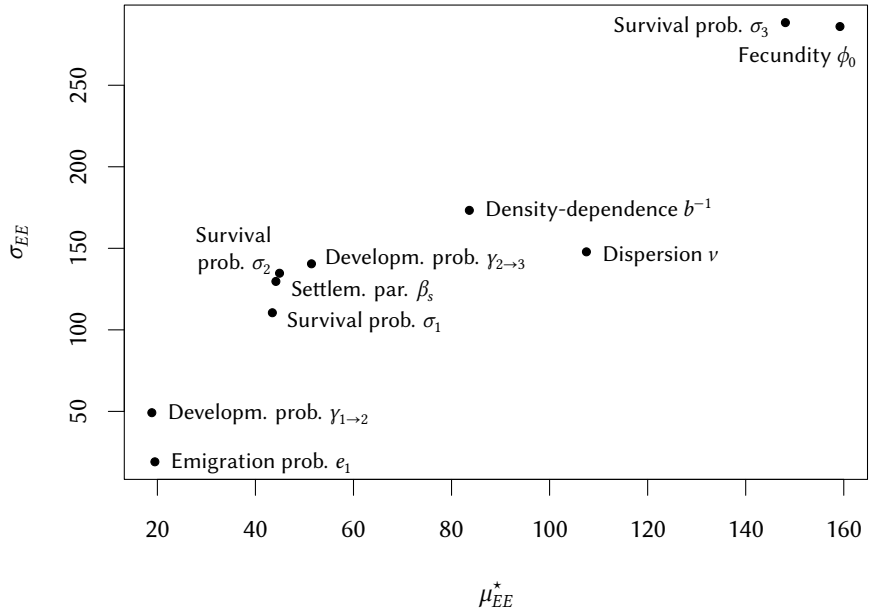

Figure B.8.: Global sensitivity analysis using Morris' elementary effects screening method (Morris, 1991). Shown are the mean of the absolute value of the elementary effect $\mu^\star_{EE}$ and the standard deviation of the elementary effect σ_{EE} for each calibrated parameter θ_i. An estimate of the overall sensitivity of θ_i on the likelihood $l(\theta)$ is provided by $\mu^\star_{EE}$, whereas σ_{EE} indicates a non-linear relation or potential interactions.

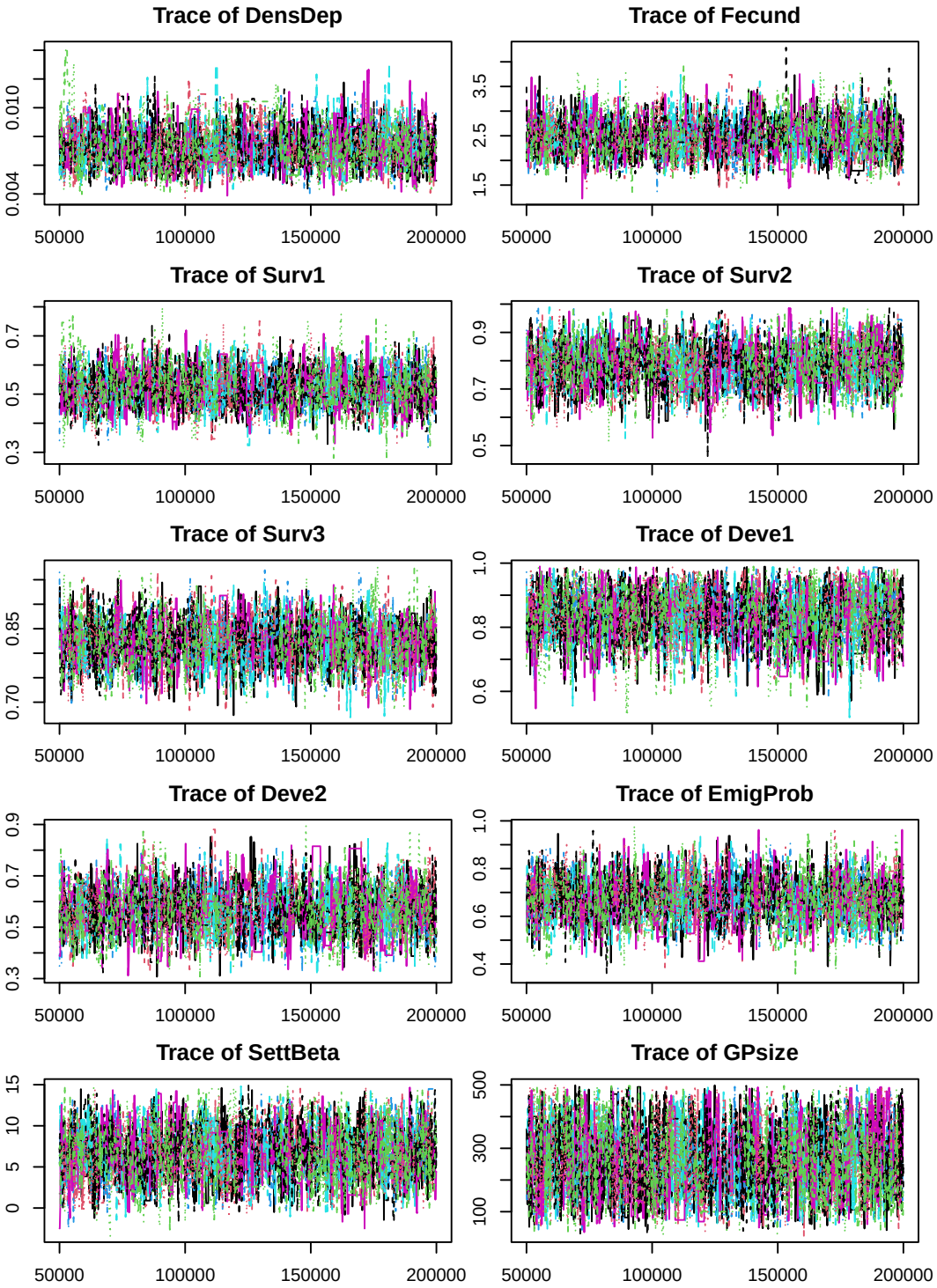

Figure B.9.: Trace plots: Parameter value sampled by each chain in each iteration.

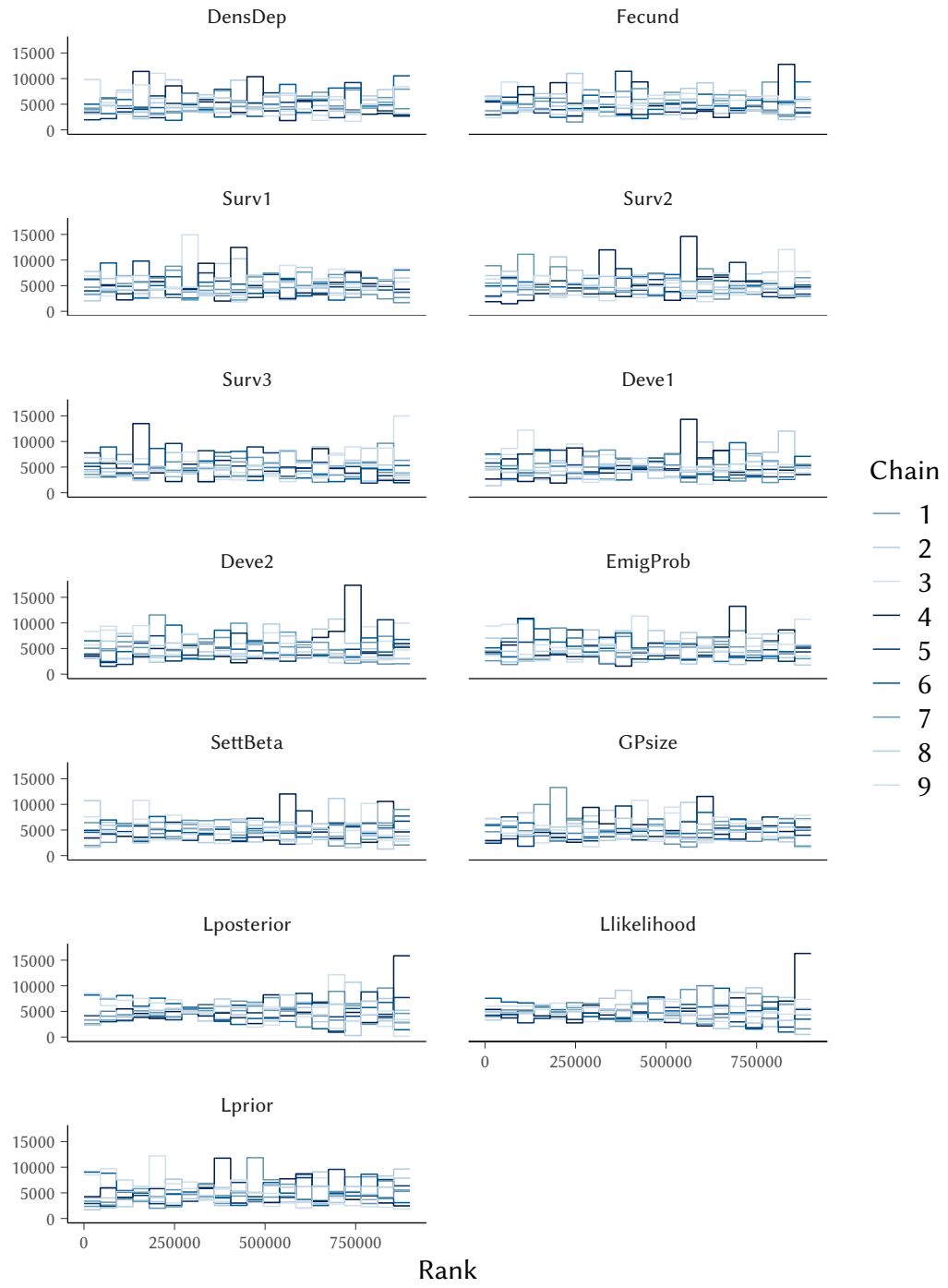

Figure B.10.: Trace rank plots: Histograms of the rank of the parameter values sampled by each chain, where ranking is done over all draws by all chains (Vehtari et al., 2021).

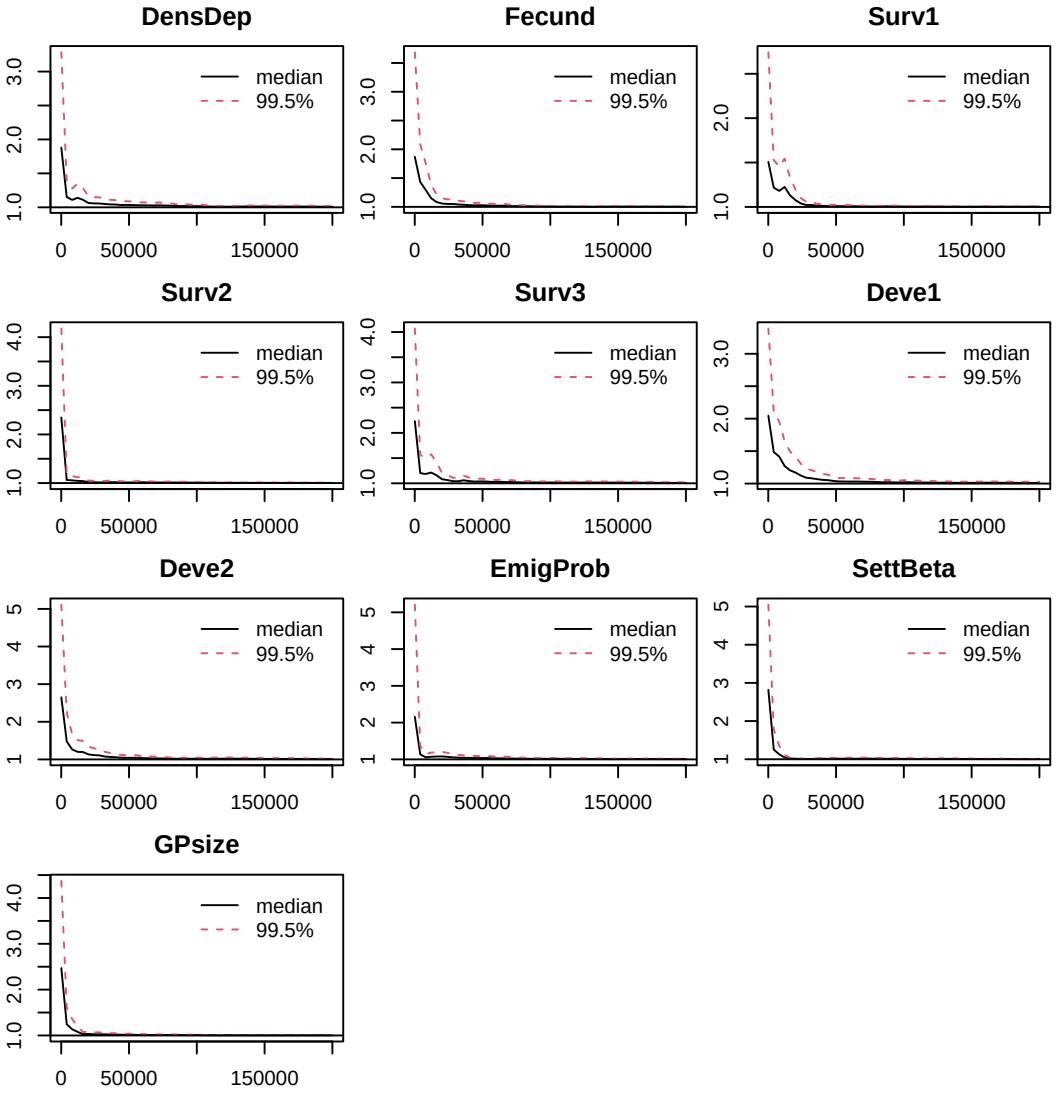

Figure B.11.: Potential scale reduction factor (psrf; Gelman & Rubin, 1992) at different chain lengths for all calibration parameters. Chain length is 2×10^5 iterations of which 0.5×10^5 are discarded as burn-in. Multivariate psrf evaluates to 1.05, 1.02, 1.05, 1.09, and 1.04 for the folds 1 to 5, and to 1.03 for the calibration run using the whole data set.

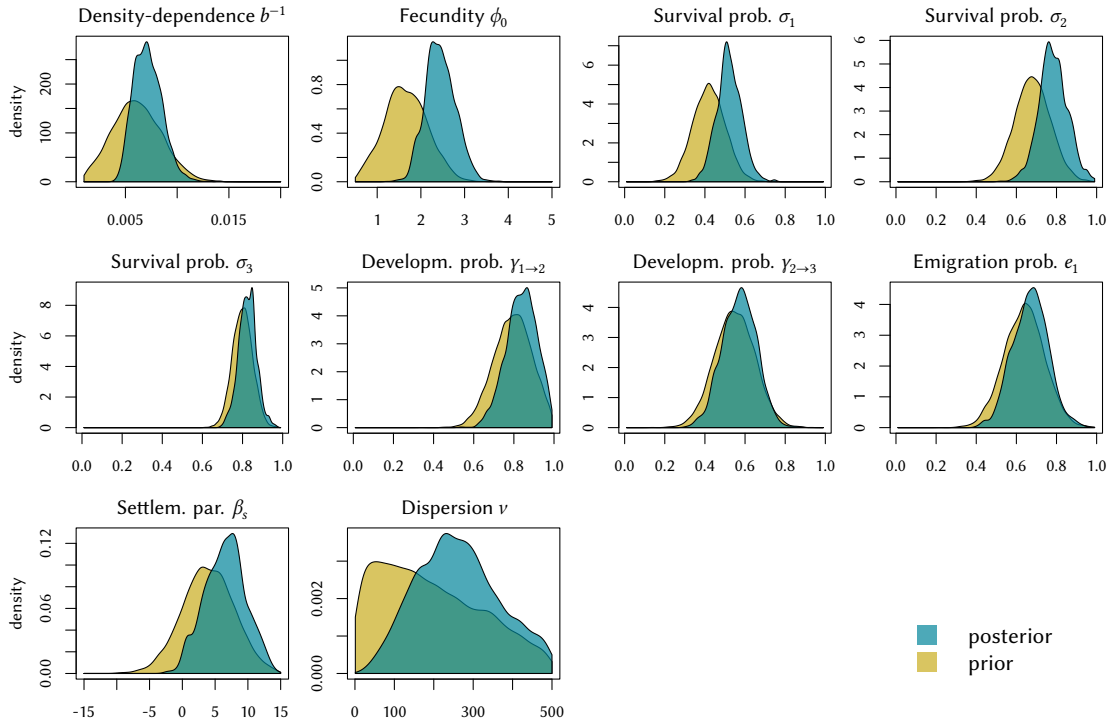

Figure B.12.: Marginal posterior distributions, fitted to full MHB data set (all five spatial folds). Combination of three independent DEzs chains with three internal chains each.

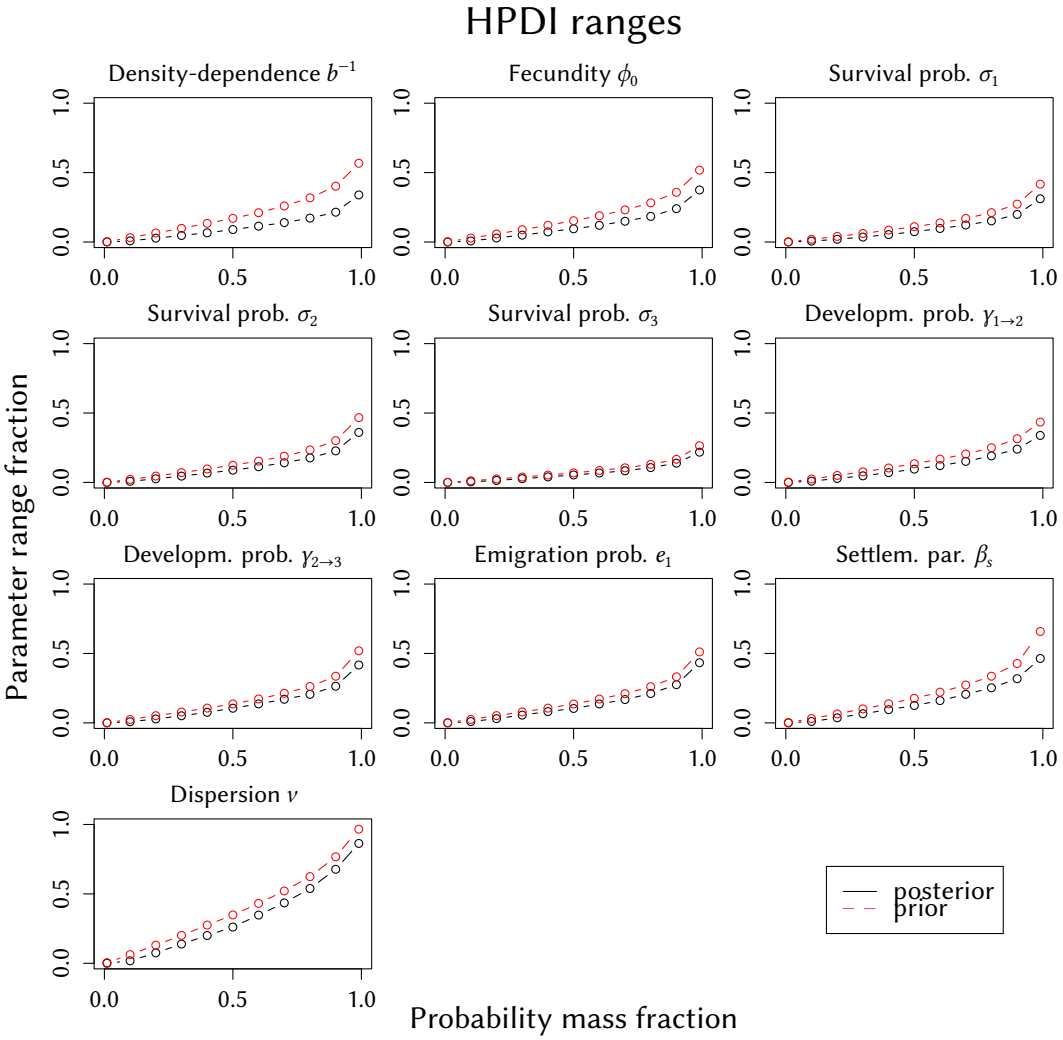

Figure B.13.: Comparison of the width of posterior versus prior marginals using highest-posterior-density intervals (HPDIs): The smaller the HPDI width and the shallower its slope with increasing probability mass, the tighter is the distribution, translating to less uncertainty around the parameters' point estimate.

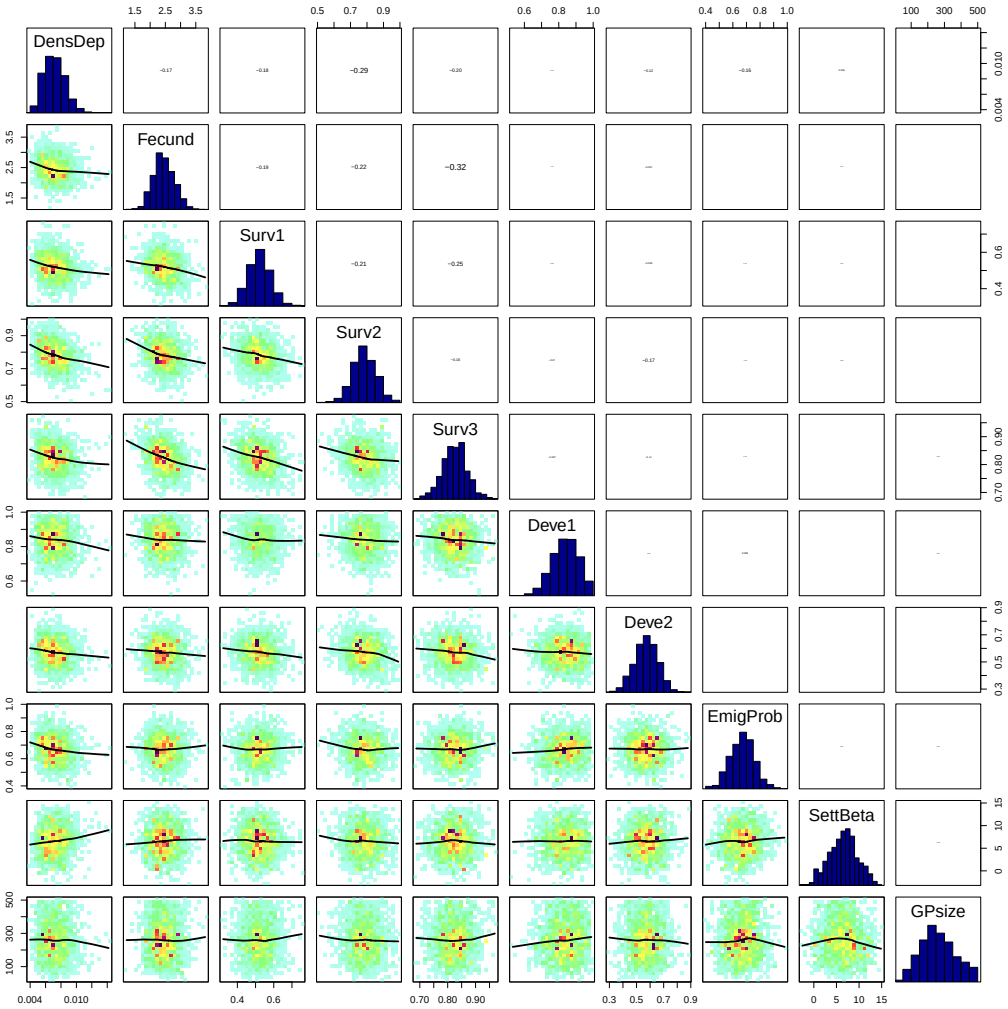

Figure B.14.: Pairwise posterior correlations

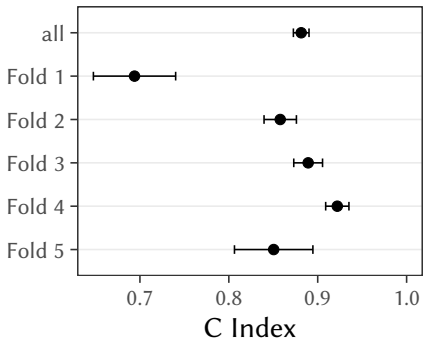

Fold ID	C index	95% CI
all	0.88	(0.87 - 0.89)
Fold 1	0.69	(0.64 - 0.74)
Fold 2	0.86	(0.84 - 0.88)
Fold 3	0.89	(0.87 - 0.91)
Fold 4	0.92	(0.91 - 0.93)
Fold 5	0.85	(0.81 - 0.89)

Figure B.15.: C-index of projections to the test data of the cross-validation. Given are the mean and 95%-confidence interval. ”all” refers to the whole MHB data set, where each observation was predicted from the particular calibration that had it in its test fold. The other rows provide the same info, but separate per fold (and calibration). Here, the c-index is calculated over all observation (site-year combination) independently.

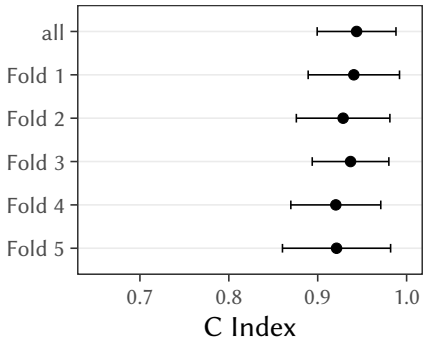

Fold ID	C index	95% CI
all	0.94	(0.90 - 0.98)
Fold 1	0.94	(0.89 - 0.99)
Fold 2	0.93	(0.88 - 0.98)
Fold 3	0.94	(0.90 - 0.98)
Fold 4	0.92	(0.87 - 0.97)
Fold 5	0.92	(0.86 - 0.98)

Figure B.16.: As Fig. B.15, but the c-index is calculated over the time series of total abundance per fold.

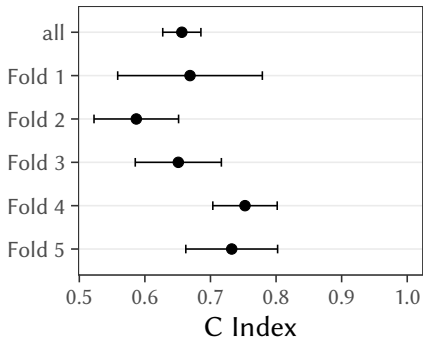

Fold ID	C index	95% CI
all	0.66	(0.63 - 0.69)
Fold 1	0.67	(0.56 - 0.78)
Fold 2	0.59	(0.53 - 0.65)
Fold 3	0.65	(0.58 - 0.72)
Fold 4	0.75	(0.70 - 0.80)
Fold 5	0.73	(0.66 - 0.80)

Figure B.17.: As Fig. B.15, but the c-index is calculated for the 15% cells with highest variance in their local abundance time series.

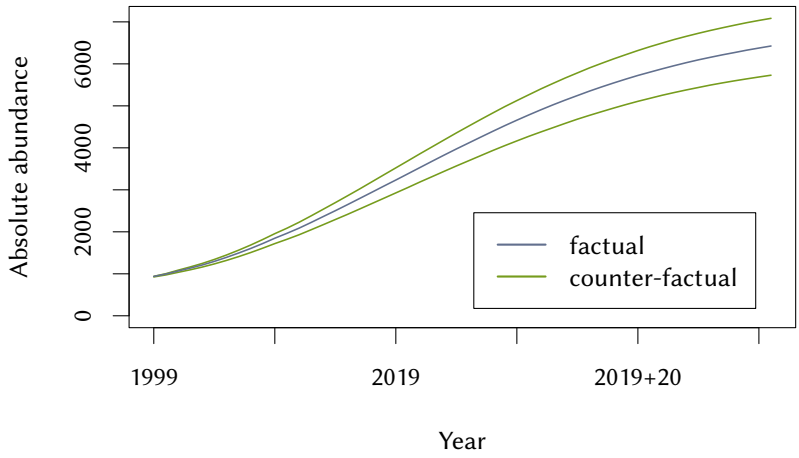

Figure B.18.: Sensitivity of the median posterior predictions to changes in the underlying habitat suitability maps. Shown are the time series of the median of total red kite abundance in Switzerland for the factual and two counter-factual scenarios. The factual scenario (blue line) is based on the observed environmental predictors and was used in the calibration. The two counter-factual scenarios (green lines) use habitat suitability maps in which the habitat suitability of each cell was increased or, respectively, decreased by five (out of a maximum of 100) points.

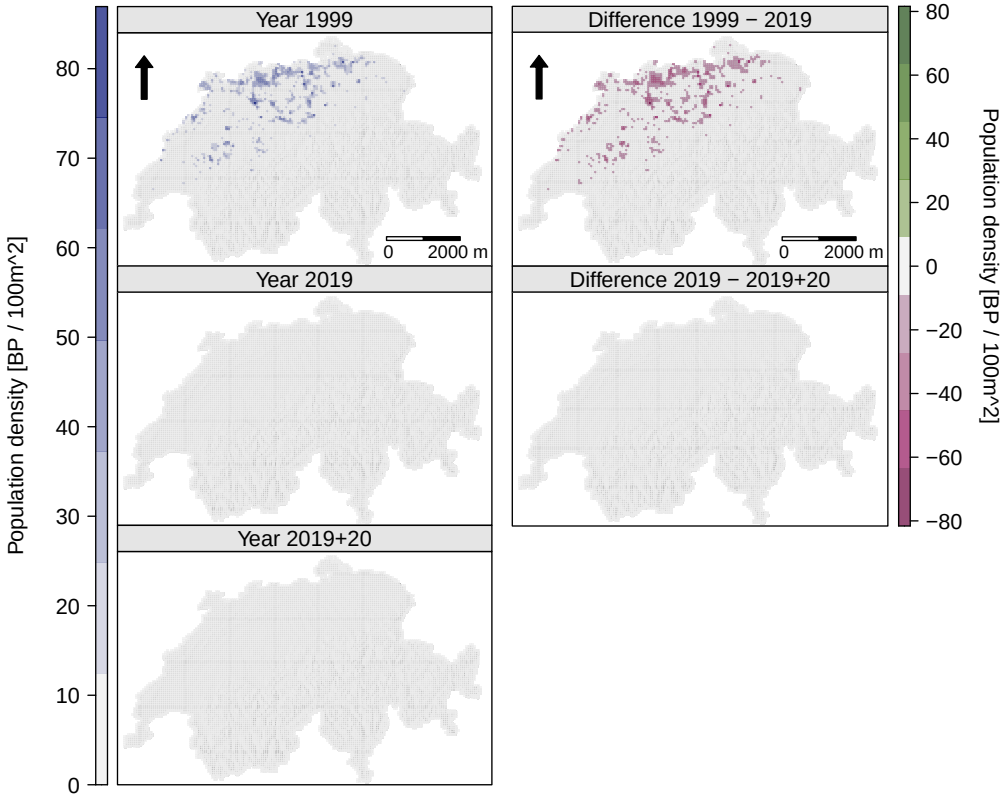

Figure B.19.: Mean prior predicted population densities for the years 1999 and 2019, and after 20 further years under constant conditions (left column) as well as the differences between those years (right column)..

References

European Union (2022). *Copernicus Land Monitoring Service*. https://land.copernicus.eu/. European Environment Agency (EEA).

Gelman, A. and Rubin, D. B. (1992). „Inference from Iterative Simulation Using Multiple Sequences". *Statistical Science* 7.4, pp. 457–472. DOI: 10.1214/ss/1177011136.

Karger, D. N., Conrad, O., Böhner, J., Kawohl, T., Kreft, H., Soria-Auza, R. W., Zimmermann, N. E., Linder, H. P., and Kessler, M. (2017). „Climatologies at high resolution for the earth's land surface areas". *Scientific Data* 4, p. 170122. DOI: 10.1038/sdata.2017.122.

– (2018). *Data from: Climatologies at high resolution for the earth's land surface areas*. DOI: 10.5061/dryad.kd1d4.

Katzenberger, J., Gottschalk, E., Balkenhol, N., and Waltert, M. (2019). „Long-term decline of juvenile survival in German Red Kites". *Journal of Ornithology* 160.2, pp. 337–349. DOI: 10.1007/s10336-018-1619-z.

Knaus, P., Strebel, N., and Sattler, T. (2022). *The State of Birds in Switzerland 2022*. Sempach: Swiss Ornithological Institute.

Knaus, P., Jérôme, G., Sattler, T., Wechsler, S., Kéry, M., Strebel, N., and Antoniazza, S. (2018). *Schweizer Brutvogelatlas 2013-2016*. Sempach, Schweiz: Schweizerische Vogelwarte. ISBN: 978-3-85949-009-3.

Morris, M. D. (1991). „Factorial Sampling Plans for Preliminary Computational Experiments". *Technometrics* 33.2, pp. 161–174. DOI: 10.1080/00401706.1991.10484804.

Nachtigall, W. (2008). „Der Rotmilan (Milvus milvus, L. 1758) in Sachsen und Südbrandenburg–Untersuchungen zu Verbreitung und Ökologie". *Diss., Univ. Halle-Wittenberg*.

Nägeli, M., Scherler, P., Witczak, S., Catitti, B., Aebischer, A., Bergen, V. van, Kormann, U., and Grüebler, M. U. (2021). „Weather and food availability additively affect reproductive output in an expanding raptor population". *Oecologia*. DOI: 10.1007/s00442-021-05076-6.

Newton, I., Davis, P., and Davis, J. (1989). „Age of first breeding, dispersal and survival of Red Kites Milvus milvus in Wales". *Ibis* 131.1, pp. 16–21.

Schaub, M. (2012). „Spatial distribution of wind turbines is crucial for the survival of red kite populations". *Biological Conservation* 155, pp. 111–118. DOI: 10.1016/j.biocon.2012.06.021.

Schmid, H., Luder, R., Naef-Daenzer, B., Graf, R., and Zbinden, N. (1998). *Schweizer Brutvogelatlas 1993–1996*. Sempach, Schweiz: Schweizerische Vogelwarte. ISBN: 978-3-9521064-5-7.

Schmid, H. and Volet, B. (2004). „Der Bestand des Rotmilans Milvus milvus im Winter 2002/03 in der Schweiz“. *Der Ornithologische Beobachter* 101, pp. 192–200.

Sergio, F., Tavecchia, G., Blas, J., Tanferna, A., and Hiraldo, F. (2021). „Demographic modeling to fine-tune conservation targets: importance of pre-adults for the decline of an endangered raptor“. *Ecological Applications* 31.3, e2266. DOI: 10.1002/eap.2266.

Vehtari, A., Gelman, A., Simpson, D., Carpenter, B., and Bürkner, P.-C. (2021). „Rank-Normalization, Folding, and Localization: An Improved R^ for Assessing Convergence of MCMC (with Discussion)“. *Bayesian Analysis* 16.2, pp. 667–718. DOI: 10.1214/20-BA1221.

Appendix C

Supporting information: Demography-environment relationships improve mechanistic understanding of range dynamics under climate change

C.1. Supplementary figures and tables

Table C.1.: Mean ($\langle\cdot\rangle$) and standard deviation (SD; σ) of the truncated Gaussian prior distributions for demographic and dispersal parameters for each species, taken from the published data in (Storchová & Horák, 2018) (demographic traits) and (Fandos et al., 2023) (dispersal traits). Columns: fecundity ρ and its SD σ_ρ; juvenile survival probability s_j, adult survival probability s_a, emigration probability p_e, and their SDs $\sigma_{s,p}$; mean dispersal distance $\bar{d}$ and its SD $\sigma_{\bar{d}}$ given in kilometres. The prior of overall demographic density dependence is given by $1/b = 0.003 \pm 0.002$ for all species. ρ, s_j, and s_a denote the intercepts of their respective demography-climate relationships. The truncated Gaussian prior for ρ is bounded to 1×10^{-4} from below and 1.0 from above; the priors for s_j and s_a are bounded between 0.01 and 0.99; and for $\bar{d}$ between 1 km (the cell size) and 20 km.

Species	$\langle\rho\rangle$	σ_ρ	$\langle s_j\rangle$	$\langle s_a\rangle$	$\langle p_e\rangle$	$\sigma_{s,p}$	$\langle\bar{d}\rangle$	$\sigma_{\bar{d}}$
Bullfinch	2.25	0.50	0.50	0.47	0.37	0.20	1.36	0.50
Crested tit	1.62	0.06	0.50	0.27	0.50	0.20	1.44	0.50
Eurasian treecreeper	2.06	0.56	0.50	0.50	0.42	0.20	1.37	0.50
Eurasian nuthatch	1.75	0.44	0.50	0.45	0.16	0.20	1.69	0.50
Goldcrest	5.00	0.88	0.50	0.50	0.52	0.20	1.48	0.50
Dunnock	2.50	0.50	0.50	0.49	0.79	0.20	2.66	0.50
Common linnet	3.12	0.62	0.50	0.38	0.51	0.20	1.46	0.50
Ring ouzel	1.50	0.28	0.38	0.52	0.09	0.20	2.38	0.50
Alpine accentor	1.75	0.38	0.50	0.50	0.45	0.20	1.39	0.50

Table C.2.: Species habitat preferences reflected in habitat maps. Habitat types from (Storchová & Horák, 2018): Deciduous forest (Dec. F.), Coniferous forest (Con. F.), Woodland (Wdl.), Shrub, Grassland (Grl.), Mountain meadows (M. mead.), Rocks. Indices of CORINE classes that were mapped from habitat types: 231 - Pastures, 311 - Broad-leaved forest, 312 - Coniferous forest, 313 - Mixed forest, 321 - Natural grasslands, 322 - Moors and heathland, 324 - Transitional woodland-shrub, 332 - Bare rocks, 333 - Sparsely vegetated areas.

Name english	Habitat preference	Corine classes
Bullfinch	Dec. F., Con. F.	311, 312, 313
Crested tit	Dec. F., Con. F.	311, 312, 313
Eurasian treecreeper	Dec. F., Con. F.	311, 312, 313
Eurasian nuthatch	Dec. F., Con. F.	311, 312, 313
Goldcrest	Con. F.	312, 313
Dunnock	Dec. F., Con. F., Wdl., Shrub	311, 312, 313, 321, 324
Common linnet	Wdl., Shrub, M. mead.	231, 321, 322, 324, 333
Ring ouzel	Con. F., Grl., Rocks	312, 322, 332, 333
Alpine accentor	M. mead., Rocks	322, 332, 333

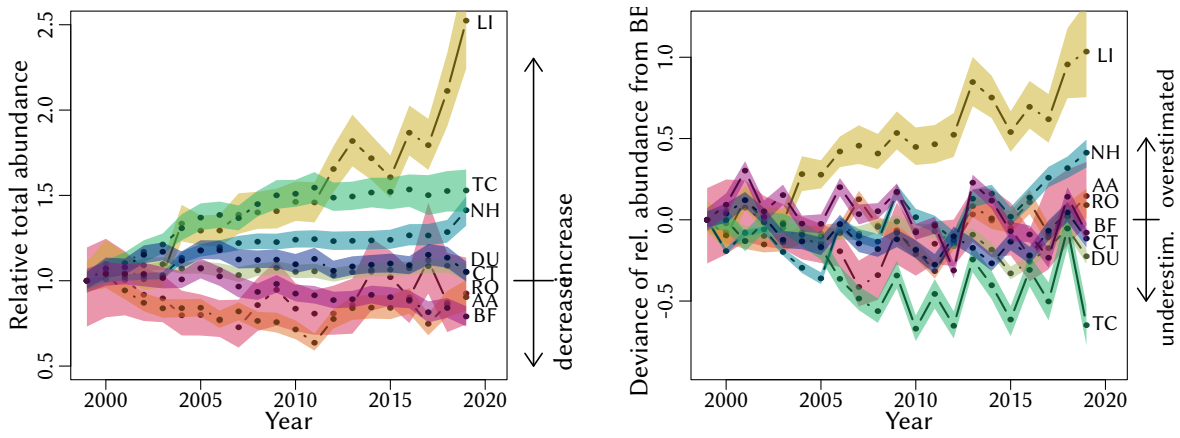

Figure C.1.: Same as Fig. 4.2 in main text but showing 95% credible intervals and medians: Total relative abundance time series (left) and its deviation from the Swiss breeding bird index (BBI, right), with 1999 (the first year of MHB data) as reference year. BF - Bullfinch (pink); CT - Crested tit (dark blue); TC - Eurasian treecreeper (dark green); NH - Eurasian nuthatch (light blue); DU - Dunnock (light green); LI - Common linnet (yellow); RO - Ring ouzel (orange); AA - Alpine accentor (red).

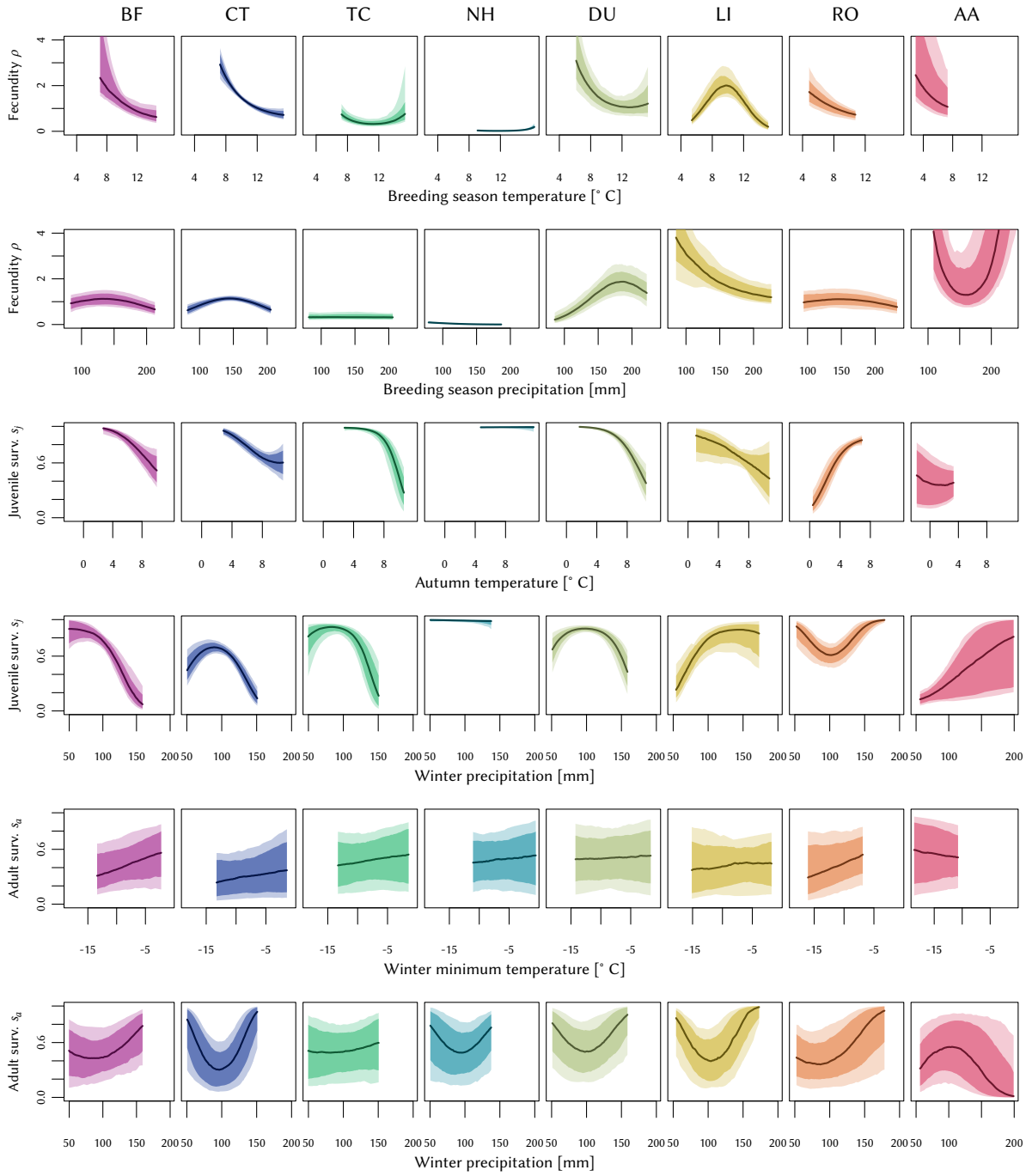

Figure C.2.: Same as Fig. 4.3 in main text, but showing each demography-climate relationship (DCR) in individual panels: DCRs for all species, evaluated over their respective typical climatic ranges. Shown are the median, 80% and 95% credible interval. BF - Bullfinch (pink); CT - Crested tit (dark blue); TC - Eurasian treecreeper (dark green); NH - Eurasian nuthatch (light blue); DU - Dunnock (light green); LI - Common linnet (yellow); RO - Ring ouzel (orange); AA - Alpine accentor (red).

Table C.3.: Model performance of the species-specific (column one) RangeShifter individual-based models (IBMs) as measured by RMSE (column two), spatial AUC (column three), and temporal c-index (column six). The latter two indices are further used for comparison with two other model types presented in Briscoe et al. (2021), namely dynamic occupancy models (DOMs, columns four and seven) and correlative species distribution models (SDMs, columns five and eight). SDMs are represented as the mean results of generalised linear mixed models and boosted regression trees. (*) For the comparison by spatial AUC, the abundances predicted by our IBMs were compressed to presence-absence data (P/A). (**) The results for DOMs and SDMs were taken from Briscoe et al. (2021), using the model variants with the largest training data set; details on the models can be found therein. The alpine accentor was not included in Briscoe et al. (2021). (†) The temporal c-index is named 'temporal AUC' in Briscoe et al. (2021).

Species	RMSE	Spatial AUC			Temporal c-index†		
		IBM*	DOM**	SDMs**	IBM	DOM**	SDMs**
Bullfinch	2.2	0.84	0.88	0.89	0.57	0.54	0.57
Crested tit	5.0	0.79	0.87	0.88	0.60	0.67	0.59
Eurasian treecreeper	3.5	0.82	0.87	0.89	0.64	0.70	0.51
Eurasian nuthatch	4.2	0.82	0.89	0.92	0.65	0.45	0.42
Dunnock	5.7	0.77	0.83	0.87	0.42	0.43	0.30
Common linnet	1.9	0.74	0.77	0.80	0.80	0.54	0.51
Ring ouzel	3.5	0.86	0.93	0.94	0.61	0.64	0.40
Alpine accentor	1.3	0.89	–	–	0.51	–	–

References

Briscoe, N. J., Zurell, D., Elith, J., König, C., Fandos, G., Malchow, A.-K., Kéry, M., Schmid, H., and Guillera-Arroita, G. (2021). „Can dynamic occupancy models improve predictions of species' range dynamics? A test using Swiss birds". *Global Change Biology* 27.18, pp. 4269–4282. DOI: 10.1111/gcb.15723.

Fandos, G., Talluto, M., Fiedler, W., Robinson, R. A., Thorup, K., and Zurell, D. (2023). „Standardised empirical dispersal kernels emphasise the pervasiveness of long-distance dispersal in European birds". *Journal of Animal Ecology* 92.1, pp. 158–170. DOI: 10.1111/1365-2656.13838.

Storchová, L. and Horák, D. (2018). „Life-history characteristics of European birds". *Global Ecology and Biogeography* 27.4, pp. 400–406. DOI: 10.1111/geb.12709.

Appendix D

ODD protocol of the red kite RangeShiftR model

This ODD protocol (Overview, Design concepts, and Details; Grimm el at. 2020) was generated by the RangeShiftR package. Its contents are part of the RangeShifter project user manual, written by Greta Bocedi, Stephen C. F. Palmer and Justin M. J. Travis from the University of Aberdeen, UK. It is available from the public github repository https://github.com/RangeShifter/RangeShifter-software-and-documentation/.

D.1. Purpose and patterns

The RangeShiftR model is a single species, spatially-explicit and stochastic individual-based model (IBM), built around the integration of two fundamental components: population dynamics and dispersal behaviour. In this model of the red kite in Switzerland, population dynamics, represented as stage-structured, female-only population, with overlapping generations, and dispersal (explicitly modelled in its three phases of emigration, transfer and settlement, where the latter is accounting for context dependency as well as stage specificity) are played out on top of a gridded habitat suitability landscape.

D.2. Entities, state variables and scales

Individuals

Individuals are the basic entities of the RangeShiftR model. Each individual has a unique ID number and here is defined by the following state variables:

- status
- initial (natal) and current location
- age and stage

Populations

Populations are defined by the individuals occupying a single cell and they represent the scale at which individuals interact and density-dependencies act. Populations are characterised by their size and location and the number in each stage class.

Landscape units

The model runs over a grid-based map.
Here, each cell stores a habitat suitability index, ranging from 0 to 100. This index is derived from a correlative species distribution model. Its value mediates the local strength of demographic density-dependence. Each cell is defined as suitable or not suitable for the red kite if its habitat suitability is above or equal to zero, respectively.

D.2.1. Spatial and temporal scales

The cell size (resolution) is 2000 m by 2000 m. The cell resolution represents the spatial scale at which the two fundamental processes of population dynamics and dispersal occur. This means that the density-dependency in the model (which here on reproduction and settlement) acts at the cell scale and cells are the single step unit for the discrete movement model used in the transfer phase. There are three distinct temporal scales: The highest-level represents years and encompass a full model cycle. The intermediate scale is the species' reproductive season. The model simulates one reproductive season per year. Finally, the smallest time scale is represented by the number of steps that dispersers take during the movement phase of dispersal. This is determined by the maximum number of steps.

D.3. Process overview and scheduling

At the beginning of each year, reproduction is the first process to be modelled. Reproduction is followed by natal dispersal. After each reproductive season, survival and successive development of all the stages are modelled. Aging occurs at the end of the year.

The comprehensive simulation schedule is represented in Figures D.1 and D.2.

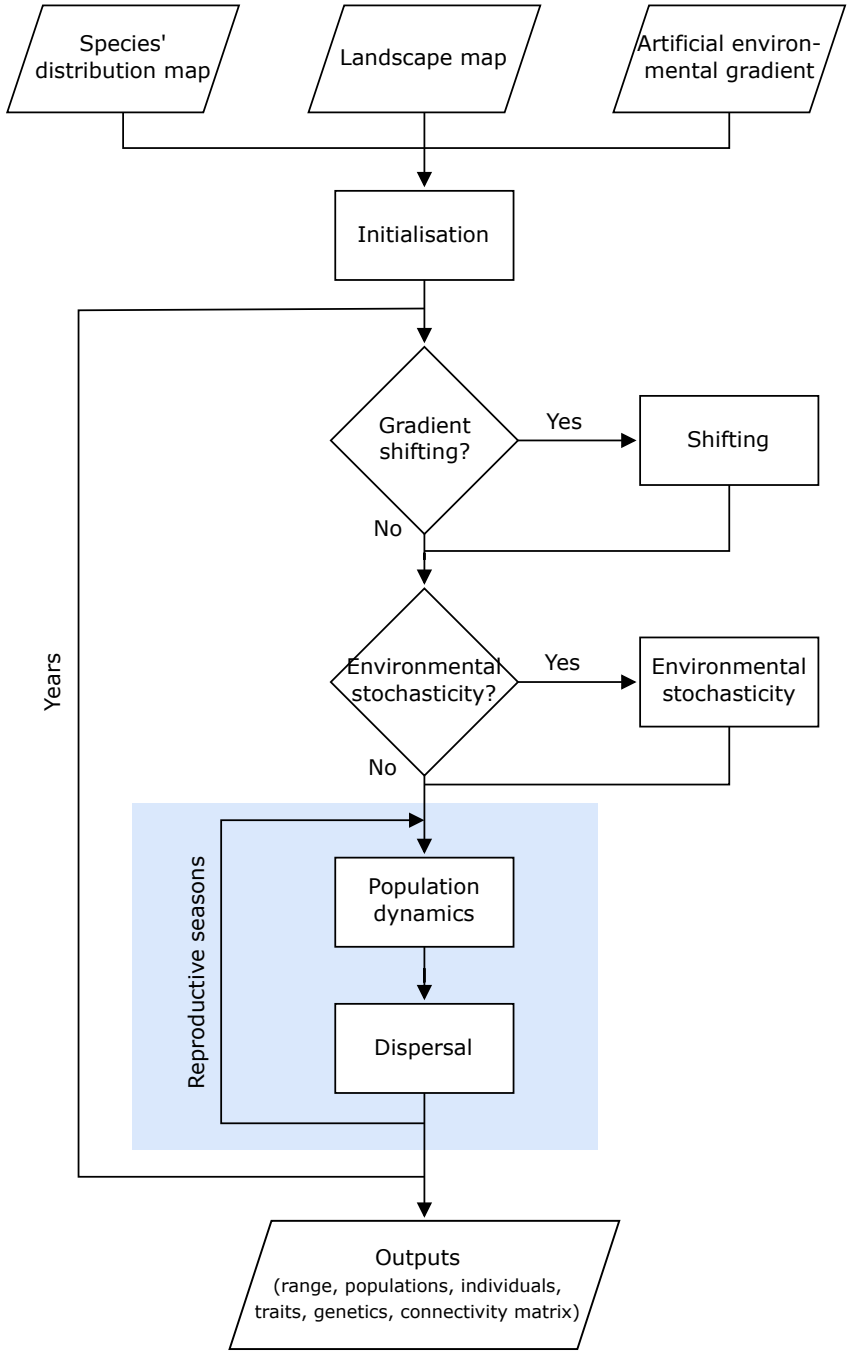

Figure D.1.: General model workflow and schedule. The model core (highlighted in blue) is expanded in Figure D.2.

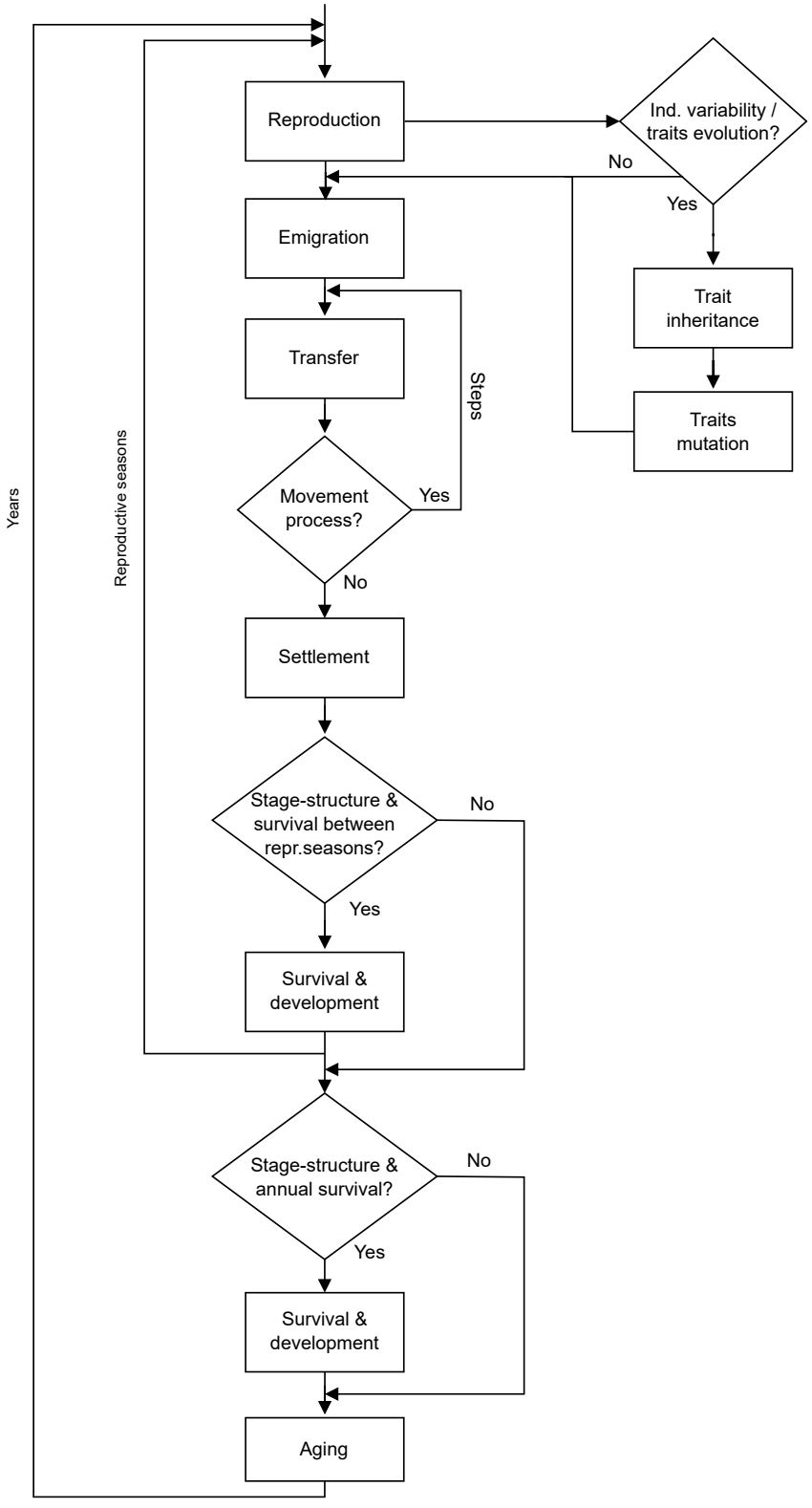

Figure D.2.: General flowchart of the core model, representing the yearly loop.

D.4. Design concepts

Basic principles

Population dynamics

Demographic stochasticity is fundamentally important for the dynamics of populations that are naturally small or have declined to low abundances owing to anthropogenic pressures. Additionally, inter-individual variability within populations can have a major influence on dynamics. Modelling stochastic events that happen to individuals is crucial for avoiding systematic overestimation of population viability or rate of spread (Clark et al. 2001, Kendall and Fox 2003, Robert et al. 2003, Grimm and Railsback 2005, Jongejans et al. 2008, Travis et al. 2011). Thus, population dynamics in RangeShiftR were constructed to be fully individual-based and stochastic. Each reproductive individual produces a discrete number of offspring sampled from a Poisson distribution with a mean that is influenced by the species' demographic parameters and the local population density.

Definition of populations

The cell is the scale at which processes such as population dynamics and dispersal act. The individuals present in a cell define a distinct population, and density-dependencies for reproduction and settlement both operate at this scale. Even in the case where two habitat cells are adjacent, they still hold separate populations.

Population structure

Implementing overlapping generations which are stage-structured is the appropriate choice for species in which generations can overlap and individuals can be classified in different stages (e.g. immature vs. breeding individuals) differing in their demographic parameters. Individuals are characterized by their age and stage. Each stage has a certain fecundity, survival and probability of developing to the next stage. The parameters are provided through classical transition matrices (Caswell 2001). However, in RangeShiftR, these are not multiplied with the population vector as is typical for matrix models but, instead, the parameters are applied stochastically in an individual-based manner. Presenting the demographic parameters in the standard matrix notation, is meant to ease parameterisation Bocedi et al. (2014), as most population modellers are used to matrix models. It has the further important benefit of helping bridging the gap between analytical models and IBMs, the joint use of which has considerable potential, especially for improving modelling for conservation (Travis et al. 2011).

Dispersal

Dispersal is defined as movement leading to spatial gene flow, and it typically involves three phases: emigration, transfer and settlement (Stenseth and Lidicker 1992, Clobert et al. 2001, Bowler and Benton 2005, Ronce 2007). The key role of dispersal in species persistence and responses to environmental change is increasingly recognized (Travis et al. 2014). Moreover, the importance of modelling dispersal as a complex process, explicitly considering its three phases, each of which has its own mechanisms and costs, has been recently highlighted (Travis et al. 2012, 2014, Bonte et al. 2012). The implementation of the

dispersal process in RangeShiftR is based on these recent frameworks and the substantial dispersal theory that has been developed so far (Clobert et al. 2012).

Emigration Emigration is the first phase of dispersal. Emigration itself can be a complex process determined by multiple proximate and ultimate causes. Multiple emigration strategies can be present across the species' range, inside a single population or even within the same individual in form of plastic emigration behaviour.

The theory on emigration accounts for context dependencies, plasticity and inter-individual variability in emigration strategies. Much work has been conducted to understand the role of density dependence in emigration (Travis et al. 1999, Metz and Gyllenberg 2001, Poethke and Hovestadt 2002, Matthysen 2005, Kun and Scheuring 2006, Chaput-Bardy et al. 2010, De Meester and Bonte 2010).

In RangeShiftR, emigration is modelled as the probability that an individual will leave its natal patch during the present year. See the description of the submodel for further details.

Transfer Transfer is the second phase of dispersal, and consists of the movement of an individual starting from when it emigrates from its natal patch and ending with settlement in another patch or with dispersal mortality. The main components of this phase are the individual movement ability and navigation capacity in response to the characteristics of the environment. The interaction between these components and their associated costs will determine the distance moved, the movement path and the chance of surviving the transfer phase.

Understanding and modelling how species move is not a simple task, and, perhaps more than for the other phases of dispersal, much effort has been spent in two separate and not always interacting fields: dispersal ecology (Travis et al. 2010) and movement ecology (Nathan et al. 2008). While the former seeks to understand movements as a part of the dispersal process and has often described transfer with phenomenological dispersal kernels (but see recent developments in fitting mechanistic kernels: (Schurr 2012)), the latter is more focused on understanding the mechanisms of the movement process itself, even though recent emphasis has been put on the consequences of movements for population dynamics (Morales et al. 2010). Modelling dispersal in IBMs needs to draw from both fields.

It is increasingly acknowledged that individual movements within and between habitat patches, and consequently also population dynamics, are strongly affected by the behavioural and physical traits of individuals and by the landscape structure and composition (Morales and Ellner 2002, Hawkes 2009, Stevens and Coulon 2012, Baguette et al. 2013). This has led to the development of mechanistic models where movement behaviour and its interaction with the environment is explicitly described (Nathan et al. 2008, Revilla and Wiegand 2008, Morales et al. 2010, Palmer et al. 2011, Pe'er et al. 2011). The classical method to represent individuals' movements mechanistically is to use a random walk (Codling et al. 2008), or its diffusion approximation, assuming that individuals are moving randomly in a homogeneous landscape and that they are all following the same rules. From

this basis, there have been recent developments in diffusion models for including landscape heterogeneity and some behavioural responses, like reaction to habitat boundaries, directly derived from empirical data through state-space models (Ovaskainen and Cornell 2003, Ovaskainen 2004, Patterson et al. 2008, Ovaskainen et al. 2008, Ovaskainen and Crone 2009, Zheng et al. 2009). Yet, these models do not account for individual variability or for many behavioural components including memory, perceptual range and movement modes. Despite this simplicity, diffusion models, and especially their recent developments, can still be satisfactory at large temporal and spatial scales and serve as a null hypothesis against which to test more complex movement models. Moreover they can provide basis for building blocks for population dynamics models.

Mechanistic IBMs allow extending the "random paradigm" by incorporating behavioural elements that are likely to be crucial in affecting species' spatial dynamics (Lima and Zollner 1996, Baguette and Van Dyck 2007, Knowlton and Graham 2010, Shreeve and Dennis 2011). These elements can be assigned into six main categories: (i) the switching between different movement modes [for example foraging within the home range vs. dispersal (Fryxell et al. 2008, Delattre et al. 2010, Pe'er et al. 2011)]; (ii) the individuals' perceptual range (Zollner and Lima 1997, Olden et al. 2004, Gardner and Gustafson 2004, Zollner and Lima 2005, Vuilleumier et al. 2006, Vuilleumier and Metzger 2006, Pe'er and Kramer-Schadt 2008, Palmer et al. 2011); (iii) the use of information in movement choices (Clobert et al. 2009) and the memory of previous experience (Smouse et al. 2010); (iv) the influence of habitat fragmentation and matrix heterogeneity on movement behaviours (Ricketts 2001, Vandermeer and Carvajal 2001, Schtickzelle and Baguette 2003, Revilla et al. 2004, Wiegand et al. 2005, Fahrig 2007, Dover and Settele 2009); (v) the individual responses to habitat boundaries (Schultz and Crone 2001, Morales 2002, Merckx et al. 2003, Ovaskainen 2004, Stevens et al. 2006, Pe'er et al. 2011); and (vi) the period of activity (Revilla et al. 2004) and the time scale of movements (Lambin et al. 2012).

A general framework for a mechanistic representation of movements has been outlined by Nathan et al. (2008), who identified four basic components: the internal state of the individual (why does it move?), its motion capacities (how does it move?), its navigation capacities (when and where does it move?) and external factors that affect the movement. This framework allows us, starting from individual movements, and taking into account individual variability, to predict movement patterns over large temporal and spatial scales and potentially to scale up to populations, communities, ecosystems and to multi-generation / evolutionary processes (Holyoak et al. 2008). The ultimate limitation is likely to be the quantity and the type of data needed to parameterize this /these kind of models; therefore, the challenge is to understand which level of detail is needed to make reliable projections in different contexts and for different purposes (Lima and Zollner 1996, Morales et al. 2010).

Movement behaviours during the transfer phase are a core component of the dispersal strategy of an individual, and therefore they come under selection and they can evolve (Merckx et al. 2003, Fahrig 2007, Hawkes 2009, Travis et al. 2012). Ultimately, it is the evolution of movement behaviours that leads to what we consider the evolution of dispersal kernels. A handful of theoretical studies have so far explored the evolution of movement rules. For example, it has been shown how the landscape composition and configuration, in

interaction with the ecology of the species, can affect the evolution of movement patterns, such that the greater the costs of dispersal the more highly correlated are the emerging walks (Heinz and Strand 2006, Bartoń et al. 2009). Moreover, straighter movement paths (Phillips et al. 2010) and riskier strategies seem to be selected during range expansion in such a way that the rate of expansion is maximized at the expense of the survival probability of the single individual (Bartoń et al. 2012).

Here, transfer is implemented as a strongly correlated random walk. This submodel is fully individual-based and explicitly describes the movement behaviour of individuals with a level of detail, and hence parameters, which is probably close to the most parsimonious for a mechanistic movement model. However, it facilitates considerably increasing the complexity and realism with which the transfer phase is modelled.

See the submodel description for further details.

Settlement Settlement, or immigration, is the last phase of dispersal, when the organism stops in a new cell or patch of breeding habitat. This phase is determined by a suite of strategies, behaviours and reaction norms that lead individuals to the decision to stop in a particular place. Habitat selection, mate finding and density dependence are probably three of the main processes involved, but not the only ones. Like emigration, settlement is a complex process affected by multiple criteria including inter-individual variability and context dependencies. It can be influenced by the causes and mechanisms of the previous phases of dispersal (Clobert et al. 2009) and it has associated specific costs (Bonte et al. 2012), which can also feed back to the previous phases (Le Galliard et al. 2012).

As for the previous phases, the use of different sources of abiotic and biotic information is likely to be crucial in the settlement decision, for which evidence is now accumulating. For example, studies have demonstrated that in some species, dispersing individuals exhibit a preference for habitat that is similar to the natal one, philopatry being a stronger predictor of habitat preferences for settlement than intrinsic habitat quality (Haughland and Larsen 2004, Stamps and Blozis 2006, Stamps et al. 2009). Conspecific density and performance have also been demonstrated to be important cues for settlement decisions (conspecific attraction), because they can provide a rapid approximation of the habitat quality (Stamps 1988, Doligez et al. 2004, Fletcher 2007, Vercken et al. 2012, Clotuche et al. 2013).

From the theoretical point of view, much work has been conducted on habitat selection during settlement decisions and its consequences for species' population dynamics and spatial genetic structure. The basic assumption is that individuals are expected to select habitat patches where their expected fitness is greater than the one expected in the natal patch, weighted by the costs of searching (Ruxton and Rohani 1998, Stamps 2001, Baker and Rao 2004, Stamps et al. 2005, Armsworth and Roughgarden 2008, Bonte et al. 2012). Recently the idea of 'matching habitat choice' has been proposed, for which individuals aim to settle where the environment best matches with their phenotype. This process, expected to be more important for species with limited phenotypic plasticity, can have important implications for processes such as local adaptation, adaptive peak shifts and evolution of niche width, and speciation (Edelaar et al. 2008). Other factors affecting settlement such as density dependence (Poethke et al. 2011), conspecific attraction (Fletcher 2006) or mate

finding (Gilroy and Lockwood 2012), their evolution and their consequences on species' responses to environmental changes, have been much less theoretically investigated.

This model incorporates density-dependent settlement rules. Dispersing individuals are not allowed to settle in their natal cell or a non-suitable cell and settlement probability is dependent on the size of the target cell's local population. For more details, see the description of the submodel.

Dispersal mortality

Dispersal is often a costly process for an organism (Bonte et al. 2012) and, in some cases, a dispersing individual may suffer mortality. Obtaining a sensible representation of dispersal requires that these mortality costs are described appropriately and, for this, it is important to recognize how dispersal mortality is incorporated in RangeShiftR. First, dispersal mortality can arise as a result of individuals failing to reach suitable habitat. For example, some individuals may fail to find suitable habitat before they use up a maximum number of movement steps. In this first case, dispersal mortality clearly depends on the proportion of suitable habitat in the landscape and will increase as the availability of habitat declines.

A second source of dispersal mortality can be a per-step probability of mortality. This can be useful for representing mortality risks that increase with distance or time spent travelling.

For more details, see the description of the submodel.

Emergence

Species range distributions emerge from the population dynamics and the dispersal behaviour of the individuals.

Adaptation

Not applicable.

Objectives

Not applicable.

Learning

Not applicable.

Prediction

Not applicable.

Sensing

Dispersing individuals can perceive the density in their current cell and potentially decide to settle if local density is low or to continue dispersing if it is high.

Interaction

No interaction is considered in the model.

Stochasticity

Demographic stochasticity is explicitly included in all processes.

Collectives

Not applicable

Observation

Populations

The population output consists of a raster stack with layers for each year and for each simulation replicate. The layers are gridded maps of the simulation domain in which each cell holds the number of breeding adults in its population.

D.5. Initialization

Initialization of landscape

Landscapes are initialized according to input raster maps, that are generated as projections from a correlative species distribution model. Thus, the habitat suitability in each cell is assumed as the modelled red kite occurrence probability in this cell. The landscape is re-initialised each year as the species distribution model is evaluated with the current predictors in each year and thus the habitat suitabilities slightly change. The demographic density-dependence of each cell is given as the maximum density-dependence (denoted $1/b$) times the cell's habitat suitability index in percent.

Initialization of populations

Populations are initialized from a data frame that lists the initial individuals with their given age, stage, and natal (i.e. initial) cell. This initial condition is generated from a Poisson model that takes into account the local habitat suitability and spatial correlation. The distributions of stages and ages of initialised individuals are calculated from the transition matrix as the quasi-equilibrium distributions.

D.6. Input data

The model requires the following input data:

- Landscape maps as 'raster' objects in R.
  Several maps may be given if the landscape shall change at specific years during the simulation. The grids need to contain habitat suitability values for each cell. Each cell in the landscapes is assigned a continuous percentage value between 0.0 and 100.0 (of the maximum density-dependence $1/b$). There are no explicit habitat or land-cover types. This allows integrating different methods for calculating the habitat suitability for a given species. For example, qualities can result from different methods of suitability modelling, which incorporate multiple variables like habitat types, elevation, climate, etc. A linear relationship between the habitat quality and the actual density-dependence of the population dynamics is assumed. Therefore, the quality should be scaled accordingly in case of a curvilinear relationship. Any part of the original landscape which was a 'no-data' region (e.g. the sea or land beyond a study area boundary) must remain in that state for the whole simulation.

- A list of initial individuals.
  The population is initialised according to a list of initial individuals (of given age and stage) in specified cells and years. This option allows simulation of a reintroduction scenario.

D.7. Submodels

Landscape

Dynamic landscapes are imported as a set of gridded maps that come into effect at specified years during the simulation. Each gridded map holds continuous values in its cells, ranging from 0.0 to 100.0, that represent percentages of habitat cover or quality. Thus, at a maps change some populations may be extirpated (all individuals either die or have an immediate opportunity to disperse) if suitable habitat is lost, and new populations may arise from colonisation of newly suitable areas.

In addition, the demographic density-dependence $1/b$ is given in units of the number of individuals per hectare. The given density dependence is interpreted as the maximum stregnth of demographic density-dependence reached in cells with 100% habitat. All other cells hold the respective fraction of the stregnth of density-dependence.

Reproduction

At the beginning of each year, reproduction is the first process to be modelled. The model simulates one reproductive season per year. Reproduction is followed by dispersal. After each reproductive season, survival and successive development of all the stages are modelled. Aging occurs at the end of the year.

Generations overlap and individuals are classified in different stages (e.g. immature vs. breeding individuals) differing in their demographic parameters. Individuals are characterized by their age and stage. Each stage has a certain fecundity ϕ, survival σ and probability of developing to the next stage γ. The parameters are provided through classical transition matrices (Caswell 2001). However, these are not multiplied with a population state vector as is typical for matrix models but, instead, the parameters are applied stochastically in an individual-based manner. At each reproductive season, two parameters control the likelihood that each individual / female reproduces:

- First, it is determined whether a reproductively mature female is a potential reproducer. Only those mature females that are able to reproduce, are potential breeders.
- Potential breeders all reproduce with a set probability ϕ.

In this model of the red kite, a female-only model was implemented. It models the three stages of juveniles, sub-adults and breeding adults. To allow offspring to developing to the next stage in the same year without losing an explicit offspring stage in which post-natal dispersal can happen, an explicit newborn stage (stage 0) is added, for example in a generic 3-stage model:

$$A = \begin{pmatrix} 0 & \phi_1 & \phi_2 & \phi_3 \\ 1 & \sigma_1 & 0 & 0 \\ 0 & \gamma_{1-2} & \sigma_2 & 0 \\ 0 & 0 & \gamma_{2-3} & \sigma_3 \end{pmatrix}$$

Newborn have to develop to stage 1 in the same year they are born. It is important to note that juvenile mortality can be accounted for in two ways. Either it is included in adult fecundity ϕ (by appropriately reducing its value), and γ_{0-1} is equal to 1.0. This is how it is typically accounted for in matrix models. Or, alternatively, ϕ is equal to the true maximum fecundity and γ_{0-1} is less than 1.0. In any case, σ_0 needs to be zero. Only the first approach allows straightforward direct comparison with standard analytical matrix models. The parameters in the matrix are used in a stochastic way at the individual level. Each individual/female at stage 3, if it reproduces, produces a number of offspring given by Poisson(ϕ_3).

Reproduction is density- and stage-dependent. Following Neubert & Caswell (2000), density and stage dependence in fecundity is implemented as an exponential decay:

$$\phi_i = \phi_{0,i} * e^{-b \sum_{j=1}^{S} \omega_{ij} N_{j,t}}$$

where ϕ_i is the fecundity of stage i, $\phi_{0,i}$ is its maximum fecundity at low densities, b is the strength of density dependence, S indicates the number of stages and ω_{ij} is contribution of stage j to the density dependence in the fecundity of stage i and $N_{j,t}$ the number of individuals in stage j at time t (e.g. (Caswell et al. 2004)).

Survival & Development

Reproduction is first followed by dispersal. Only then survival and successive development of all the stages are modelled.

Here, survival is neither density- nor stage- dependent. Bernoulli trials $Bern(\sigma)$ determine if an individual survives or not.

Likewise, development is neither density- nor stage- dependent. Bernoulli trials $Bern(\gamma)$ determine if an individual develops to the next stage or not.

Emigration

Emigration is the first phase of dispersal. It is modeled as the probability e that an individual will leave its natal patch during the present year. If a stage having non-zero e can last for more than one year, an individual has multiple opportunities to emigrate, each with probability e, and hence the realised overall emigration rate will be larger than e. Here, the emigration probability e is density-independent but stage-specific, so that only juveniles and sub-adults emigrate.

Transfer

Transfer is the second phase of dispersal, and consists of the movement of an individual starting from when it emigrates from its natal cell and ending with settlement in another cell or mortality. The main components of this phase are the individual movement ability and navigation capacity in response to the characteristics of the environment. The interaction between these components and their associated costs will determine the distance moved, the movement path and the chance of surviving the transfer phase.

The movement model is fully individual-based and explicitly decribes the movement behaviour of individuals with a level of detail, and hence parameters, which is probably close to the most parsimonious for a mechanisctic movement model.

For this model, a simple correlated random walk is used. This transfer submodel is implemented in continuous space on the top of the landscape grid. Individuals take steps of a constant step length, the direction is sampled from a wrapped Cauchy distribution having a correlation parameter ρ in the range 0 to 1 (Zollner and Lima 1999, Bartoń et al. 2009). All individuals take each step simultaneously.

Settlement

Settlement, or immigration, is the last phase of dispersal, when the organism stops in a new cell of breeding habitat. Dispersing individuals are not allowed to settle in their natal cell.

At each step, made simultaneously by all dispersing individuals, each evaluates their current cell for the possibility of settling. The individual decides to stop if there is suitable habitat; this is a necessary condition. Additionally, the settlement decision is density-dependent. The individual has a probability p_s of settling in the cell i, given by:

$$p_s = \frac{S_0}{1 + e^{-(bN_i - \beta_i) * \alpha_s}}$$

Here, N_i is the number of individuals of the cell i, b represents the strength of density dependence used for the population dynamics, S_0 is the maximum settlement probability, β_s is the inflection point and α_s is the slope of the function.

To avoid having individuals moving perpetually because they cannot find suitable conditions to settle, the model includes a maximum number of steps. The maximum number of steps defines the maximum time length of the transfer period. When an individual reaches the maximum number of steps, it stops where it is regardless of the suitability of the location. In the next season, if still alive, it will continue to move again.

Aging

Aging occurs at the end of each year.

D.8. Model parameter settings

Table D.1.: Simulation parameters

Parameter	Description	Values
Year	Number of simulated years	24
Replicates	Number of simulation iterations	20
Absorbing	Whether non-valid cells lead to direct mortality of the individual during transfer	FALSE
LocalExt	Local extinction	FALSE
EnvStoch	Environmental stochasticity (0: none, 1: global, 2: local) stochasticity acts (0: growth rate/fecundity, 1: demographic density dependence)	0
OutIntRange	Output of range file	0
OutIntOcc	Output of occupancy file	0
OutIntPop	Output of population file	1
OutIntInd	Output of individual file	0
OutIntConn	Output of connectivity file	0
OutIntPaths	Output of SMS paths file	0
OutStartPop	Starting year for output population file	2
OutStartInd	Starting year for output individual file	0
OutStartConn	Starting year for output connectivity file	0
OutStartPaths	Starting year for output SMS paths file	0
SMSHeatMap	Output SMS heat map raster file	FALSE

Table D.2.: Landscape parameters

Parameter	Description	Values
Landscape file	Landscape map(s)	habitatmaps
Resolution	Resolution in meters	2000
HabPercent	Whether habitat types/codes or habitat cover/quality	TRUE
NHabitats	Number of different habitat codes	2
K_or_DensDep	Demographic density-dependence	0.006
PatchFile	Filename(s) of the patch map(s)	NULL
CostsFile	Filename(s) of the SMS cost map(s)	NULL
DynamicLandYears	Years of landscape changes	0, 1, 2, 3, 4, 5, 6, 7, 8, 9, 10, 11, 12, 13, 14, 15, 16, 17, 18, 19
InitIndsFile	Filename of the species initial distribution list	NULL
InitIndsList	Species initial distribution data frame	createInitIndsFile_Pois()

Table D.3.: Demography parameters

Parameter	Description	Values
Stages	Number of life stages	4
TransMatrix	Transition matrix Defines the development probabilities from each stage into the next as well as the respective survival probabilities and fecundities	$\begin{bmatrix} 0 & 0 & 0 & 1.65 \\ 1 & 0.084 & 0 & 0 \\ 0 & 0.336 & 0.306 & 0 \\ 0 & 0 & 0.374 & 0.8 \end{bmatrix}$
MaxAge	Maximum age in years	12
MinAge	Ages which an individual in stage i-1 must already have reached before it can develop into the next stage i.	0, 0, 0, 0
RepSeasons	Number of potential reproduction events per year	1

Parameter	Description	Values
RepInterval	Number of reproductive seasons which must be missed following a reproduction attempt before another reproduction attempt may occur	0
PRep	Probability of reproducing in subsequent reproductive seasons	1
SurvSched	Scheduling of survival (0: at reproduction, 1: between reproductive events, 2: annually)	1
FecDensDep	whether density dependent fecundity probability is modelled	TRUE
DevDensDep	Whether density dependent development probability is modelled	FALSE
SurvDensDep	Whether density dependent survival probability is modelled	FALSE
DevDensCoeff	Relative density dependence coefficient for development	1
SurvDensCoeff	Relative density dependence coefficient for survival	1
FecStageWtsMatrix	Stage-dependent weights in density dependence of fecundity	$\begin{bmatrix} 0 & 0 & 0 & 0 \\ 0 & 0 & 0 & 0 \\ 0 & 0 & 0 & 0 \\ 0 & 0 & 1 & 1 \end{bmatrix}$
DevStageWtsMatrix	Stage-dependent weights in density dependence of development	Not selected.
SurvStageWtsMatrix	Stage dependent weights in density dependence of survival	Not selected.
PostDestrictn	Whether individuals of a population die (FALSE) or disperse (TRUE) if its patch gets destroyed	FALSE
ReproductionType	Decribes the reproduction type (0: asexual/only female; 1: simple sexual model; 2: sexual model with explicit mating system)	0

Table D.4.: Dispersal parameters

Process	Parameter	Description	Values
Emigration	EmigProb	Emigration probabilities per stage	$\begin{bmatrix} 0 & 0 \\ 1 & 0.64 \\ 2 & 0 \\ 3 & 0 \end{bmatrix}$
	SexDep	Sex-dependent emigration probability?	FALSE
	StageDep	Stage-dependent emigration probability?	TRUE
	DensDep	Density-dependent emigration probability?	FALSE
	UseFullKern	Shall the emigration probability be derived from dispersal kernel?	FALSE
Transfer	Model	Type of transfer model	Correlated Random Walk
	StepLength	Step length given in meters	2000
	Rho	Correlation parameter	0.85
	Straighten-Path	Straighten path after decision not to settle in a patch?	FALSE
	StepMort	Per-step mortality probability	0.00
Settlement	DensDep	Density-dependent settlement requirements?	TRUE
	SexDep	Sex-dependent settlement requirements?	FALSE
	StageDep	Stage-dependent settlement requirements?	FALSE
	Settle	Settlement probability parameters for all stages/sexes.	$\begin{bmatrix} 0.85 & -1 & 1.67 \end{bmatrix}$
	MinSteps	Minimum number of steps	0
	MaxSteps	Maximum number of steps	10
	MaxStepsYear	Maximum number of steps per year	5
	FindMate	Mating requirements to settle?	FALSE

Table D.5.: Initialisation parameters

Parameter	Description	Values
InitType	Type of initialisation (0: free initialisation according to habitat map, 1: from loaded species distribution map, 2: from initial individuals list file) (0: random in given number of cells, 1: all suitable cells/patches) species distribution map (0: all suitable cells within all distribution presence cells, 1: all suitable cells within given number of randomly chosen presence cells)	2
InitDens	Number of individuals seeded in each cell/patch (0: at demographic density dependence, 1: at half of the demographic density dependence, 2: according to quasi-equilibrium distribution) (0: minimum age for the respective stage, 1: random age between the minimum and maximum age for the respective stage, 2: according to a quasi-equilibrium distribution)	0
InitFreezeYear	Year until which species is confined to its initial range limits	0
RestrictRows	Number of rows at northern front to restrict range.	0
RestrictFreq	Frequency in years at which range is restricted to northern front.	0
FinalFreezeYear	The year after which species is confined to its new, current range limits, after a period of range expansion.	0

References

Armsworth, Paul R. and Roughgarden, Joan E. 2008. The Structure of Clines with Fitness-Dependent Dispersal. - The American Naturalist 172: 648–657.

Baguette, M. and Van Dyck, H. 2007. Landscape connectivity and animal behavior: functional grain as a key determinant for dispersal. - Landscape Ecol 22: 1117–1129.

Baguette, M. et al. 2013. Individual dispersal, landscape connectivity and ecological networks. - Biological Reviews 88: 310–326.

Baker, M. B. and Rao, S. 2004. Incremental Costs and Benefits Shape Natal Dispersal: Theory and Example with Hemilepistus reaumuri. - Ecology 85: 1039–1051.

Bartoń, K. A. et al. 2009. The evolution of an "intelligent" dispersal strategy: biased, correlated random walks in patchy landscapes. - Oikos 118: 309–319.

Bartoń, K. A. et al. 2012. Risky movement increases the rate of range expansion. - Proceedings of the Royal Society B: Biological Sciences 279: 1194–1202.

Bocedi, G. et al. 2014. RangeShiftR: a platform for modelling spatial eco-evolutionary dynamics and species' responses to environmental changes. - Methods in Ecology and Evolution 5: 388–396.

Bonte, D. et al. 2012. Costs of dispersal. - Biol Rev Camb Philos Soc 87: 290–312.

Bowler, D. E. and Benton, T. G. 2005. Causes and consequences of animal dispersal strategies: relating individual behaviour to spatial dynamics. - Biol Rev Camb Philos Soc 80: 205–225.

Caswell, H. 2001. Matrix Population Models: Construction, Analysis, and Interpretation. - Oxford University Press.

Caswell, H. et al. 2004. Sensitivity analysis of equilibrium in density-dependent matrix population models. - Ecology Letters 7: 380–387.

Chaput-Bardy, A. et al. 2010. Condition and Phenotype-Dependent Dispersal in a Damselfly, Calopteryx splendens. - PLOS ONE 5: e10694.

Clark, J. S. et al. 2001. Invasion by extremes: population spread with variation in dispersal and reproduction. - Am Nat 157: 537–554.

Clobert, J. et al. 2001. Dispersal. - Oxford University Press.

Clobert, J. et al. 2012. Dispersal Ecology and Evolution - Oxford University Press.

Clobert, J. et al. 2009. Informed dispersal, heterogeneity in animal dispersal syndromes and the dynamics of spatially structured populations. - Ecol Lett 12: 197–209.

Clotuche, G. et al. 2013. Settlement decisions by the two-spotted spider mite Tetranychus urticae. - Comptes Rendus Biologies 336: 93–101.

Codling, E. A. et al. 2008. Random walk models in biology. - J R Soc Interface 5: 813–834.

De Meester, N. and Bonte, D. 2010. Information use and density-dependent emigration in an agrobiont spider. - Behavioral Ecology 21: 992–998.

Delattre, T. et al. 2010. Dispersal mood revealed by shifts from routine to direct flights in the meadow brown butterfly Maniola jurtina. - Oikos 119: 1900–1908.

Doligez, B. et al. 2004. Availability and Use of Public Information and Conspecific Density for Settlement Decisions in the Collared Flycatcher. - Journal of Animal Ecology 73: 75–87.

Dover, J. and Settele, J. 2009. The influences of landscape structure on butterfly distribution and movement: a review. - J Insect Conserv 13: 3–27.

Edelaar, P. et al. 2008. Matching Habitat Choice Causes Directed Gene Flow: A Neglected Dimension in Evolution and Ecology. - Evolution 62: 2462–2472.

Fahrig, L. 2007. Non-optimal animal movement in human-altered landscapes. - Functional Ecology 21: 1003–1015.

Fletcher, R. J. 2007. Species interactions and population density mediate the use of social cues for habitat selection. - J Anim Ecol 76: 598–606.

Fryxell, J. M. et al. 2008. Multiple movement modes by large herbivores at multiple spatiotemporal scales. - PNAS 105: 19114–19119.

Gardner, R. H. and Gustafson, E. J. 2004. Simulating dispersal of reintroduced species

within heterogeneous landscapes. - Ecological Modelling 171: 339–358.
Gilroy, J. J. and Lockwood, J. L. 2012. Mate-Finding as an Overlooked Critical Determinant of Dispersal Variation in Sexually-Reproducing Animals. - PLOS ONE 7: e38091.
Grimm, V. and Railsback, S. F. 2005. Individual-based Modeling and Ecology. - Princeton University Press.
Grimm, V., Railsback, S. F., Vincenot, C. E., Berger, U., Gallagher, C., Deangelis, D. L., Edmonds, B., Ge, J., Giske, J., Groeneveld, J., Johnston, A. S. A., Milles, A., Nabe-Nielsen, J., Polhill, J. G., Radchuk, V., Rohwäder, M. S., Stillman, R. A., Thiele, J. C., and Ayllón, D. 2020. The ODD protocol for describing agent-based and other simulation models: A second update to improve clarity, replication, and structural realism. - Journal of Artificial Societies and Social Simulation, 23(2), Article 2.
Haughland, D. L. and Larsen, K. W. 2004. Exploration correlates with settlement: red squirrel dispersal in contrasting habitats. - Journal of Animal Ecology 73: 1024–1034.
Hawkes, C. 2009. Linking movement behaviour, dispersal and population processes: is individual variation a key? - Journal of Animal Ecology 78: 894–906.
Heinz, S. K. and Strand, E. 2006. Adaptive Patch Searching Strategies in Fragmented Landscapes. - Evolutionary Ecology: 113–130.
Holyoak, M. et al. 2008. Trends and missing parts in the study of movement ecology. - PNAS 105: 19060–19065.
Jongejans, E. et al. 2008. Dispersal, demography and spatial population models for conservation and control management. - Perspectives in Plant Ecology, Evolution and Systematics 9: 153–170.
Kendall, B. E. and Fox, G. A. 2003. Unstructured Individual Variation and Demographic Stochasticity. - Conservation Biology 17: 1170–1172.
Knowlton, J. L. and Graham, C. H. 2010. Using behavioral landscape ecology to predict species' responses to land-use and climate change. - Biological Conservation 143: 1342–1354.
Kun, Á. and Scheuring, I. 2006. The Evolution of Density-Dependent Dispersal in a Noisy Spatial Population Model. - Oikos 115: 308–320.
Lambin, X. et al. 2012. High connectivity despite high fragmentation: iterated dispersal in a vertebrate metapopulation. - In: Dispersal Ecology and Evolution. Oxford University Press, in press.
Le Galliard, J.-F. et al. 2012. Patterns and processes of dispersal behaviour in arvicoline rodents. - Mol Ecol 21: 505–523.
Lima, S. L. and Zollner, P. A. 1996. Towards a behavioral ecology of ecological landscapes. - Trends in Ecology & Evolution 11: 131–135.
Matthysen, E. 2005. Density-dependent dispersal in birds and mammals. - Ecography 28: 403–416.
Merckx, T. et al. 2003. The evolution of movements and behaviour at boundaries in different landscapes: a common arena experiment with butterflies. - Proceedings of the Royal Society of London. Series B: Biological Sciences 270: 1815–1821.
Metz, J. a. J. and Gyllenberg, M. 2001. How should we define fitness in structured metapopulation models? Including an application to the calculation of evolutionarily stable dispersal strategies. - Proceedings of the Royal Society of London. Series B: Biological

Sciences 268: 499–508.
Morales, J. 2002. Behavior at Habitat Boundaries Can Produce Leptokurtic Movement Distributions. - The American Naturalist 160: 531–538.
Morales, J. M. and Ellner, S. P. 2002. Scaling up Animal Movements in Heterogeneous Landscapes: The Importance of Behavior. - Ecology 83: 2240–2247.
Morales, J. M. et al. 2010. Building the bridge between animal movement and population dynamics. - Philosophical Transactions of the Royal Society B: Biological Sciences 365: 2289–2301.
Nathan, R. et al. 2008. A movement ecology paradigm for unifying organismal movement research. - PNAS 105: 19052–19059.
Neubert, M. G. and Caswell, H. C. 2000. Density-dependent vital rates and their population dynamic consequences. - J Math Biol 41: 103–121.
Olden, J. D. et al. 2004. Context-dependent perceptual ranges and their relevance to animal movements in landscapes. - Journal of Animal Ecology 73: 1190–1194.
Ovaskainen, O. 2004. Habitat-Specific Movement Parameters Estimated Using Mark–Recapture Data and a Diffusion Model. - Ecology 85: 242–257.
Ovaskainen, O. and Cornell, S. J. 2003. Biased Movement at a Boundary and Conditional Occupancy Times for Diffusion Processes. - Journal of Applied Probability 40: 557–580.
Ovaskainen, O. and Crone, E. E. 2009. Modeling animal movement with diffusion. - Spatial Ecology in press.
Ovaskainen, O. et al. 2008. An empirical test of a diffusion model: predicting clouded apollo movements in a novel environment. - Am Nat 171: 610–619.
Palmer, S. C. F. et al. 2011. Introducing a “stochastic movement simulator” for estimating habitat connectivity. - Methods in Ecology and Evolution 2: 258–268.
Patterson, T. A. et al. 2008. State–space models of individual animal movement. - Trends in Ecology & Evolution 23: 87–94.
Pe’er, G. and Kramer-Schadt, S. 2008. Incorporating the perceptual range of animals into connectivity models. - Ecological Modelling 213: 73–85.
Pe’er, G. et al. 2011. Breaking Functional Connectivity into Components: A Novel Approach Using an Individual-Based Model, and First Outcomes. - PLOS ONE 6: e22355.
Phillips, B. L. et al. 2010. Life-history evolution in range-shifting populations. - Ecology 91: 1617–1627.
Poethke, H. J. and Hovestadt, T. 2002. Evolution of density–and patch–size–dependent dispersal rates. - Proceedings of the Royal Society of London. Series B: Biological Sciences 269: 637–645.
Poethke, H. J. et al. 2011. The ability of individuals to assess population density influences the evolution of emigration propensity and dispersal distance. - J Theor Biol 282: 93–99.
Revilla, E. and Wiegand, T. 2008. Individual movement behavior, matrix heterogeneity, and the dynamics of spatially structured populations. - PNAS 105: 19120–19125.
Revilla, E. et al. 2004. Effects of Matrix Heterogeneity on Animal Dispersal: From Individual Behavior to Metapopulation-Level Parameters. - The American Naturalist 164: E130–E153.
Ricketts, T. H. 2001. The matrix matters: effective isolation in fragmented landscapes. - Am Nat 158: 87–99.

Robert, A. et al. 2003. Variation among Individuals, Demographic Stochasticity, and Extinction: Response to Kendall and Fox. - Conservation Biology 17: 1166–1169.

Ronce, O. 2007. How Does It Feel to Be Like a Rolling Stone? Ten Questions About Dispersal Evolution. - Annual Review of Ecology, Evolution, and Systematics 38: 231–253.

Ruxton, G. D. and Rohani, P. 1998. Fitness-dependent dispersal in metapopulations and its consequences for persistence and synchrony. - Journal of Animal Ecology: 530–539.

Schtickzelle, N. and Baguette, M. 2003. Behavioural responses to habitat patch boundaries restrict dispersal and generate emigration–patch area relationships in fragmented landscapes. - Journal of Animal Ecology 72: 533–545.

Schultz, C. B. and Crone, E. E. 2001. Edge-Mediated Dispersal Behavior in a Prairie Butterfly. - Ecology 82: 1879–1892.

Schurr, F. M. 2012. How random is dispersal? From stochasticity to process in the description of seed movement. - In: Clobert, J. et al. (eds), Dispersal Ecology and Evolution. Oxford University Press, pp. 240–247.

Shreeve, T. G. and Dennis, R. L. H. 2011. Landscape scale conservation: resources, behaviour, the matrix and opportunities. - J Insect Conserv 15: 179–188.

Smouse, P. E. et al. 2010. Stochastic modelling of animal movement. - Philosophical Transactions of the Royal Society of London. Series B, Biological Sciences: 2201–2211.

Stamps, J. A. 1988. Conspecific Attraction and Aggregation in Territorial Species. - The American Naturalist 131: 329–347.

Stamps, J. 2001. Habitat selection by dispersers: integrating proximate and ultimate approaches. - In: Clobert, J. et al. (eds), Dispersal. Oxford University Press, pp. 230–242.

Stamps, J. A. and Blozis, S. A. 2006. Effects of natal experience on habitat selection when individuals make choices in groups: A multilevel analysis. - Animal Behaviour 71: 663–672.

Stamps, J. A. et al. 2005. Search Costs and Habitat Selection by Dispersers. - Ecology 86: 510–518.

Stamps, Judy A. et al. 2009. How Different Types of Natal Experience Affect Habitat Preference. - The American Naturalist 174: 623–630.

Stenseth, N. C. and Lidicker, W. Z. (Eds.) 1992. Animal Dispersal: Small mammals as a model. - Springer, Netherlands.

Stevens, V. M. and Coulon, A. 2012. Landscape effects on spatial dynamics: the natterjack toad as a case study. - In: Dispersal Ecology and Evolution. Oxford University Press, in press.

Stevens, V. M. et al. 2006. Quantifying functional connectivity: experimental assessment of boundary permeability for the natterjack toad (Bufo calamita). - Oecologia 150: 161–171.

Travis, J. M. J. et al. 1999. The evolution of density-dependent dispersal. - Proc Biol Sci 266: 1837.

Travis, J. M. J. et al. 2010. Towards a mechanistic understanding of dispersal evolution in plants: conservation implications. - Diversity and Distributions 16: 690–702.

Travis, J. M. J. et al. 2011. Improving prediction and management of range expansions by combining analytical and individual-based modelling approaches. - Methods in

Ecology and Evolution 2: 477–488.
Travis, J. M. J. et al. 2012. Modelling dispersal: an eco-evolutionary framework incorporating emigration, movement, settlement behaviour and the multiple costs involved. - Methods in Ecology and Evolution 3: 628–641.
Travis, J. M. J. et al. 2014. Dispersal and species' responses to climate change. - Oikos 122: 1532–1540.
Vandermeer, J. and Carvajal, R. 2001. Metapopulation dynamics and the quality of the matrix. - Am Nat 158: 211–220.
Vercken, E. et al. 2012. The importance of a good neighborhood: dispersal decisions in juvenile common lizards are based on social environment. - Behavioral Ecology: 1059–1067.
Vuilleumier, S. and Metzger, R. 2006. Animal dispersal modelling: Handling landscape features and related animal choices. - Ecological Modelling 190: 159–170.
Vuilleumier, S. et al. 2006. Effects of Cognitive Abilities on Metapopulation Connectivity. - Oikos 113: 139–147.
Wiegand, T. et al. 2005. Effects of Habitat Loss and Fragmentation on Population Dynamics. - Conservation Biology 19: 108–121.
Zheng, C. et al. 2009. Modelling dispersal with diffusion and habitat selection: Analytical results for highly fragmented landscapes. - Ecological Modelling 220: 1495–1505.
Zollner, P. and Lima, S. L. 1997. Landscape-level perceptual abilities in white-footed mice : perceptual range and the detection of forested habitat. - Oikos 80: 51–60.
Zollner, P. and Lima, S. L. 1999. Search Strategies for Landscape-Level Interpatch Movements. - Ecology 80: 1019–1030.
Zollner, P. A. and Lima, S. L. 2005. Behavioral tradeoffs when dispersing across a patchy landscape. - OIKOS 108: 219–230.

Declaration

I herewith declare that I independently prepared this dissertation. I did not use any sources other than those specified in the list of references. All parts, which originate literally or meaningfully from other sources, are marked as such. This thesis has not been submitted to any other university of examination board before.

Anne-Kathleen Malchow
Potsdam, 03.10.2022